universität wien

DISSERTATION / DOCTORAL THESIS

Titel der Dissertation /Title of the Doctoral Thesis

„On the Quantum Gross-Pitaevskii Equation“

verfasst von / submitted by

Mag. Damian Draxler

angestrebter akademischer Grad / in partial fulfilment of the requirements for the degree of

Doktor der Naturwissenschaften (Dr.rer.nat.)

Wien, 2016

Studienkennzahl lt. Studienblatt / degree programme code as it appears on the student record sheet:	A 791 411
Dissertationsgebiet lt. Studienblatt / field of study as it appears on the student record sheet:	Physik
Betreut von / Supervisor:	Univ. Prof. Dr. Frank Verstraete

To Alma and David

Contents

Zusammenfassung

Gegenstand dieser Dissertation ist die Entwicklung neuer variationeller Algorithmen zur Untersuchung von stark korrelierten eindimensionalen Quantenfeldtheorien. Zu diesem Zweck wird das Dirac-Frenkel zeitabhängige Variationsprinzip auf die Klasse der kontinuierlichen Matrix Produkt Zustände (cMPS) angewandt. Diese Zustände gehören zu der Familie der Tensor-Netzwerk Zustände, sind jedoch direkt im Kontinuum formuliert. Die Dissertation beinhaltet im wesentlichen drei Hauptresultate: einen Ansatz zur Beschreibung von Anregungszuständen niedriger Energie, ein Algorithmus für die Zeitentwicklung von Systemen mit offenen Randbedingungen sowie ein weiterer für jene mit periodischen Randbedingungen. Die Algorithmen sind sowohl für endliche nicht translationsinvariante Systeme als auch für Systeme im thermodynamischen Limes anwendbar und können gleichsam relativistische und nicht-relativistische Theorien beschreiben. Es wird daher ein umfangreicher methodologischer Rahmen zur numerischen Untersuchung von stark korrelierten eindimensionalen Quantenfeldtheorien erarbeitet. Darüber hinaus verallgemeinern wir die renommierte Theorie von Gross und Pitaevskii, omnipräsent in der theoretischen Beschreibung von ultrakalten Bose Gasen, auf den Fall von stark korrelierten, eindimensionalen Systemen wo Molekularfeldnäherungen typischerweise nicht anwendbar sind. Diese Verallgemeinerung beinhaltet die Gross-Pitaevskii Gleichung im Molekularfeldlimes aber geht weit darüber hinaus indem Verschränkung und Quantenkorrelationen mitberücksichtigt werden. Die Linearisierung dieser sogenannten Quantum Gross-Pitaevskii Gleichungen führt zu einer quantenmechanischen Version der Bogoliubov de-Gennes Gleichungen welche die Untersuchung der nicht perturbativen linearen response-Theorie oder der quantenmechanischen Kontrolltheorie ermöglicht. Diese Methoden werden dann dazu verwendet die Anregungen und die dynamischen Korrelationsfunktionen des Lieb-Liniger Models und einer nicht integrablen Erweiterung desselben zu untersuchen, wobei im Spektrum des ersteren solitonische Anregungen und im Spektrum des letzteren ein nicht trivialer, gebundener Zustand identifiziert wurde. Des Weiteren wird ein wechselwirkendes Bose Gas studiert, welches in der Anwesenheit eines $U(1)$-Eichpotentials auf eine ringförmige Geometrie beschränkt ist. Hierbei liegt der Fokus auf der Berechnung der dissipationsfreien Teilchen Ströme, wobei zusätzlich eine lokale Barriere in das System eingeführt wurde. Darüber hinaus werden Grundzustandseigenschaften eines zwei-komponentigen Bose Gases simuliert. Dies ebnet den Weg zur Beschreibung von quasi zwei (oder höher) dimensionalen Systemen deren Beschreibung mit den derzeit vorhanden cMPS Methoden nicht möglich sind.

Abstract

This thesis is concerned with the development of new variational algorithms to study strongly correlated one dimensional quantum field theories. To this end we apply the Dirac-Frenkel time-dependent variational principle to the class of continuous Matrix Product States (cMPS) which are a certain type of tensor-network states directly formulated in the continuum. Three main results are presented in this thesis: an ansatz for low lying excitations, a time-evolution algorithm for systems with open boundary conditions and a time evolution algorithm for systems with periodic boundary conditions. These algorithms can be applied equally well to finite translationally and non-translationally invariant systems, to systems in the thermodynamic limit and to both relativistic and non-relativistic theories. Hence, we provide an almost complete toolbox for the numerical study of strongly correlated one dimensional quantum field theories. Moreover, we thereby generalize the renowned theory of Gross and Pitaevskii, central to the theoretical study of ultracold Bose gases, to the case of strongly correlated one dimensional systems where mean-field descriptions typically fail. Our generalization includes the Gross-Pitaevskii equation in the mean-field limit but goes well beyond this regime by capturing entanglement and quantum correlations. Linearizing these quantum Gross-Pitaevskii equations gives then rise to a quantum version of the Bogoluibov de-Gennes equations which allow the study of non-perturbative linear response or quantum control theory. These methods are then used to study excitations and dynamical correlation functions of the Lieb-Liniger model, as well as a non-integrable extension thereof where we identify clear solitonic signatures in the spectrum of the former one and a non-trivial bound state in the spectrum of the latter one. We then investigate an interacting Bose gas loaded into a ring shaped geometry in the presence of a $U(1)$-gauge potential, and focus on the persistent currents behaviour in the presence of a barrier. In addition, ground state properties of the two-component Bose gas are studied thereby paving the way towards quasi two (or higher) dimensional systems which are currently not accessible with cMPS based methods.

Acknowledgements

I would like to thank my supervisor Prof. Frank Verstraete for his support and encouragement during my graduate studies.

I would like to thank all my collaborators and especially Jutho Haegeman, Vid Stojevic and Matteo Rizzi for their engagement in our joint projects. I would also like to thank Vid for proofreading many of my drafts.

I would like to thank Valentin Zauner-Stauber not only for his countless assistance in getting the cluster working again but also for being a very pleasant office neighbour.

I gratefully acknowledge the generous support by the Austrian FWF SFB project FoQuS and ViCoM.

I would especially like to thank my wife Agnes and my parents, and my parents in-law for their encouragement throughout the time of my graduate studies and for being such wonderful babysitters.

Introduction

The origins of this thesis may be traced back to the early days of quantum many-body physics when in two seminal works Gross [45] (1963) and Pitaevskii [93] (1961) independently derived an equation that has become one of the cornerstones of the theoretical study of ultracold Bose gases. The success of this equation stems from the fact that for large dilute systems in three dimensions a significant fraction of the systems constituent particles condense into the lowest possible energy state at low temperatures. Thus a mean-field description, such as the Gross-Pitaevskii (GP) wave function, can be applied. In 1947 Bogoliubov [10] derived a perturbative formula for the ground state energy of the three dimensional uniform Bose gas thereby developing a general theory for the study of excitations in the weak coupling limit. Both the GP and the Bogoliubov ansatz depend crucially on the *condensate* hypothesis as the Bogoliubov excitations can be interpreted as small fluctuations around the condensate wave function [94]. In the case of an inhomogenous system the Bogoliubov equations are derived by linearizing the time dependent GP equation around its fixed point, resulting in a set of linear equations that are typically referred to as the Bogoliubov-de Gennes equations [16]. The first experimental realisation of a Bose Einstein condensate in 1995/1996 has led to an outburst of both experimental and theoretical work on this subject. This has demonstrated a remarkably good agreement between the theoretical predictions of the GP/Bogoliubov theory and the experimental findings thus validating their application in three- (or two-) dimensional systems [73].

However, in one dimension strong quantum correlations dominate and the GP/Bogoliubov theory is not applicable anymore. From a quantum information theoretical perspective this is best understood by the fundamental monogamous nature of entanglement [24, 112] which leads in general to a decrease of entanglement with increasing spatial dimension. Hence, in the limit of infinite dimension mean field theory becomes exact. On the contrary, quantum many-body systems in one dimension are dominated by entanglement and require tools which go beyond the mean-field realm.

In 1981 Haldane realised that many of these one dimensional models exhibit a linear dispersion of the low lying excitations and have algebraically decaying ground state correlation functions. This led him to the definition of a universality class named *Tomonaga-Luttinger liquids* (TLL) [55]. TTL theory is an effective low energy theory that is exactly solvable once the two defining parameters of the theory are known, the sound velocity and the so called Luttinger-Liquid parameter. These two parameters are model specific and have to be calculated numerically unless the underlying model is exactly solvable. This in turn means that the TTL theory can not be used as a black box to study one dimensional systems as it relies on other numerical methods. The very powerful and statistically exact Monte Carlo approach is one method of choice. However, Monte Carlo methods are plagued by the infamous sign problem and are thus mostly restricted to bosonic systems. The sign problem can partially be

resolved by means of the variational Monte Carlo method but the accuracy of this approach strongly depends on the specific trial wave function at hand and thus demands in general for an educated guess about the structure of the quantity which one aims to compute. Moreover, Monte Carlo methods can not straightforwardly be applied to systems in the thermodynamic limit or to systems out of equilibrium.

In 1992 Steve White opened a new chapter in the field of one dimensional strongly correlated quantum many-body systems by introducing the *Density Matrix Renormalization Group* algorithm (DMRG) [127]. This algorithm arose by merging ideas from renormalization group and quantum information theory and can be regarded as the initial ignition of a whole new research area named *Tensor-Network* (TN) methods [121]. Indeed, it took very little time to realise that the DMRG algorithm is a variational optimisation procedure over the class of *Matrix Product States* (MPS) which are the most prominent example of one dimensional TN states. Other examples of TN states are the two dimensional generalisation of MPS called *Projected Entangled Pair States* (PEPS), *Tree Tensor-Network* (TTN) states for tree like graphs or the *Multi-scale Entanglement Renormalization Ansatz* (MERA) used in the study of critical systems [121, 85, 124]. With the exception of MERA, all these tensor network classes satisfy an *area law* by construction, i.e. the entanglement entropy of a subregion scales with the boundary of this region and not with its volume. In fact it can be proven that ground states of local one dimensional gaped Hamiltonians always obey an area law [58] and it is believed, but not proven, that this generically also holds for higher dimensions. For critical models, the area law receives corrections that scale logarithmically in the length of the subregion. These results on area laws have led to the widely accepted picture of a small *corner* in Hilbert space which incorporates all physically relevant states, namely those with little entanglement, and that TN states provide an efficient parametrization of this intriguing corner. Inspired by this intuition TN related methods have been succesfully applied to a plethora of different subjects including the classification of gapped-phases in one dimension [19, 104, 117], the study of topological [103] and symmetry protected topological order [18], gauge theories [110] and even quantum chemistry [83]. The toolbox of TN methods further allows the study of both in and out of equilibrium phenomena, and of systems at finite temperature thus providing an unprecedented platform to pursue the quests of quantum many-body physics.

In 2010 the family of TN states was further enlarged by the introduction of the class of *continuous Matrix Product States* (cMPS) [119]. These states are the continuum limit of a certain subclass of MPS and allow to study one dimensional quantum field theories directly in the continuum. However, in contrast to the aforementioned TN states, the theory of cMPS is not as advanced, and especially lacks efficient optimization methods. It is the central goal of this thesis to partially fill this gap and develop efficient time-evolution and optimization methods for cMPS. This is accomplished by applying the Dirac-Frenkel time-dependent variational principle (TDVP) [30, 38, 70] to both, uniform cMPS in the thermodynamic limit and to inhomogenous finite systems with open or periodic boundary conditions. Hence, a complete toolbox is provided for probing ground state properties, low lying excitations and the dynamics of one dimensional quantum field theories. These methods are not restricted to a certain model, but can be applied to bosons and to fermions, as well as to both relativistic or non-relativistic theories.

The methodological framework presented in this dissertation is also directly related to the mean-field treatment of ultracold quantum gases mentioned in the beginning of this chapter. Indeed, the TDVP equations for cMPS reduce to the time-dependent GP equation in a certain

mean-field limit. Moreover, linearizing these equations around its fix point gives rise to a quantum version of the Bogoliubov-de Gennes equations. The methods developed in this thesis may thus as well be seen in a bigger and rather historical context as they enable the ingeniuity of Gross, Pitaevskii and Bogoliubov to eventually enter the world of one dimensional strongly correlated quantum many-body systems. The thesis is organised as follows:

Outline and Summary of the results

Chapter 1: In this chapter we introduce a variational method for constructing low lying excitations of translational invariant $(1+1)$-dimensional quantum field theories in the thermodynamic limit. The method is based upon applying the time independent variational principle, also known as the Raleigh-Ritz principle, to the variational class of cMPS tangent states. The method crucially relies on the assumption that low lying excitations are well approximated by momentum superpositions of local disturbances in the many-body ground state. This assumption can be even proven for excitations in translational invariant quantum lattice systems with local interactions if the corresponding eigenvalue is separated from the rest of the spectrum [53]. While not providing any exact results we give strong numerical evidence that the method produces reliable results for generic field theories. We first consider the integrable Lieb-Liniger model [74] and reproduce the exact results to a high degree of accuracy. Within our method Lieb's Type I and Type II excitation branches are identified as topological excitations, and we illustrate the solitonic nature of the latter. Moreover a non-integrable model is studied by adding a $U(1)$-symmetry breaking term to the Lieb-Liniger Hamiltonian and we find that the spectrum of this Hamiltonian contains non-trivial bound states.

Chapter 2: This chapter is devoted to the problem of generalizing the ubiquitous GP equation to one dimensional systems by including entanglement and quantum correlations. We do so by applying the time dependent variational principle to the class of cMPS which results in a non-commutative generalization of the GP equation. This so called *quantum Gross-Pitaevskii* equation (qGPE) is not only an extension to one dimension, but also allows the study of fields with arbitrary statistics including relativistic or non-relativistic theories alike. Linearizing the qGPE around its fix point leads to a quantum version of the Bogoliubov-de Gennes equations. The solutions of these *quantum Bogoliubov-de Gennes* (qBdG) equations may be at first interpreted as excitations above the many-body ground state. Indeed, in the case of a uniform system in the thermodynamic limit one recovers the excitation formalism developed in chapter 1. However, the qBdG equations in its most general form go well beyond this interpretation and allow the study of linear response theory in the strongly correlated regime thereby delivering a new approach to study dynamical correlation functions or even aspects of quantum control theory. As a first example we study the response of the Lieb-Liniger ground state against a static external potential of cosine form. It is found that the response amplitude, also known as the inverse energy-weighted moment of the dynamic structure factor, as a function of the wavevector of the external potential shows a strong peak around twice the Fermi momentum. This effect can not be explained within the classical Bogoliubov approach. It is a clear signature of the second gap closing of Lieb's Type II excitation branch closing, and should be observable in experiments similar to those in [33, 35, 80].

Chapter 3: In this chapter we derive the TDVP equations for uniform cMPS with periodic boundary conditions. Systems with periodic boundary conditions are in general much more

costly to simulate with tensor network based methods than systems with open boundary conditions. This difficulty can partially be overcome by additional approximations in the contraction of the network. In our setting this is done by allowing for a cutoff in the spectrum of the cMPS transfer matrix. The method is then used to study an interacting rotating Bose gas in a ring which is interrupted by a localised barrier. We focus on the system's ground state properties such as the dependence of the persistent currents amplitude on the interaction and the barrier strength. The results are thoroughly benchmarked against TTN based lattice simulations and classical GP calculations to demonstrate the wide applicability of our method for all interactions, densities or system sizes.

Appendix A: The thesis is concluded by a brief discussion of dynamical correlation functions and by a study of the two-component Bose gas. For the former we use the results from chapter 1 to calculate dynamical density-density correlation functions (also known as the dynamical structure factor (DSF)) of the Lieb-Liniger model. The results have to be taken with a grain of salt as also excitations that are not well captured within the ansatz of chapter 1, i.e non local multi particle/hole excitations, significantly contribute to the DSF. We give an outlook on how to generalize our ansatz and discuss the possibility of using the results of chapter 2 on the qBdG equations to establish a different approach towards the simulation of such dynamical quantities.

The second part on the two component Bose gas contains a complete derivation of the TDVP equations for a newly defined cMPS ansatz for coupled fields. We focus on the repulsive case with equal species density and study the mixing/demixing transition (or phase seperation). We give an outlook on how to use the results of chapter 1 and 2 to study the bosonic equivalence of spin/charge separation, and how to address questions concerning the dynamics of quasi two (or higher) dimensional systems of coupled Lieb-Liniger arrays.

Chapter 1

Particles, holes and solitons: a matrix product state approach

Synopsis:

We introduce a variational method for calculating dispersion relations of translation invariant (1+1)-dimensional quantum field theories. The method is based on continuous matrix product states and can be implemented efficiently. We study the critical Lieb-Liniger model as a benchmark and excelent agreement with the exact solution is found. Additionally, we observe solitonic signatures of Lieb's Type II excitation. In addition, a non-integrable model is introduced where a $U(1)$-symmetry breaking term is added to the Lieb-Liniger Hamiltonian. For this model we find evidence of a non-trivial bound-state excitation in the dispersion relation.

Based on:

D. Draxler, J. Haegeman, T. J. Osborne, V. Stojevic, L. Vanderstraeten, and F. Verstraete
Phys. Rev. Lett. **111**, 020402 (2013)

1.1 Introduction

The last decades have witnessed an explosion in the experimental realization of strongly correlated one-dimensional quantum systems [40]. Often a discretised description in terms of a lattice Hamiltonian is possible, which can then be studied using White's density matrix renormalization group [127]. The underlying variational ansatz, the set of matrix product states (MPS) [3, 36, 87, 121, 23], explains both the success of this method and has been used to develop generalizations beyond the setting of ground states, *e.g.* to the study of time evolution [123, 47], dissipative dynamics [120, 130] and dispersion relations [91, 54].

The use of elongated optical or magnetic atom traps has opened the possibility of creating one-dimensional quantum gases in the lab [43, 82, 68, 67, 34, 71]. It is natural to study these systems directly using quantum fields, without resorting to a lattice discretisation. A continuum limit of the class of matrix product states, known as *continuous matrix product states* (cMPS) [119, 86, 49], was recently developed and has demonstrated to be able to provide an efficient description of the ground-state properties of the Lieb-Liniger (LL) model [75].

Apart from ground-state properties, there has also been experimental interest in localized excitations in these systems [11, 8, 107, 126]. While Lieb determined the spectrum of excitations for the LL model [74], a systematic method for studying excitations of non-integrable quantum fields is still lacking. In this Letter we fill the gap by extending the recently introduced ansatz for excitations of translation invariant spin chains in the thermodynamic limit [69] to the setting of cMPS. This yields a new variational ansatz for elementary excitations of translation invariant quantum fields that allows us to simulate dispersion relations for integrable and non-integrable models alike. The corresponding variational states are faithful eigenstates and have therefore an infinite lifetime, out of which we can construct localized wavepackets by taking linear combinations. With this method, we can reconstruct the spectrum of the LL Hamiltonian and illustrate the solitonic effects in Lieb's Type II excitation —first observed in Refs. [72, 64] in the weak-interaction limit— for arbitrary interaction strength. We can equally well construct the spectrum for non-integrable models, which we illustrate by adding a pairing term to the LL Hamiltonian which opens a gap. For a certain parameter regime, our method provides strong evidence for the existence of a non-trivial bound state.

1.2 Ansatz for Excitations

A cMPS for a translation invariant infinite system with open boundary conditions is defined as [119]

$$|\Psi(Q,R)\rangle = v_L^\dagger \left(\mathcal{P} \mathrm{e}^{\int_{-\infty}^{\infty} \mathrm{d}x \, [Q\otimes\mathbb{1} + R\otimes\hat{\psi}^\dagger(x)]} \right) v_R |\Omega\rangle \tag{1.1}$$

where $Q, R \in \mathbb{C}^{D\times D}$, v_L and v_R are D-dimensional boundary vectors acting on an ancillary system, $|\Omega\rangle$ is the Fock vacuum and $\mathcal{P}$ the path-ordering operator. For bosonic systems the field operators satisfy the commutation relation $[\hat{\psi}(x), \hat{\psi}^\dagger(y)] = \delta(x-y)$. For a generic normalizable cMPS, all eigenvalues of the transfer matrix $T = Q\otimes\mathbb{1} + \mathbb{1}\otimes\bar{Q} + R\otimes\bar{R}$ have non-positive real part and there is a non-degenerate zero eigenvalue. The corresponding left and right zero eigenvectors, $\langle l|T = 0$, $T|r\rangle = 0$ may be reshaped to give positive, hermitian matrices l and r which have full rank and are normalized so that $\langle l|r\rangle = \mathrm{Tr}(lr) = 1$. Since the boundary vectors have no variational importance they are chosen so that the state has norm 1, i.e. $\langle\Psi(\bar{Q},\bar{R})|\Psi(Q,R)\rangle = (v_L^\dagger \otimes v_L^\top)|r\rangle\langle l|\,(v_R\otimes\bar{v}_R) = (v_L^\dagger r v_L)(v_R^\dagger l v_R) = 1$.

Suppose we have approximated the ground state of a system as a cMPS parametrized by the matrices (Q,R). An ansatz for a particle-like eigenstate or excitation is obtained by locally

replacing the matrices Q and R by V and W — which has the effect of perturbing the ground state in a spatial region of the size of the correlation length — and then building a state with definite momentum via a plane wave superposition:

$$|\Phi_p(V,W)\rangle := \int_{-\infty}^{\infty} \mathrm{d}x\, \mathrm{e}^{\mathrm{i}px} v_L^\dagger \hat{U}_1(-\infty,x)\Big(V\otimes\mathbb{1} + W\otimes\hat{\psi}^\dagger(x)\Big)\hat{U}_2(x,\infty)v_R|\Omega\rangle \tag{1.2}$$

where $\hat{U}_a(x,y) = \mathcal{P}\exp(\int_x^y \mathrm{d}z\,(Q_a\otimes\mathbb{1} + R_a\otimes\hat{\psi}^\dagger(z)))$ for $a = 1,2$. The crucial feature here is a single strictly local disturbance described by the matrices $V, W \in \mathbb{C}^{D\times D}$, which is nevertheless able to influence the state up to a distance determined by the bond dimension and appears to efficiently capture single-particle excitations, as we illustrate below. The states $|\Phi_p(V,W)\rangle$ are momentum eigenstates and obey a δ-orthogonality. Note that they depend linearly on the variational parameters V and W, so they span a linear subspace of Hilbert space. Asymptotically the states $|\Phi_p(V,W)\rangle$ look like $|\Psi(Q_1,R_1)\rangle$ at $x = -\infty$ and $|\Psi(Q_2,R_2)\rangle$ at $x = +\infty$, which are supposed to be equally good but potentially different ground states (in the case of symmetry breaking). Our ansatz thus includes the possibility of capturing *topologically non-trivial* excitations, henceforth referred to as topological excitations for the sake of brevity. For $|\Psi(Q_1,R_1)\rangle = |\Psi(Q_2,R_2)\rangle$, the ansatz describes (topologically) trivial excitations and can be interpreted as a state in the momentum sector p of the tangent space obtained by an infinitesimal position dependent variation of $|\Psi(Q,R)\rangle$ [49].

To compute excitations we apply the *Rayleigh-Ritz* method, which results in a generalized eigenvalue problem for an effective Hamiltonian. In our case the generalized eigenvalue equation is given by

$$H_p \begin{bmatrix} V \\ W \end{bmatrix} = E N_p \begin{bmatrix} V \\ W \end{bmatrix} \tag{1.3}$$

with $\left[\begin{smallmatrix} V \\ W \end{smallmatrix}\right]$ being the $2D^2$-dimensional vector corresponding to V and W, E is the energy, H_p the effective Hamiltonian and N_p the effective norm matrix. Both H_p and N_p are $2D^2\times 2D^2$-dimensional matrices defined by

$$\begin{aligned}\langle\Phi_p(\overline{V},\overline{W})|\hat{H} - E_0|\Phi_{p'}(V,W)\rangle &= 2\pi\delta(p-p')\left[V^\dagger W^\dagger\right] H_p \begin{bmatrix} V \\ W \end{bmatrix} \\ \langle\Phi_p(\overline{V},\overline{W})|\Phi_{p'}(V,W)\rangle &= 2\pi\delta(p-p')\left[V^\dagger W^\dagger\right] N_p \begin{bmatrix} V \\ W \end{bmatrix}\end{aligned} \tag{1.4}$$

where E_0 is the ground state energy obtained with the ground state approximation $|\Psi(Q,R)\rangle$.

Note that H_p and N_p have zero eigenvalues corresponding to a redundancy in the representation of the states $|\Phi_p(V,W)\rangle$, which can be traced back to the gauge invariance of the states $|\Psi(Q,R)\rangle$ under the transformation $Q \leftarrow g^{-1}Qg$ and $R \leftarrow g^{-1}Rg$ [49]. One finds that for all $X \in \mathbb{C}^{D\times D}$, $|\Phi_p([X,Q] + \mathrm{i}pX, [X,R])\rangle = 0$. Hence, $|\Phi_p(V',W')\rangle = |\Phi_p(V,W)\rangle$ if $V' = V + [X,Q] + \mathrm{i}pX$ and $W' = W + [X,R]$. If, for $p = 0$, one also restricts to states orthogonal to the ground state by imposing $\langle l|\left(V\otimes\mathbb{1} + W\otimes\bar{R}\right)|r\rangle = 0$, there are D^2 redundant degrees of freedom for every momentum p. These can be eliminated by constraining V and W to satisfy a 'gauge-fixing' condition such as

$$\langle l|\left(V\otimes\mathbb{1} + W\otimes\bar{R}\right) = 0 \tag{1.5}$$

with $\langle l|$ the left eigenvector of T_{11}, the transfer matrix corresponding to $|\Psi(Q_1,R_1)\rangle$. It can be shown that this choice of gauge reduces the effective norm matrix to the identity (Ref. [49]

and Supplementary Material), so that the Rayleigh-Ritz problem becomes an ordinary eigenvalue problem. The explicit calculation of the effective Hamiltonian H_p in this gauge is more involved and is derived in full detail in the Supplementary Material. The lowest eigenvalues of H_p can then be obtained with a computational time scaling as $\mathcal{O}(D^3)$ using a sparse eigensolver exploiting the tensor product structure of the effective Hamiltonian.

1.3 Results

1.3.1 The Lieb-Liniger Hamiltonian

We now discuss the results obtained for the LL model. The LL Hamiltonian is given by

$$\hat{H}_{\mathrm{LL}} = \int_{-\infty}^{+\infty} \left[\frac{\mathrm{d}\hat{\psi}^\dagger}{\mathrm{d}x} \frac{\mathrm{d}\hat{\psi}}{\mathrm{d}x} - \mu \hat{\psi}^\dagger \hat{\psi} + c \hat{\psi}^\dagger \hat{\psi}^\dagger \hat{\psi} \hat{\psi} \right] \mathrm{d}x \tag{1.6}$$

with a repulsive interaction strength $c > 0$ and where the argument of the field operators has been omitted for the sake of brevity. Since a variational approach targets the lowest energy state, this Hamiltonian was formulated in the grand-canonical ensemble (with chemical potential $\mu > 0$). The Hamiltonian is gapless and only depends on a single parameter $\gamma = c/\rho$, with ρ the ground state particle density which is set by μ. The cMPS ansatz generalizes a coherent state ansatz and breaks the U(1)-symmetry of the model, whereas the exact Bethe-ansatz ground state does not and has a fixed total number of particles. This follows from the fact that it is often energetically beneficial to break the symmetry in the presence of a constraint on the total amount of entanglement. Hence, the order parameter $\langle \Psi(\bar{Q}, \bar{R}) | \hat{\psi} | \Psi(Q, R) \rangle \neq 0$ (and in fact slowly converges to 0 for increasing D). For any $\theta \in [0, 2\pi)$, $|\Psi(Q, e^{i\theta} R)\rangle$ is again a valid ground state so that we can also consider topological excitations interpolating between two different ground states characterized by a different order parameter. They can also be understood as momentum superpositions of a local perturbation at position x which has a half-infinite string $\hat{S}(x) = \exp(\mathrm{i}\theta \int_{-\infty}^{x} \hat{\psi}^\dagger(z)\hat{\psi}(z)\,\mathrm{d}z)$ attached to it. Even for the exact solution with fixed particle number N, the elementary particle ($N+1$) and hole ($N-1$) excitations have a topological nature and need to be studied using antiperiodic boundary conditions [69]. For $\theta = \pi$, the string $\hat{S}(x)$ has exactly the effect of flipping the sign of the field operators at $-\infty$ ($\hat{S}(x)^\dagger \hat{\psi}(-\infty) \hat{S}(x) = -\hat{\psi}(-\infty)$) and Fig. 1.1 does indeed confirm that the elementary excitations are perfectly captured by using the ansatz for topological excitations with the choice $Q_1 = Q_2 = Q$, $R_1 = -R_2 = R$. The dispersion relation is centered around 0 and the *hole* branch (red stars) is obtained as the lowest excitation energy with momentum between $-\pi\rho$ and $+\pi\rho$, with ρ the particle density. The *particle* branch (blue diamonds) shows the eigenvalues of the eigenvectors that have the largest overlap with the state $\int_{-\infty}^{\infty} \mathrm{d}x\, \mathrm{e}^{\mathrm{i}px} \hat{\psi}^\dagger(x) e^{\mathrm{i}\pi \int_{-\infty}^{x} \hat{\psi}^\dagger(z)\hat{\psi}(z)\,\mathrm{d}z} |\Psi(Q, R)\rangle$. All parameters plotted in the figures are normalized such that they are dimensionless ($p/\rho, e/\rho^2$), as in Ref. [75].

Lieb determined the spectrum with fixed particle number (*i.e.* topologically trivial) in first quantization [74] and isolated two types of excitations, which he labeled Type I and Type II excitations. Either can be used to construct the full spectrum of excitations with equal particle number. Fig. 1.2 shows the eigenvalues of the effective Hamiltonian H_p as a function of the momentum p obtained using the trivial ansatz ($Q_1 = Q_2$ and $R_1 = R_2$). However, it is well-known [69] that the Type I excitations should be understood as one *hole* at momentum $-\pi\rho$ plus one *particle* with momentum $p \geq \pi\rho$, whereas the Type II excitations at momentum p are obtained by combining one *particle* with momentum $\pi\rho$ plus one *hole* with momentum

$-\pi\rho \leq p \leq \pi\rho$. By combining momentum and variational energies of our topological excitations according to this recipe, we can accurately reproduce (5 digits of precision) the Bethe ansatz dispersion relations of Lieb's Type I [blue diamonds in Fig. 1.2 and 1.1(a)] and II excitations [red stars in Fig. 1.2 and 1.1(b)]. If we would have used the trivial excitation energies directly [also sketched in Fig. 1.1(b)], a worse precision would have been obtained, as this single particle ansatz cannot accurately represent the two unbound constituents of Lieb's Type I and Type II excitations and tries to confine them into a small spatial region. Since the repulsive Lieb-Liniger model does not have any bound states [69], all trivial excitations have a similar structure consisting of an even sum of topological hole and particle excitations.

Without knowing the exact result, this information could be inferred from looking at the convergence of the variational energies as a function of increasing D. There are two competing effects within our variational strategy. Firstly, by modifying Q and R locally, we assume that the excitation is confined in a spatial region, the width of which is set by the bond dimension. This is the variational approximation and it produces a positive variational error. Secondly, we subtract from the Hamiltonian a variational estimate of the ground state energy which is too large. This second effect results in a negative error and is dominant for truly elementary excitations for which the assumed locality is valid and the first error is negligible. If an excited state cannot be approximated locally, *e.g.* an excitation that is composed of several unbound elementary excitations, then the first effect will likely be dominant as the ansatz confines these different excitations in a finite spatial region. Indeed, for increasing D, the particle and hole energies in Fig. 1.1 are increasing (which is true for all $\gamma \gtrsim 3$) because a smaller variational estimate for the ground state energy is subtracted. In contrast, the energies of trivial excitations in Fig. 1.2 decrease for increasing D, in line with our expectations.

Our ansatz does not depend on γ and works in principle equally well for both limiting cases $\gamma \to \infty$ and $\gamma \to 0$, as is confirmed by the results for small values of γ in the Supplementary Material. However, for small γ ($\gamma \lesssim 3$) we observe a transition of the topological hole excitation to a solitonic excitation. This observation was first discussed in Refs. [72, 64] or recently received renewed attention following the experimental realization [107, 101, 4]. In the Tonks-Girardeau limit (large γ) [41], the hole excitation maps exactly to the fermion-like hole excitation and produces a change in particle number of -1. For very small γ, the hole excitation is related to the classical dark soliton of the non-linear Schrödinger equation [116] and produces a large change in particle number [4]. The relative change in particle number can easily be calculated using our ansatz. It is illustrated in Fig. 1.3 for momentum $p = 0$, and the results perfectly coincide with the recent exact calculations [4].

1.3.2 A non integrable model

Next, we study a non-integrable model obtained by adding a pairing term to $\hat{H}_{\mathrm{LL}}$ that breaks the $\mathsf{U}(1)$ symmetry down to a residual $\mathbb{Z}_2$ symmetry

$$\hat{H}' = \hat{H}_{\mathrm{LL}} + \int_{-\infty}^{\infty} dx \, \left(u\hat{\psi}^\dagger\hat{\psi}^\dagger + \bar{u}\hat{\psi}\hat{\psi} \right). \tag{1.7}$$

As long as $\mu > 0$ the cMPS ground state approximation $|\Psi(Q,R)\rangle$ spontaneously breaks the $\mathbb{Z}_2$ symmetry for any nonzero pairing strength $u \in \mathbb{C}_0$, and a second ground state $|\Psi(Q,-R)\rangle$ is obtained. This also opens up a gap in the spectrum. The magnitude of the order parameter $\langle\Psi(\bar{Q},\bar{R})|\hat{\psi}(x)|\Psi(Q,R)\rangle$ is determined by the competing effects of the pairing term and the repulsive interaction. As an example we consider an intermediate parameter range where we have found strong evidence that the lowest lying excitation in the trivial spectrum is a bound state. In the top plot of Fig. 1.4, the lowest lying trivial excitations of $\hat{H}'$ for $\gamma \approx 26.4$, $\mu = 1$

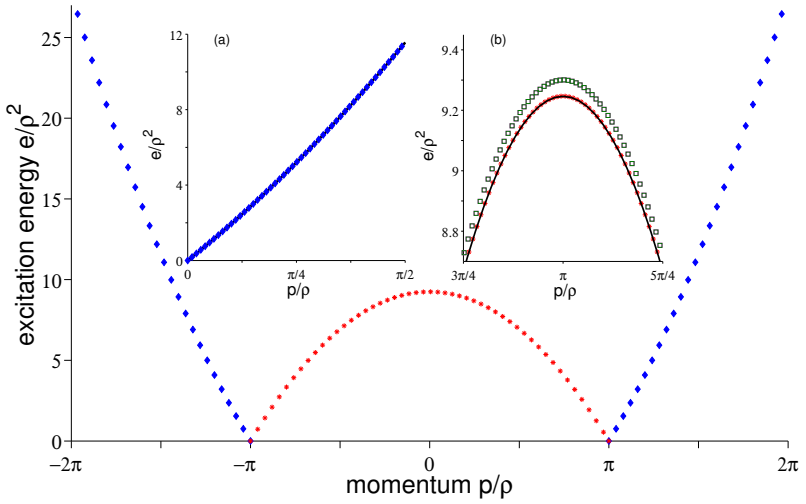

Figure 1.1: Elementary topological excitation branches for $\gamma = c/\rho \approx 60.16$ at $D = 64$ with $\theta = \pi$. Blue diamonds are *particle* excitations and red stars *hole* excitations. (a) Dispersion relation of Lieb's Type I excitation obtained from the topological ansatz (blue diamonds) and from the Bethe ansatz solution (black line). (b) Dispersion relation of Lieb's Type II excitation obtained from the topological ansatz (red stars), the trivial ansatz (green squares) and from the Bethe ansatz solution (black line).

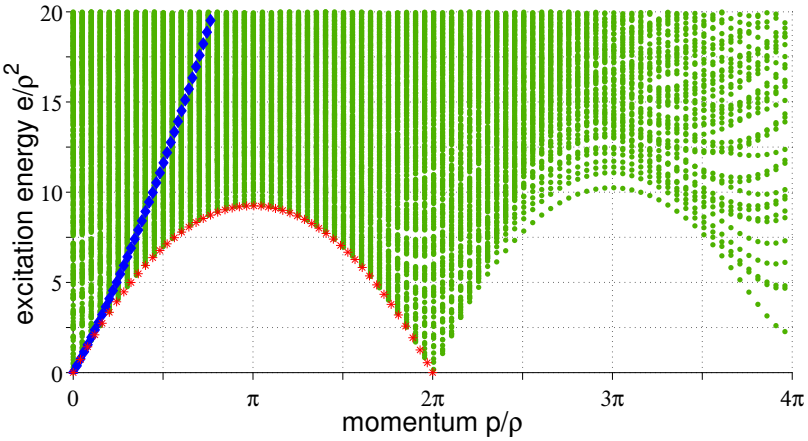

Figure 1.2: Dispersion relation for the Lieb-Liniger model with $D = 64$ for $\gamma = c/\rho \approx 60.16$. Bulk excitations (dots) are trivial excitations. Blue diamonds (Type I) and red stars (Type II) are obtained by combining momenta and energy of two topological excitations (hole and particle) of Fig. 1.1.

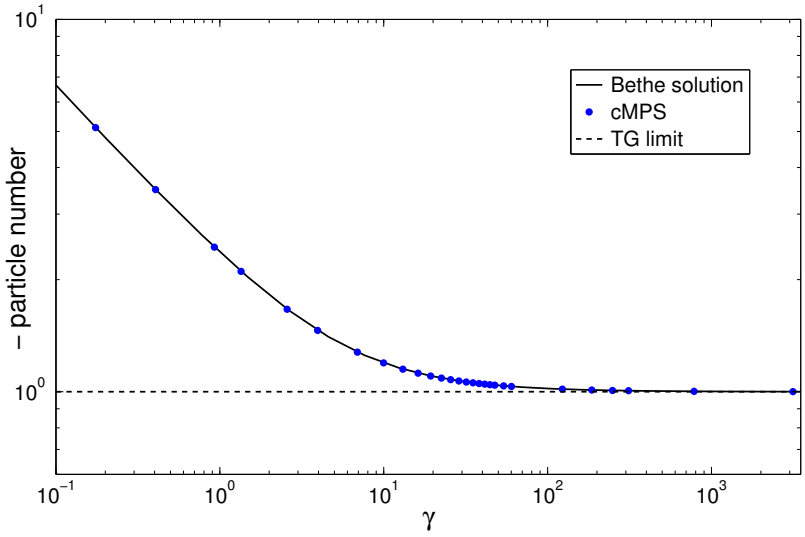

Figure 1.3: The change in particle number expectation value for the hole state at momentum $p = 0$ as a function of γ, as predicted by the Bethe solution [4] and with the cMPS excitation ansatz.

and $u = 1$ with $D = 22$ are shown with red circles. Due to the symmetry breaking, we can again construct topological excitations (right insert of Fig. 1.4), for which the lowest lying eigenvalues constitute an isolated branch that can be interpreted as the kink excitation that interpolates between the two degenerate ground states. The blue dots in the trivial spectrum of Fig. 1.4 are obtained by considering all possible pairs of two such topological excitations by adding their momentum and energy. Around momentum zero, the lowest lying trivial excitation produced by the trivial ansatz lies well below the two-kink continuum starting at twice the kink mass.

It is tempting to interpret this excitation as a bound state of two kinks, and this claim is further supported by considering the convergence behavior of (twice) the kink mass and the two lowest trivial excitation energies as a function of D in the bottom plot of Fig. 1.4. The kink is the elementary excitation; it has a negative error that vanishes quickly for increasing D. As in the LL case, unbound multi-particle states are not expected to converge quickly, because the different constituents are confined within a spatial region, the size of which is determined by the bond dimension. For the energy of a two-particle state, we thus expect a positive finite size error. The energy of a bound state should also exhibit a large positive error as long as the spatial support of the excitation ansatz is below the binding length, but should then stagnate when the binding length is exceeded by increasing D. Fig. 1.4 confirms that the lowest lying energy of the trivial ansatz converges to a value well below twice the kink mass in a way that is characteristic for a bound state.

1.4 Conclusions

In conclusion, we have introduced a variational ansatz for the study of elementary excitations for one-dimensional quantum field theories, based on continuous matrix product states. The ansatz produces very accurate results even for the critical Lieb-Liniger model. The local aspect of the ansatz made the solitonic feature of the lowest lying hole eigenstates of the LL model very explicit, and the particle number in those solitons could be reproduced to great accuracy. We also applied the method to a gapped non-integrable variant of LL, and obtained

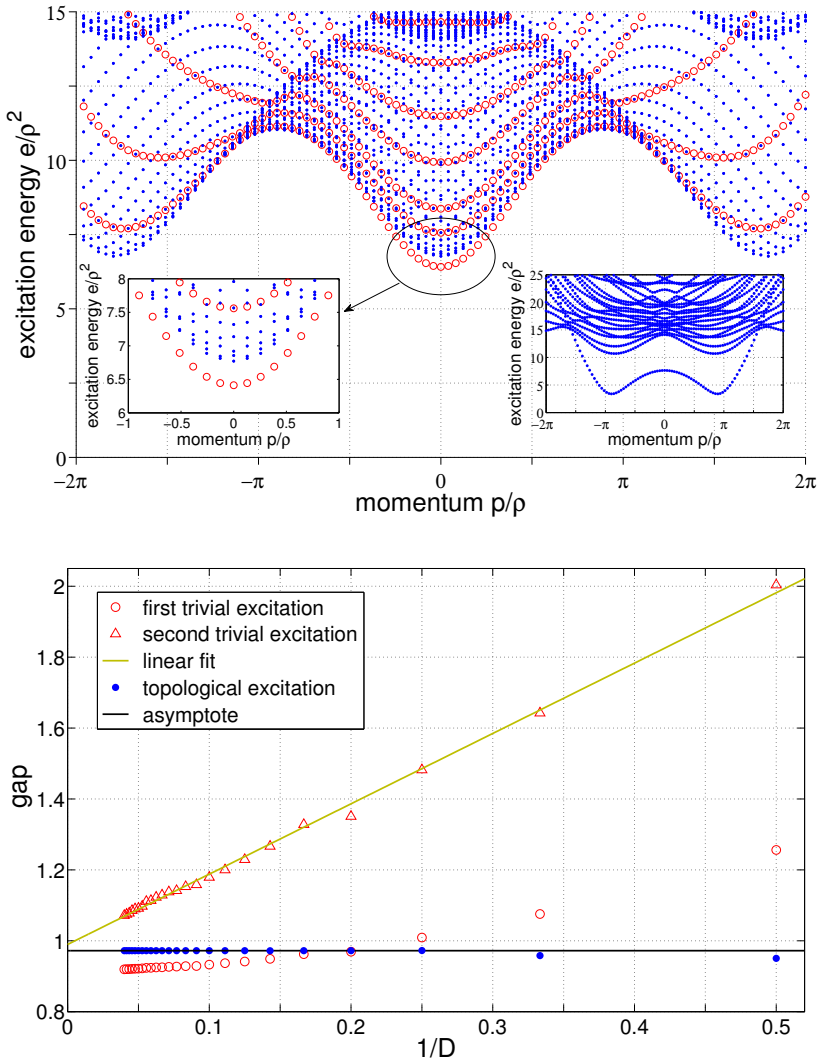

Figure 1.4: Top: Dispersion relation of $\hat{H}'$ with $D = 22$ for $\gamma \approx 26.4$, $\mu = 1$ and $u = 1$. Blue dots are the pairwise sum of all topological excitations. Red circles are trivial excitations and the right insert shows the topological spectrum. Bottom: Convergence of the two lowest trivial eigenvalues and the lowest two-kink excitation energy as a function of D^{-1} at $p = 0$.

strong evidence for the existence of a bound state. As an outlook, we can remark that this method provides a stepping stone to a further understanding of the low-energy dynamics of one-dimensional interacting quantum field theories. In order to calculate *e.g.* dynamical correlation functions, it would be interesting to study scattering states of topological excitations.

1.5 Supplementary Material

In this Supplementary Material we explain in full detail how to calculate expectation values of bosonic field operators with the variational states introduced in this paper. In particular, we will derive the effective Hamiltonian for the Lieb-Liniger model $\hat{H}_{\mathrm{LL}}$ and for the non-integrable Hamiltonian $\hat{H}'$ that was introduced in the paper. Moreover, some more results for the spectrum of $\hat{H}_{\mathrm{LL}}$ for small values of the interaction strength are shown. The variational ansatz states for excitations in a uniform system are defined as

$$|\Phi_p(V,W)\rangle := \int_{-\infty}^{\infty} \mathrm{d}x\, \mathrm{e}^{\mathrm{i}px} v_L^\dagger \hat{U}_1(-\infty,x)\Big(V\otimes \mathbb{1} + W\otimes \hat{\psi}^\dagger(x)\Big)\hat{U}_2(x,\infty)v_R|\Omega\rangle\ , \quad (1.8)$$

with $V,W\in\mathbb{C}^{D\times D}$ and $\hat{U}_a(x,y)=\mathcal{P}\exp(\int_x^y \mathrm{d}z\,(Q_a\otimes\mathbb{1}+R_a\otimes\hat{\psi}^\dagger(z)))$ for $a=1,2$ where (Q_a,R_a) are two equally good ground states. The field operators satisfy the usual commutation relaltion $[\hat{\psi}(x),\hat{\psi}^\dagger(y)]=\delta(x-y)$. We assume that all eigenvalues of the ground state transfer matrix $T_{aa}=Q_a\otimes\mathbb{1}+\mathbb{1}\otimes\bar{Q}_a+R_a\otimes\bar{R}_a$ with $a=1,2$ have non-positive real part and there is a non-degenerate zero eigenvalue with corresponding left and right zero eigenvectors, $\langle l_a|T_{aa}=0$, $T_{aa}|r_a\rangle=0$. Moreover, it is possible to work in a gauge such that $\langle l_a|$ always reshapes to $\mathbb{1}_{D\times D}$ and $|r_a\rangle$ to the right $(D\times D)$-dimensional density matrix r_a. The boundary vectors are chosen such that the ground state is normalised, i.e. $\langle\Psi(\bar{Q}_a,\bar{R}_a)|\Psi(Q_a,R_a)\rangle = (v_L^\dagger\otimes v_L^\top)|r_a\rangle\langle l_a|\,(v_R\otimes\bar{v}_R)=1$. When $|\Psi(Q_1,R_1)\rangle$ and $|\Psi(Q_2,R_2)\rangle$ represent inequivalent ground states, the mixed transfer matrix T_{12} has only eigenvalues with a strictly negative real part. Vice versa, if the mixed transfer matrix has an eigenvalue with real part zero, then there exists a gauge transform G such that $Q_1=G^{-1}Q_2G$ and $R_1=G^{-1}R_2G$. We will always assume that (Q_1,R_1) and (Q_2,R_2) either parametrize different ground states, or that they are identical such that $G=1$ and $T_{11}=T_{12}=T_{22}$. All of these statements are analogous to well-known results for the case of matrix product states [see *e.g.* D. Perez-Garcia, M.M. Wolf, M. Sanz, F. Verstraete, J.I. Cirac, Phys. Rev. Lett. **100**, 167202 (2008)].

To calculate expectation values, it is useful to know how an annihilation operator acts on the states of Eq. (1.8),

$$\begin{aligned}
&\hat{\psi}(y)|\Phi_p(V,W)\rangle = \\
&+\int_y^\infty \mathrm{d}x\,\mathrm{e}^{\mathrm{i}px} v_L^\dagger \hat{U}_1(-\infty,y)R_1\hat{U}_1(y,x)\Big(V\otimes\mathbb{1}+W\otimes\hat{\psi}^\dagger(x)\Big)\hat{U}_2(x,\infty)v_R|\Omega\rangle \\
&+\int_{-\infty}^y \mathrm{d}x\,\mathrm{e}^{\mathrm{i}px} v_L^\dagger \hat{U}_1(-\infty,x)\Big(V\otimes\mathbb{1}+W\otimes\hat{\psi}^\dagger(x)\Big)\hat{U}_2(x,y)R_2\hat{U}_2(y,\infty)v_R|\Omega\rangle \\
&+\mathrm{e}^{\mathrm{i}py} v_L^\dagger \hat{U}_1(-\infty,y)W\hat{U}_2(y,\infty)v_R|\Omega\rangle\ . \qquad (1.9)
\end{aligned}$$

The same can be done for two annihilation operators $\hat{\psi}(z)$, $\hat{\psi}(y)$ where we assume $z\le y$,

$$\begin{aligned}
&\hat{\psi}(z)\hat{\psi}(y)|\Phi_p(V,W)\rangle = \\
&\int_y^\infty \mathrm{d}x\,\mathrm{e}^{\mathrm{i}px} v_L^\dagger \hat{U}_1(-\infty,z)R_1\hat{U}_1(z,y)R_1\hat{U}_1(y,x)\Big(V\otimes\mathbb{1}+W\otimes\hat{\psi}^\dagger(x)\Big)\hat{U}_2(x,\infty)v_R|\Omega\rangle \\
&+\int_z^y \mathrm{d}x\,\mathrm{e}^{\mathrm{i}px} v_L^\dagger \hat{U}_1(-\infty,z)R_1\hat{U}_1(z,x)\Big(V\otimes\mathbb{1}+W\otimes\hat{\psi}^\dagger(x)\Big)\hat{U}_2(x,y)R_2\hat{U}_2(y,\infty)v_R|\Omega\rangle \\
&+\int_{-\infty}^z \mathrm{d}x\,\mathrm{e}^{\mathrm{i}px} v_L^\dagger \hat{U}_1(-\infty,x)\Big(V\otimes\mathbb{1}+W\otimes\hat{\psi}^\dagger(x)\Big)\hat{U}_2(x,z)R_2\hat{U}_2(z,y)R_2\hat{U}_2(y,\infty)v_R|\Omega\rangle \\
&+\mathrm{e}^{\mathrm{i}pz} v_L^\dagger \hat{U}_1(-\infty,z)W\hat{U}_2(z,y)R_2\hat{U}_2(y,\infty)v_R|\Omega\rangle \\
&+\mathrm{e}^{\mathrm{i}py} v_L^\dagger \hat{U}_1(-\infty,z)R_1\hat{U}_1(z,y)W\hat{U}_2(y,\infty)v_R|\Omega\rangle\ . \qquad (1.10)
\end{aligned}$$

For the kinetic energy we need to know how $\frac{d\hat{\psi}(y)}{dy}$ acts on Eq. (1.8), i.e. we have to take the derivative of Eq. (1.9), where we use $\mathrm{d}\hat{U}_a(x,y)/\mathrm{d}y = \hat{U}_a(x,y)[Q_a \otimes \mathbb{1} + R_a \otimes \hat{\psi}^\dagger(y)]$ and $\mathrm{d}\hat{U}_a(y,x)/\mathrm{d}y = -[Q_a \otimes \mathbb{1} + R_a \otimes \hat{\psi}^\dagger(y)]\hat{U}_a(y,x)$ in order to obtain

$$\begin{aligned}
&\frac{d\hat{\psi}(y)}{dy}|\Phi_p(V,W)\rangle = \\
&\int_y^\infty \mathrm{d}x\, \mathrm{e}^{\mathrm{i}px} v_L^\dagger \hat{U}_1(-\infty,y)\,[Q_1, R_1\otimes\mathbb{1}]\,\hat{U}_1(y,x)\Big(V\otimes\mathbb{1} + W\otimes\hat{\psi}^\dagger(x)\Big)\hat{U}_2(x,\infty)v_R|\Omega\rangle \\
&+\int_{-\infty}^y \mathrm{d}x\, \mathrm{e}^{\mathrm{i}px} v_L^\dagger \hat{U}_1(-\infty,x)\Big(V\otimes\mathbb{1} + W\otimes\hat{\psi}^\dagger(x)\Big)\hat{U}_2(x,y)\,[Q_2, R_2]\,\hat{U}_2(y,\infty)v_R|\Omega\rangle \\
&+ v_L^\dagger \hat{U}_1(-\infty,y)\Big(\,(VR_2 - R_1V) + (Q_1W - WQ_2) + \mathrm{i}pW\Big)\hat{U}_2(y,\infty)v_R|\Omega\rangle\,. \qquad (1.11)
\end{aligned}$$

One can check that a number of potentially problematic (infinite norm) terms which have a creation operator $\hat{\psi}^\dagger(y)$ at the fixed position y all nicely cancel.

Expectation values can now easily be calculated by taking the overlap of the above expressions. We start with the scalar product of Eq. (1.8)

$$\begin{aligned}
&\langle\Phi_p(\overline{V},\overline{W})|\Phi_{p'}(V,W)\rangle = \\
&\int_{-\infty}^\infty \mathrm{d}x\, \mathrm{e}^{\mathrm{i}p'x}\int_x^\infty \mathrm{d}y\, \mathrm{e}^{-\mathrm{i}py}\langle l_1|\Big(V\otimes\mathbb{1} + W\otimes\overline{R}_1\Big)\mathrm{e}^{(y-x)T_{12}}\Big(\mathbb{1}\otimes\overline{V} + R_2\otimes\overline{W}\Big)|r_2\rangle \\
&+\int_{-\infty}^\infty \mathrm{d}x\, \mathrm{e}^{\mathrm{i}p'x}\int_{-\infty}^x \mathrm{d}y\, \mathrm{e}^{-\mathrm{i}py}\langle l_1|\Big(\mathbb{1}\otimes\overline{V} + R_1\otimes\overline{W}\Big)\mathrm{e}^{(x-y)T_{21}}\Big(V\otimes\mathbb{1} + W\otimes\overline{R}_2\Big)|r_2\rangle \\
&+\int_{-\infty}^\infty \mathrm{d}x\, \mathrm{e}^{\mathrm{i}(p'-p)x}\langle l_1|W\otimes\overline{W}|r_2\rangle \\
=&2\pi\delta(p'-p)\Bigg[\int_0^\infty \mathrm{d}y\,\langle l_1|\Big(V\otimes\mathbb{1} + W\otimes\overline{R}_1\Big)\mathrm{e}^{y(T_{12}-\mathrm{i}p)}\Big(\mathbb{1}\otimes\overline{V} + R_2\otimes\overline{W}\Big)|r_2\rangle \\
&\qquad+\int_0^{+\infty}\mathrm{d}y\,\langle l_1|\Big(\mathbb{1}\otimes\overline{V} + R_1\otimes\overline{W}\Big)\mathrm{e}^{y(T_{21}+\mathrm{i}p)}\Big(V\otimes\mathbb{1} + W\otimes\overline{R}_2\Big)|r_2\rangle \\
&\qquad+\langle l_1|W\otimes\overline{W}|r_2\rangle\Bigg]\,. \qquad (1.12)
\end{aligned}$$

The non-local character of the perturbation (V,W) to the ground state results in two non-local terms in the above expression, connected by the mixed transfer matrix T_{12}.

Throughout this supplementary material, we will have to compute many integrals of the form $\int_0^{+\infty}\mathrm{e}^{x(T_{ab}\pm\mathrm{i}p)}\,\mathrm{d}x$. For the mixed transfer matrix in the expression above, in case of two inequivalent ground states, this integral is well defined and results in $-(T_{ab}\pm\mathrm{i}p)^{-1}$, since all eigenvalues have a strictly negative real part. We then obtain

$$\begin{aligned}
&\langle\Phi_p(\overline{V},\overline{W})|\Phi_{p'}(V,W)\rangle = \\
&2\pi\delta(p'-p)\Bigg[\langle l_1|\Big(V\otimes\mathbb{1} + W\otimes\overline{R}_1\Big)(-T_{12}+\mathrm{i}p)^{-1}\Big(\mathbb{1}\otimes\overline{V} + R_2\otimes\overline{W}\Big)|r_2\rangle \\
&\qquad+\langle l_1|\Big(\mathbb{1}\otimes\overline{V} + R_1\otimes\overline{W}\Big)(-T_{21}-\mathrm{i}p)^{-1}\Big(V\otimes\mathbb{1} + W\otimes\overline{R}_2\Big)|r_2\rangle \\
&\qquad+\langle l_1|W\otimes\overline{W}|r_2\rangle\Bigg]\,. \qquad (1.13)
\end{aligned}$$

For topologically trivial states [$(Q_1, R_1) = (Q_2, R_2)$], the situation is more complicated. In this case, we can define a unique transfer matrix $T := T_{12} = T_{11} = T_{22}$ which has a unique eigenvalue zero with corresponding left eigenvector $\langle l| := \langle l_1| = \langle l_2|$ and right eigenvector $|r\rangle := |r_1\rangle = |r_2\rangle$. We can then define a projector $P = \mathbb{1} - |r\rangle\langle l|$ and compute $\int_0^{+\infty} P\mathrm{e}^{x(T\pm \mathrm{i}p)}P\,\mathrm{d}x = -P(T \pm \mathrm{i}p)^{-1}P = -(T \pm \mathrm{i}p)^{\mathsf{P}}$ where we have introduced the notation of superscript P to denote a kind of pseudo-inverse where the eigenspace zero of the transfer matrix has been projected out. The remaining 'singular' part evaluates to $\int_0^{+\infty} |r\rangle\langle l|\,\mathrm{e}^{x(T\pm\mathrm{i}p)}\,|r\rangle\langle l|\,\mathrm{d}x = |r\rangle\langle l|\int_0^{+\infty}\mathrm{e}^{\pm\mathrm{i}px}\,\mathrm{d}x$, and by combining the singular parts of the first and second line in Eq. (1.12) we obtain

$$\begin{aligned}
&\langle\Phi_p(\overline{V},\overline{W})|\Phi_{p'}(V,W)\rangle = \\
&2\pi\delta(p'-p)\Bigg[\langle l|\Big(V\otimes\mathbb{1}+W\otimes\overline{R}\Big)(-T+\mathrm{i}p)^{\mathsf{P}}\Big(\mathbb{1}\otimes\overline{V}+R\otimes\overline{W}\Big)|r\rangle \\
&\qquad + \langle l|\Big(\mathbb{1}\otimes\overline{V}+R\otimes\overline{W}\Big)(-T-\mathrm{i}p)^{\mathsf{P}}\Big(V\otimes\mathbb{1}+W\otimes\overline{R}\Big)|r\rangle \\
&\qquad + \langle l|W\otimes\overline{W}|r\rangle + 2\pi\delta(p)\langle l|\mathbb{1}\otimes\overline{V}+R\otimes\overline{W}\,|r\rangle\,\langle l|\,V\otimes\mathbb{1}+W\otimes\overline{R}|r\rangle\Bigg].
\end{aligned} \tag{1.14}$$

The singular term for momentum $p = 0$ inside the square brackets can be traced back to the non-orthogonality of the $|\Phi_p(V,W)\rangle$ with the ground state $|\Psi(Q,R)\rangle$, which is given by $\langle\Psi(Q,R)|\Phi_p(V,W)\rangle = 2\pi\delta(p)\langle l|\mathbb{1}\otimes\overline{V}+R\otimes\overline{W}\,|r\rangle$. For topologically trivial excitations at momentum zero, we henceforth restrict to V and W which satisfy $\langle l|\mathbb{1}\otimes\overline{V}+R\otimes\overline{W}\,|r\rangle = 0$, so that this singular term vanishes.

The gauge freedom in the cMPS parametrization induces a redundancy in the parametrization of the states $|\Phi_p(V,W)\rangle$, *i.e.* these states are invariant under the additive gauge transformation $V \leftarrow V + Q_1X - XQ_2 + \mathrm{i}pX$ and $W \leftarrow W + R_1X - XR_2$ for $X \in \mathfrak{gl}(D) = \mathbb{C}^{D\times D}$. This gauge freedom can be used to choose a parametrization that allows us omit the non-local terms in the expressions above, *e.g.* by restriction to representations (V,W) that satisfy

$$\langle l_1|\Big(V\otimes\mathbb{1}+W\otimes\overline{R}_1\Big) = 0. \tag{1.15}$$

This condition is henceforth referred to as the *left gauge condition*. Similarly one can choose instead a right gauge condition by imposing $\Big(V\otimes\mathbb{1}+W\otimes\overline{R}_2\Big)|r_2\rangle = 0$. With this, Eq. (1.12) reduces to the local expression

$$\langle\Phi_p(\overline{V},\overline{W})|\Phi_{p'}(V,W)\rangle = 2\pi\delta(p-p')\langle l_1|W\otimes\overline{W}|r_2\rangle \tag{1.16}$$

for the topologically trivial and non-trivial cases alike. Note however the subtle difference between both cases. In the topologically non-trivial case (inequivalent ground states $|\Psi(Q_1,R_1)\rangle$ and $|\Psi(Q_2,R_2)\rangle$), it is really all D^2 gauge degrees of freedom in X that are used to impose D^2 equations that are encoded by the left or right gauge condition. For the topologically trivial case, this is still true for momenta $p \neq 0$. However, at momentum zero the choice $X = \mathbb{1}$ does not induce any transformation at all, and the gauge transformations can only be used to fulfil $D^2 - 1$ conditions. The remaining requirement is $\langle l|\mathbb{1}\otimes\overline{V}+R\otimes\overline{W}\,|r\rangle = 0$, which expresses orthogonality to the ground state and cannot be imposed by a mere gauge transform. Hence, the left or right gauge condition automatically include the restriction of orthogonality to the ground state for topologically trivial excitations with momentum $p = 0$.

Next we will calculate the expectation value of the terms in the Hamiltonian. Evaluating these expressions will involve more integrals of the form $\int_0^{+\infty} \mathrm{e}^{x(T_{ab}\pm \mathrm{i}p)}\,\mathrm{d}x$ or $\int_0^{+\infty} \mathrm{e}^{xT_{aa}}\,\mathrm{d}x$, and we now introduce the general notation $(T_{ab} \pm \mathrm{i}p)^{\mathsf{P}}$, which is defined as the inverse of $T_{ab} \pm \mathrm{i}p$ in the complement of the zero eigenspace of T_{ab} (which is the whole space $\mathbb{C}^{D^2}$ if T_{ab} doesn't have a zero eigenvalue). When acting with the left or right zero eigenvector of T_{ab} on $(T_{ab} \pm \mathrm{i}p)^{\mathsf{P}}$, it reduces to zero. We will always be able to cancel all singular contributions, either by using the fact that we choose $\langle l|\mathbb{1}\otimes\overline{V} + R\otimes\overline{W}\,|r\rangle = 0$ in the case of topologically trivial excitations at momentum zero or by subtracting the ground state energy. Let us elaborate on the latter. There will be contributions where the local operators in the Hamiltonian do not act directly on the perturbation V and W. However, the nonlocal effect of this perturbation is expressed by the fact that there is a transfer matrix connecting that Hamiltonian term to the perturbation. The regular part of this transfer matrix is actually responsible for the genuine nonlocal effect of the perturbation, whereas the singular part contains the projection $|r\rangle\langle l|$ and just returns the ground state energy density with a singular volume integral. It is only at the very end, by subtracting the total ground state energy (*i.e.* the energy density times the volume) that these singular contributions disappear. This also requires that $|\Psi(Q_1,R_1)\rangle$ and $|\Psi(Q_2,R_2)\rangle$ have identical energy densities in the case of topologically nontrivial excitations. However, keeping in mind this final step, we will not include these singular contributions in the expressions below. Note that the use of the left gauge condition allows to omit additional non-singular terms.

The expectation value of the density operator is obtained by computing the overlap of Eq. (1.9) with itself

$$\begin{aligned}
&\int_{-\infty}^{\infty} \mathrm{d}x\, \langle \Phi_p(\overline{V},\overline{W})|\hat{\psi}^\dagger(x)\hat{\psi}(x)|\Phi_{p'}(V,W)\rangle = 2\pi\delta(p-p')\times \\
&\Big\{\langle l_1|\Big[R_1\otimes\overline{R}_1\Big(-T_{11}\Big)^{\mathsf{P}}W\otimes\overline{W} + W\otimes\overline{W}\Big(-T_{22}\Big)^{\mathsf{P}}R_2\otimes\overline{R}_2 \\
&\quad + R_1\otimes\overline{R}_1\Big(-T_{11}\Big)^{\mathsf{P}}\Big(V\otimes\mathbb{1} + W\otimes\overline{R}_1\Big)\Big(-T_{21}+\mathrm{i}p\Big)^{\mathsf{P}}\Big(\mathbb{1}\otimes\overline{V} + R_2\otimes\overline{W}\Big) \\
&\quad + R_1\otimes\overline{R}_1\Big(-T_{11}\Big)^{\mathsf{P}}\Big(\mathbb{1}\otimes\overline{V} + R_1\otimes\overline{W}\Big)\Big(-T_{12}-\mathrm{i}p'\Big)^{\mathsf{P}}\Big(V\otimes\mathbb{1} + W\otimes\overline{R}_2\Big) \\
&\quad + R_1\otimes\overline{W}\Big(-T_{12}-\mathrm{i}p'\Big)^{\mathsf{P}}\Big(V\otimes\mathbb{1} + W\otimes\overline{R}_2\Big) \\
&\quad + W\otimes\overline{R}_1\Big(-T_{21}+\mathrm{i}p\Big)^{\mathsf{P}}\Big(\mathbb{1}\otimes\overline{V} + R_2\otimes\overline{W}\Big) + W\otimes\overline{W}\Big]|r_2\rangle\Big\}\,. \qquad (1.17)
\end{aligned}$$

The expectation value of the interaction energy of the δ-interaction is calculated similarly by taking the overlap of Eq. (1.10) in the limit $z \to y$,

$$\begin{aligned}
&\int_{-\infty}^{\infty} \mathrm{d}x\, \langle \Phi_p(\overline{V},\overline{W})|\hat{\psi}^\dagger(x)\hat{\psi}^\dagger(x)\hat{\psi}(x)\hat{\psi}(x)|\Phi_{p'}(V,W)\rangle = 2\pi\delta(p-p')\times \\
&\Big\{\langle l_1|\Big[R_1^2\otimes\overline{R}_1^2\Big(-T_{11}\Big)^{\mathsf{P}} W\otimes\overline{W} + W\otimes\overline{W}\Big(-T_{22}\Big)^{\mathsf{P}} R_2^2\otimes\overline{R}_2^2 \\
&\quad + R_1^2\otimes\overline{R}_1^2\Big(-T_{11}\Big)^{\mathsf{P}}\Big(V\otimes\mathbb{1}+W\otimes\overline{R}_1\Big)\Big(-T_{21}+\mathrm{i}p\Big)^{\mathsf{P}}\Big(\mathbb{1}\otimes\overline{V}+R_2\otimes\overline{W}\Big) \\
&\quad + R_1^2\otimes\overline{R}_1^2\Big(-T_{11}\Big)^{\mathsf{P}}\Big(\mathbb{1}\otimes\overline{V}+R_1\otimes\overline{W}\Big)\Big(-T_{12}-\mathrm{i}p'\Big)^{\mathsf{P}}\Big(V\otimes\mathbb{1}+W\otimes\overline{R}_2\Big) \\
&\quad + R_1^2\otimes(\overline{R}_1\overline{W}+\overline{W}\,\overline{R}_2)\Big(-T_{12}-\mathrm{i}p'\Big)^{\mathsf{P}}\Big(V\otimes\mathbb{1}+W\otimes\overline{R}_2\Big) \\
&\quad + (R_1W+WR_2)\otimes\overline{R}_1^2\Big(-T_{21}+\mathrm{i}p\Big)^{\mathsf{P}}\Big(\mathbb{1}\otimes\overline{V}+R_2\otimes\overline{W}\Big) \\
&\quad + (R_1W+WR_2)\otimes(\overline{R}_1\overline{W}+\overline{W}\,\overline{R}_2)\Big]|r_2\rangle\Big\}\,. \qquad (1.18)
\end{aligned}$$

For the kinetic energy we evaluate the overlap of Eq. (1.11),

$$\begin{aligned}
&\int_{-\infty}^{\infty} \mathrm{d}x\, \langle \Phi_p(\overline{V},\overline{W})|\frac{d\hat{\psi}^\dagger(x)}{dx}\frac{d\hat{\psi}(x)}{dx}|\Phi_{p'}(V,W)\rangle = 2\pi\delta(p-p')\times \\
&\Big\{\langle l_1|\Big[[Q_1,R_1]\otimes[\overline{Q}_1,\overline{R}_1]\Big(-T_{11}\Big)^{\mathsf{P}} W\otimes\overline{W} + W\otimes\overline{W}\Big(-T_{22}\Big)^{\mathsf{P}}[Q_2,R_2]\otimes[\overline{Q}_2,\overline{R}_2] \\
&+ [Q_1,R_1]\otimes[\overline{Q}_1,\overline{R}_1]\Big(-T_{11}\Big)^{\mathsf{P}}\Big(V\otimes\mathbb{1}+W\otimes\overline{R}_1\Big)\Big(-T_{21}+\mathrm{i}p\Big)^{\mathsf{P}}\Big(\mathbb{1}\otimes\overline{V}+R_2\otimes\overline{W}\Big) \\
&+ [Q_1,R_1]\otimes[\overline{Q}_1,\overline{R}_1]\Big(-T_{11}\Big)^{\mathsf{P}}\Big(\mathbb{1}\otimes\overline{V}+R_1\otimes\overline{W}\Big)\Big(-T_{12}-\mathrm{i}p'\Big)^{\mathsf{P}}\Big(V\otimes\mathbb{1}+W\otimes\overline{R}_2\Big) \\
&+ (Q_1W-WQ_2)\otimes[\overline{Q}_1,\overline{R}_1]\Big(-T_{21}+\mathrm{i}p\Big)^{\mathsf{P}}\Big(\mathbb{1}\otimes\overline{V}+R_2\otimes\overline{W}\Big) \\
&+ ((VR_2-R_1V)+\mathrm{i}pW)\otimes[\overline{Q}_1,\overline{R}_1]\Big(-T_{21}+\mathrm{i}p\Big)^{\mathsf{P}}\Big(\mathbb{1}\otimes\overline{V}+R_2\otimes\overline{W}\Big) \\
&+ [Q_1,R_1]\otimes(\overline{Q}_1\overline{W}-\overline{W}\overline{Q}_2)\Big(-T_{12}-\mathrm{i}p'\Big)^{\mathsf{P}}\Big(V\otimes\mathbb{1}+W\otimes\overline{R}_2\Big) \\
&+ [Q_1,R_1]\otimes((\overline{V}\,\overline{R}_2-\overline{R}_1\overline{V})-\mathrm{i}p\overline{W})\Big(-T_{12}-\mathrm{i}p'\Big)^{\mathsf{P}}\Big(V\otimes\mathbb{1}+W\otimes\overline{R}_2\Big) \\
&+ ((Q_1W-WQ_2)+(VR_2-R_1V)+\mathrm{i}pW)\otimes(\overline{Q}_1\overline{W}-\overline{W}\overline{Q}_2) \\
&+ ((Q_1W-WQ_2)+(VR_2-R_1V)+\mathrm{i}pW)\otimes((\overline{V}\,\overline{R}_2-\overline{R}_1\overline{V})-\mathrm{i}p\overline{W})\Big]|r_2\rangle\Big\}. \qquad (1.19)
\end{aligned}$$

Finally we calculate the expectation values of the pairing terms which appear in the non-integrable Hamiltonian introduced in this paper.

$$\begin{aligned}
&\int_{-\infty}^{\infty} \mathrm{d}x\, \langle \Phi_p(\overline{V},\overline{W})|\hat{\psi}^\dagger(x)\hat{\psi}^\dagger(x)|\Phi_{p'}(V,W)\rangle = 2\pi\delta(p-p')\times \\
&\quad\Big\{\langle l_1|\Big[\mathbb{1}\otimes\overline{R}_1^2\Big(-T_{11}\Big)^{\mathsf{P}} W\otimes\overline{W} + W\otimes\overline{W}\Big(-T_{22}\Big)^{\mathsf{P}}\mathbb{1}\otimes\overline{R}_2^2 \\
&\qquad + \mathbb{1}\otimes\overline{R}_1^2\Big(-T_{11}\Big)^{\mathsf{P}}\Big(V\otimes\mathbb{1}+W\otimes\overline{R}_1\Big)\Big(-T_{21}+\mathrm{i}p\Big)^{\mathsf{P}}\Big(\mathbb{1}\otimes\overline{V}+R_2\otimes\overline{W}\Big) \\
&\qquad + \mathbb{1}\otimes\overline{R}_1^2\Big(-T_{11}\Big)^{\mathsf{P}}\Big(\mathbb{1}\otimes\overline{V}+R_1\otimes\overline{W}\Big)\Big(-T_{12}-\mathrm{i}p'\Big)^{\mathsf{P}}\Big(V\otimes\mathbb{1}+W\otimes\overline{R}_2\Big) \\
&\qquad + \mathbb{1}\otimes(\overline{R}_1\overline{W}+\overline{W}\,\overline{R}_2)\Big(-T_{12}-\mathrm{i}p'\Big)^{\mathsf{P}}\Big(V\otimes\mathbb{1}+W\otimes\overline{R}_2\Big)\Big]|r_2\rangle\Big\} \qquad (1.20)
\end{aligned}$$

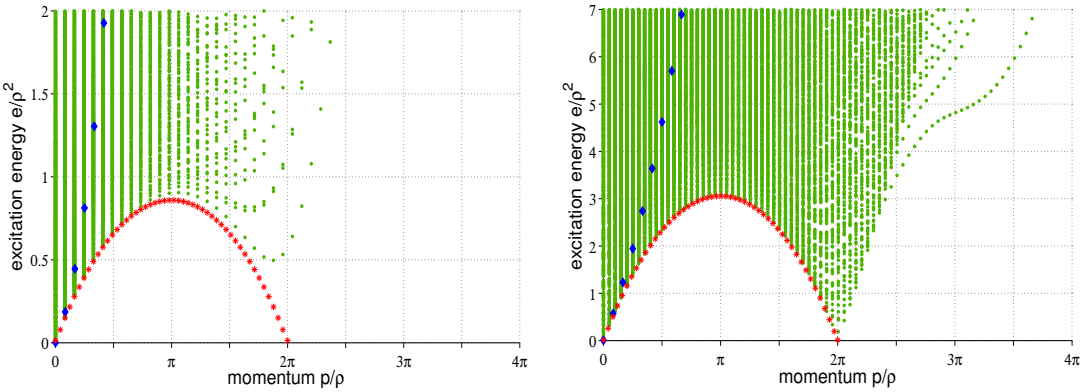

Figure 1.5: Dispersion relation for the Lieb-Liniger model with $D = 64$ for $\gamma = c/\rho \approx 0.1$ and $\gamma \approx 1.35$ (top to bottom). Bulk excitations (dots) and blue diamonds (Type I) are trivial excitations. Red stars (Type II) are obtained by combining momenta and energy of two topological excitations (hole and particle).

$$\int_{-\infty}^{\infty} \mathrm{d}x\, \langle \Phi_p(\overline{V},\overline{W})|\hat{\psi}(x)\hat{\psi}(x)|\Phi_{p'}(V,W)\rangle = 2\pi\delta(p-p')\times$$
$$\Big\{\langle l_1|\Big[R_1^2\otimes\mathbb{1}\Big(-T_{11}\Big)^{\mathsf{P}}W\otimes\overline{W}+W\otimes\overline{W}\Big(-T_{22}\Big)^{\mathsf{P}}R_2^2\otimes\mathbb{1}$$
$$+R_1^2\otimes\mathbb{1}\Big(-T_{11}\Big)^{\mathsf{P}}\Big(V\otimes\mathbb{1}+W\otimes\overline{R}_1\Big)\Big(-T_{21}+\mathrm{i}p\Big)^{\mathsf{P}}\Big(\mathbb{1}\otimes\overline{V}+R_2\otimes\overline{W}\Big)$$
$$+R_1^2\otimes\mathbb{1}\Big(-T_{11}\Big)^{\mathsf{P}}\Big(\mathbb{1}\otimes\overline{V}+R_1\otimes\overline{W}\Big)\Big(-T_{12}-\mathrm{i}p'\Big)^{\mathsf{P}}\Big(V\otimes\mathbb{1}+W\otimes\overline{R}_2\Big)$$
$$+R_1^2\otimes(\overline{R}_1\overline{W}+\overline{W}\,\overline{R}_2)\Big(-T_{12}-\mathrm{i}p'\Big)^{\mathsf{P}}\Big(V\otimes\mathbb{1}+W\otimes\overline{R}_2\Big)\Big]|r_2\rangle\Big\} \qquad (1.21)$$

The above expressions define the effective Hamiltonian for the Lieb-Liniger model and for the non-integrable model. The explicit construction of the effective Hamiltonian is done by making use of the fact that these expressions are linear in V and W. This allows us to reshape them into the form $\langle V^\dagger W^\dagger|H_{\text{eff}}|VW\rangle$ and $\langle V^\dagger W^\dagger|N_{\text{eff}}|VW\rangle$. Since we impose the left gauge condition Eq. (1.15) we can parametrize V and W in terms of one single matrix $Y \in \mathbb{C}^{D\times D}$. We can choose a parametrization such that the effective norm matrix N_{eff} is the identity by setting $W = l_1^{-1/2} Y r_2^{-1/2}$ and $V = -l_1^{-1} R^\dagger l_1^{1/2} Y r_2^{-1/2}$, where we can also use a gauge for the cMPS such that $l_1 = \mathbb{1}$. This particular parametrization is useful since it transforms the generalised eigenvalue problem for the effective Hamiltonian into an ordinary one and allows for an efficient iterative implementation with computational cost of order $\mathcal{O}(D^3)$.

Finally, we briefly discuss our results for the Lieb-Liniger model in the weak coupling limit of small γ. It is well known that in this limit the mean-field approximation derived by Bogoliubov accurately describes the Type I excitations. We therefore expect to find this branch in the trivial spectrum of our ansatz (dots in Fig. 1.5) by looking for the excitation which has largest overlap with the state $\int_{-\infty}^{\infty} \mathrm{d}x\, \mathrm{e}^{\mathrm{i}px}\hat{\psi}^\dagger(x)|\Psi(Q,R)\rangle$. These excitations are shown by blue diamonds in Fig. 1.5 . However, the branch of Type II excitations is always found by combining two excitations of the topological spectrum (red stars in Fig. 1.5), irrespective of the interaction strength. The left plot of Fig. 1.5 clearly shows that for weak interaction the lowest branch of trivial excitations is separated by a large gap from the energy of the lowest topological excitation (red stars). This can be understood from the fact that the trivial ansatz badly describes unbound multi-particle excitations, as explained in the paper . For strong

interaction the particle number of the topological *hole* excitation is -1 and therefore also the trivial ansatz gives a fairly good description of the Type II branch (Fig. 1. in the paper). However, for small γ the topological *hole* excitation experiences a diverging particle number and the trivial ansatz is no longer able to accurately describe this excitation branch which leads to the large energy gap in Fig. 1.5.

Chapter 2

Quantum Gross-Pitaevskii Equation

Synopsis:

We introduce a non-commutative generalization of the Gross-Pitaevskii equation for one-dimensional quantum gasses and quantum liquids. This generalization is obtained by applying the time-dependent variational principle to the variational manifold of continuous matrix product states. This allows for a full quantum description of many body system —including entanglement and correlations— and thus extends significantly beyond the usual mean-field description of the Gross-Pitaevskii equation, which is known to fail for (quasi) one-dimensional systems.

Based on:

J. Haegeman, D. Draxler, V. Stojevic, J. Ignacio Cirac, T. J. Osborne , and F. Verstraete
e-print arXiv: 1501.06575, submitted to PRA: Rapid Communications

2.1 Introduction

In 1961, Gross and Pitaevskii developed the mean-field theory description of cold Bose gasses [45, 93, 46], which resulted in the ubiquitous Gross-Pitaevskii equation (GPE)

$$\mathrm{i}\frac{\partial\phi(\boldsymbol{x},t)}{\partial t} = (-\Delta + v(\boldsymbol{x}))\phi(\boldsymbol{x},t) + 2g|\phi(\boldsymbol{x},t)|^2\phi(\boldsymbol{x},t),$$

where $\phi(x,t)$ is the order parameter of the Bose-Einstein condensate in a trapping potential $v(x)$. Ever since, this equation constitutes the cornerstone for the theoretical description of cold atomic gasses [28, 94, 13]. Its success can be explained by the fact that the GPE agrees with the full quantum solution for the three-dimensional problem in the weak-density limit, which corresponds with the typical experimental setup of trapped dilute gasses (see Ref. [76] and references therein).

The GPE without trapping potential [$v(x) = 0$] is also known as the nonlinear Schrödinger equation and appears in several areas of theoretical physics as it offers a canonical description for slowly varying, quasi-monochromatic wave packets in dispersive, weakly nonlinear media [109, 2]. As such, it has also stimulated an abundance of mathematical research towards showing the stability of its (solitary wave) solutions [114, 125, 12], as well as towards the development of numerical integrators [111, 6, 78, 25, 113].

In the case of one spatial dimension [77, 16], as realized in highly elongated traps [5, 32, 29, 43, 61], both the GPE [129] and the full quantum mechanical problem known as the Lieb-Liniger model [75, 74, 128] are integrable for constant potential, but the respective solutions do not agree. One-dimensional Bose gasses have no condensation (only quasi long-range order) [89], show quasi-fermionic behavior [42, 84, 88, 67] and have excitations which cannot be predicted from Bogoliubov's theory [74, 82]. This behavior has no classical counterpart and is dominated by quantum correlations.

The current Letter develops a generalization of the one-dimensional GPE that takes quantum correlations into account. It is formulated in terms of non-commuting matrices and — following the typical nomenclature of integrable systems— is referred to as the *quantum Gross-Pitaevskii equation* (QGPE). The normal GPE can be derived by applying the Dirac-Frenkel time-dependent variational principle (TDVP) [30, 38, 70] to a variational mean field ansatz $|\Psi[\phi]\rangle$ in the canonical [$|\Psi[\phi]\rangle \sim (\int \phi(x)\hat{\psi}^\dagger(x)\,\mathrm{d}x)^N\,|\Omega\rangle$ for N particles] or grand-canonical [$|\Psi[\phi]\rangle \sim \mathrm{e}^{\int \phi(x)\hat{\psi}^\dagger(x)\,\mathrm{d}x}\,|\Omega\rangle$] ensemble, where $\hat{\psi}^\dagger(x)$ is the bosonic field creation operator in second quantization and $|\Omega\rangle$ is the Fock vacuum. For one-dimensional bosonic systems, the GPE is obtained by applying this ansatz to the Lieb Liniger Hamiltonian [75]

$$\hat{H} \;=\; \int \mathrm{d}x\, \frac{\mathrm{d}\hat{\psi}^\dagger}{\mathrm{d}x}(x)\frac{\mathrm{d}\hat{\psi}}{\mathrm{d}x}(x) + v(x)\hat{\psi}^\dagger(x)\hat{\psi}(x) + g\hat{\psi}^\dagger(x)\hat{\psi}^\dagger(x)\hat{\psi}(x)\hat{\psi}(x). \qquad (2.1)$$

The variational manifold of *continuous matrix product states* (cMPS) [119, 86, 49] can be seen as a generalization of this grand-canonical ansatz in which the variational function $\phi(x)$ is replaced by a matrix valued function $R(x)$:

$$|\Psi[R,\boldsymbol{v}_1,\boldsymbol{v}_2]\rangle = \boldsymbol{v}_1^\dagger \mathcal{P}\mathrm{e}^{\int_{x_1}^{x_2} R(x)\otimes\hat{\psi}^\dagger(x)\,\mathrm{d}x}\boldsymbol{v}_2\,|\Omega\rangle\,. \qquad (2.2)$$

Here $\mathcal{P}$ denotes the path-ordered exponential and $\boldsymbol{v}_{1,2}$ are D-dimensional boundary vectors. By choosing the bond dimensions $D = 1$, we clearly recover the mean field ansatz. The cMPS ansatz was conceived as a continuum limit of the matrix product state (MPS) ansatz [36, 87, 23], which underlies the highly successful density matrix renormalization group [127]

for the description of one-dimensional quantum spin systems. By enlarging the refinement parameter D, the exact quantum state can be increasingly well approximated. Indeed, the cMPS ansatz was shown to represent both the ground state [119] and the two types of elementary excitations [31] of the Lieb-Liniger model very well for moderate values of D. The goal of this paper is to apply the TDVP formalism to the cMPS manifold in order to derive the matrix or quantum analogue of the GPE.

2.2 Quantum Gross-Pitaevskii Equation

For a complex manifold, the TDVP can be understood as a replacement of Schrödinger's equation by

$$\mathrm{i}\frac{\mathrm{d}}{\mathrm{d}t}\left|\Psi\right\rangle = \hat{P}_\Psi \hat{H}\left|\Psi\right\rangle, \tag{2.3}$$

where P_Ψ is a projector onto the tangent space of the variational manifold at the point $|\Psi\rangle$. Whereas the Schrödinger equation would immediately take an initial state away from the variational manifold, this extra projector assures that the evolution remains within the manifold. The QGPE can thus be obtained by finding a time derivative $\partial_t R$ (and $\partial_t \boldsymbol{v}_{1,2}$) such that $\mathrm{d}\left|\Psi[R,\boldsymbol{v}_1,\boldsymbol{v}_2]\right\rangle/\mathrm{d}t$ has the same inner product as $\hat{H}\left|\Psi\right\rangle$ with any possible tangent vector. Using the expressions of tangent vectors and overlaps with Hamiltonians obtained in [49], we obtain [see Supplementary Material for details]

$$\begin{aligned}\mathrm{i}\partial_t R(x) = &\left(-\partial_x^2 + v(x)\right) R(x) \\ &+ g\left(\rho_L^{-1}(x)R^\dagger(x)\rho_L(x)\right)R^2(x) + gR^2(x)\left(\rho_R(x)R^\dagger(x)\rho_R^{-1}(x)\right) \\ &- \left(\rho_L^{-1}(x)R^\dagger(x)\rho_L(x)\right)[R(x),\partial_x R(x)] - [R(x),\partial_x R(x)]\left(\rho_R(x)R^\dagger(x)\rho_R^{-1}(x)\right)\end{aligned} \tag{2.4}$$

where $\rho_L(x)$ and $\rho_R(x)$ are $D\times D$ reduced density matrices defined by the equations

$$\rho_L(x_1) = \boldsymbol{v}_1\boldsymbol{v}_1^\dagger, \qquad \partial_x\rho_L(x) = R^\dagger(x)\rho_L(x)R(x), \tag{2.5a}$$

$$\rho_R(x_2) = \boldsymbol{v}_2\boldsymbol{v}_2^\dagger, \qquad -\partial_x\rho_R(x) = R(x)\rho_R(x)R^\dagger(x). \tag{2.5b}$$

Note that the original GPE can be read off from the first line of (2.4) for $D=1$, while the second line —involving a commutator $[R(x),\partial_x R(x)]$— has no mean field analogue. Since the non-vanishing of this term is tantamount to the presence of quantum correlations, it would be extremely interesting to investigate its physical consequences in more detail.

2.2.1 Gauge invariance

As is well known in the literature of MPS, efficient and robust algorithms make crucial use of gauge transforms, i.e. transformations of the kind $R(x)\to G^{-1}(x)R(x)G(x)$ for an arbitrary matrix function $G(x)$ that leaves the physics invariant. A manifestly gauge invariant QGPE is obtained by introducing two more $D\times D$ matrix valued functions $P(x)$ and $Q(x)$, which can be interpreted as the A_0 and A_1 components of a gauge potential. The spatial and temporal derivates are then replaced by covariant derivatives

$$\partial_x R(x) \to \mathcal{D}_x R(x) \equiv \partial_x R(x) + [Q(x),R(x)] \tag{2.6a}$$

$$\partial_t R(x) \to \mathcal{D}_t R(x) \equiv \partial_t R(x) + [P(x),R(x)]. \tag{2.6b}$$

and the cMPS acquires the conventional form [119]

$$|\Psi[Q,R,\boldsymbol{v}_1,\boldsymbol{v}_2]\rangle = \boldsymbol{v}_1^\dagger \mathcal{P}\mathrm{e}^{\int_{x_1}^{x_2} Q(x)\otimes\hat{I}+R(x)\otimes\hat{\psi}^\dagger(x)\,\mathrm{d}x}\boldsymbol{v}_2\,|\Omega\rangle\,.$$

The manifestly covariant QGPE becomes

$$\begin{aligned}\mathrm{i}\mathcal{D}_t R(x) = &\left(-\mathcal{D}_x^2 + v(x)\right)R(x)\\ &+ g\left(\rho_L^{-1}(x)R^\dagger(x)\rho_L(x)\right)R^2(x) + gR^2(x)\left(\rho_R(x)R^\dagger(x)\rho_R^{-1}(x)\right)\\ &- \left(\rho_L^{-1}(x)R^\dagger(x)\rho_L(x)\right)[R(x),\mathcal{D}_x R(x)] - [R(x),\mathcal{D}_x R(x)]\left(\rho_R(x)R^\dagger(x)\rho_R^{-1}(x)\right)\end{aligned} \tag{2.7}$$

in combination with a new equation for the time evolution of $Q(x)$

$$\begin{aligned}\mathrm{i}\partial_t Q(x) - \mathrm{i}\partial_x P(x) - \mathrm{i}[Q(x),P(x)] = &-\rho_L(x)^{-1}R(x)^\dagger\rho_L(x)\{gR(x)^2\\ &-[R(x),\mathcal{D}_x R(x)]\}\rho_R(x)R(x)^\dagger\rho_R(x)^{-1}.\end{aligned}$$

Note that the left hand side can be recognised as the only nonzero component $F_{0,1}$ of the antisymmetric field tensor. The defining equations for the density matrices $\rho_{L,R}$ are changed to $\partial_x\rho_L(x) = Q(x)^\dagger\rho_L(x) + \rho_L(x)Q(x) + R^\dagger(x)\rho_L(x)R(x)$ and similarly for $\rho_R(x)$. These equations as well as the corresponding cMPS are invariant under arbitrary x- and t-dependent gauge transformation $G(x,t) \in \mathsf{GL}(D)$

$$\begin{aligned}\rho_L(x,t) &\to G^\dagger(x,t)\rho_L(x,t)G(x,t)\\ \rho_R(x,t) &\to G^{-1}(x,t)\rho_R(x,t)G^{\dagger-1}(x,t)\\ R(x,t) &\to G^{-1}(x,t)R(x,t)G(x,t)\\ Q(x,t) &\to G^{-1}(x,t)\left(Q(x,t)+\partial_x\right)G(x,t)\\ P(x,t) &\to G^{-1}(x,t)\left(P(x,t)+\partial_t\right)G(x,t).\end{aligned} \tag{2.8}$$

A great benefit from working in this representation is that the matrices $R(x,t), Q(x,t), P(x,t)$ can be chosen to be independent of x for translational invariant systems, greatly reducing the complexity of integrating the QGPE. Furthermore, it allows to fix the cMPS to remain in e.g. the left canonical form $\rho_L(x,t) = \mathbb{1}$ [and thus $Q(x)^\dagger + Q(x) + R(x)^\dagger R(x) = 0$] by choosing $P(x) = -\mathrm{i}R^\dagger(x)\mathcal{D}_x R(x) + iF(x)$ with $F(x)$ a hermitian matrix. This $F(x)$ can be chosen freely in the case of real time evolution, but has to properly chosen in the case of imaginary time evolution. One particular choice is the solution of

$$\begin{aligned}\partial_x F - Q^\dagger F - FQ - R^\dagger FR = \\ (\mathcal{D}_x R)^\dagger(\mathcal{D}_x R) + v(x)R^\dagger R + g(R^\dagger)^2R^2\end{aligned} \tag{2.9}$$

which ensures that $\partial_t Q(x) + R(x)^\dagger\partial_t R(x) = 0$.

2.2.2 Boundary Conditions

For finite systems, the QGPE needs to be supplemented with appropriate boundary conditions to fully specify the problem. These will also affect the evolution equation for the boundary vectors $\boldsymbol{v}_{1,2}$, which we derive presently. As the TDVP can be obtained from extremizing an action, there are only two types of self-consistent boundary conditions (similar to *e.g.* the classical wave equation for a vibrating string), unless explicit boundary terms are included

in the Hamiltonian from Eq. (2.1). These can be derived by considering the quantized field operator $\hat{\psi}(x)$ and expressing stability with respect to variations of $\hat{\psi}^\dagger(x)$. When the value of $\hat{\psi}(x)$ is fixed at the boundaries, Dirichlet conditions are obtained:

$$\hat{\psi}(x_1) = a \qquad \Rightarrow \qquad \boldsymbol{v}_1^\dagger R(x_1) = a\boldsymbol{v}_1^\dagger, \tag{2.10a}$$

$$\hat{\psi}(x_2) = b \qquad \Rightarrow \qquad R(x_2)\boldsymbol{v}_2 = b\boldsymbol{v}_2. \tag{2.10b}$$

Alternatively homogenous Neumann or mixed boundary conditions could be used. While the resulting boundary conditions for the variational parameters R are inherently gauge invariant, they only correspond to D instead of D^2 equations each. In e.g. the case of Dirichlet conditions, they only fix one eigenvalue and eigenvector of the matrix R. In fact, the other directions of R at the boundary do not appear in physical expectation values and can thus not be fixed from physical considerations. In order to eliminate any interplay with the gauge transformation, we will 'promote' the boundary conditions in a gauge invariant manner by imposing them as identity matrix, e.g. $R(x_1) = a\mathbb{1}_D$ in the case of Eq. (2.10a). Note that there are no separate boundary condition on $Q(x)$, as these degrees of freedom can be interpreted as pure gauge degrees of freedom. The boundary conditions then also affect the TDVP equation for the boundary vectors. For the case of Dirichlet conditions [$R(x_1) = a\mathbb{1}_D$ and $R(x_2) = b\mathbb{1}_D$], we find

$$\mathrm{i}\partial_t \boldsymbol{v}_1^\dagger - \mathrm{i}\boldsymbol{v}_1^\dagger P(x_1) = -\overline{a}\boldsymbol{v}_1^\dagger \mathcal{D}_x R(x_1) \tag{2.11a}$$

$$\mathrm{i}\partial_t \boldsymbol{v}_2 + \mathrm{i}P(x_2)\boldsymbol{v}_2 = +\overline{b}\mathcal{D}_x R(x_2)\boldsymbol{v}_2 \tag{2.11b}$$

where the left hand side contains the covariant time derivative in the conjugate and fundamental representation, respectively. These equations are also valid for the Neumann conditions, where the right hand side becomes zero.

2.2.3 Symplectic structure

Let us now discuss in more detail the mathematical structure of the QGPE. Since it contains the quantities $\rho_{L,R}(x)$, which are defined by integrating Eq. (2.5), it forms a set of coupled non-linear partial integro-differential equations[1] containing first order time derivatives and second order space derivatives. It is a non-commutative generalization of the normal GPE in that it is defined in terms of matrix variables. Indeed, the normal GPE is recovered from Eq. (2.7) in the limit $D = 1$ by setting $R(x) = \phi(x)$ and observing that commutators then vanish. In that limit, $\int_{x_1}^{x_2} Q(x)\,\mathrm{d}x$ acts as on overall scalar factor (norm and phase) that can be absorbed in the boundaries.

Just like the normal GPE and essentially any TDVP equation, the real-time QGPE evolution forms a classical Hamiltonian system where $\langle\Psi[\overline{Q}, \overline{R}, \overline{\boldsymbol{v}}_1, \overline{\boldsymbol{v}}_2]|\hat{H}|\Psi[Q, R, \boldsymbol{v}_1, \boldsymbol{v}_2]\rangle$ plays the role of the classical Hamiltonian, and is a constant of motion when $\hat{H}$ is time-independent. The symplectic structure comes for free since any complex submanifold of Hilbert space is automatically Kähler, with the metric determined by the physical overlap of two tangent vectors. When using the QGPE with imaginary time evolution $t \to -\mathrm{i}\tau$ to find a cMPS approximation for the quantum ground state, this symplectic structure is of course lost and the energy expectation value decreases monotonically until convergence.

[1] One can also formulate time evolution differential equations for $\rho_{L,R}(x)$ in order to make it into a larger set of ordinary non-linear partial differential equations.

2.2.4 Numerical integration

Developing a stable numerical integration scheme for the QGPE is challenging. Firstly, there are the inherent complexities associated with solving a set of non-linear partial integro-differential equations. Because of the second order spatial derivative and first order time derivative, the Courant-Friedrichs-Levy condition limits the time step of explicit schemes. A typical workaround for the GPE is to use a splitting scheme [111, 78, 113], where the evolution is decomposed into the local terms (external potential and interaction) and the kinetic term. The linearity of the latter allows for a solution using a Crank-Nicolson method [27] or in Fourier space [57]. While the QGPE is still linear in the second order spatial derivative, it has non-linear terms containing first-order spatial derivatives, which cannot easily be integrated in Fourier space.

Another complication of the QGPE, as formulated in Eq. (2.11), is that it depends on the inverses of the density matrices $\rho_L(x)$ and $\rho_R(x)$. These become rank deficient near respectively the left and right boundary, as is clear from the definition in Eq. (2.5). It is well known in the tensor network community that the gauge degrees of freedom in the underlying matrix product state have to be exploited to transform these density matrices into identity matrices [102]. This was implemented only recently for the TDVP equation for matrix product states [47], using a non-trivial decomposition of the tangent space projector that allows to split the non-linear differential equation for all variables into a set of linear differential equations for the individual MPS tensors [51], which is made possible by the fact that the MPS parameterization is multilinear. Here too, we have to face complications introduced by the intrinsic nonlinearity in the cMPS parameterization. A final challenge is to develop suitable continuum analogous of the factorization routines such as the QR- or singular value decomposition, which are exploited in the MPS simulations to robustly implement the required gauge transformations. Note, in addition, that in order to exploit gauge freedom, the discretization of the QGPE should not break gauge invariance. Hereto, ideas from lattice gauge theory can serve as inspiration. In the translation invariant setting (when Q and R become x-independent matrices), several of these difficulties disappear.

2.3 Quantum Bogoliubov-de Gennes equations

In the case of small perturbations around a translational invariant Hamiltonian, it might therefore be useful to linearize the QGPE around the translation invariant cMPS. The ensuing equations are "quantum" versions of the Bogoliubov-de Gennes equations. As an example, let us assume that we have found a variational minimum R_0, Q_0 and corresponding $\rho_{L0} = \hat{I}$ and ρ_{R0} for the ground state of a translation invariant Hamiltonian H_0. We now wish to study the response of the system when applying an external potential $\epsilon V(x,t)$. We can readily expand the arguments of the QGPE (2.11) to first order $R(x,t) = R_0 + \epsilon\tilde{R}(x,t)$, $Q(x,t) = Q_0 + \epsilon\tilde{R}(x,t)$, $\rho_R(x,t) = \rho_{R0} + \epsilon\tilde{\rho}_R(x,t)$ and obtain linear equations for all new variables. As the QGPE mixes R with its conjugate, the corresponding equations decouple all different Fourier modes from each other except those with opposite momenta, leading to a simple linear set of equations with $2D^2$ unknowns. In particular, if we consider a time-dependent perturbation of the form $\hat{H}_1 = \int dx v(t)\cos(kx - \omega t)\,\psi^\dagger(x)\psi(x)$, the equation for $\tilde{R} = e^{\mathrm{i}(kx-\omega t)}R_+ + e^{-\mathrm{i}(kx-\omega t)}R_-$ becomes [1]

$$\begin{bmatrix} \omega & 0 \\ 0 & -\omega \end{bmatrix} \begin{bmatrix} R_+ \\ R_-^\dagger \end{bmatrix} = \begin{bmatrix} H_{\text{eff}} & M_{\text{eff}} \\ M_{\text{eff}}^\dagger & H_{\text{eff}} \end{bmatrix} \begin{bmatrix} R_+ \\ R_-^\dagger \end{bmatrix} + \begin{bmatrix} v_1 \\ v_2 \end{bmatrix}. \tag{2.12}$$

[1] See Supplementary Material for further details.

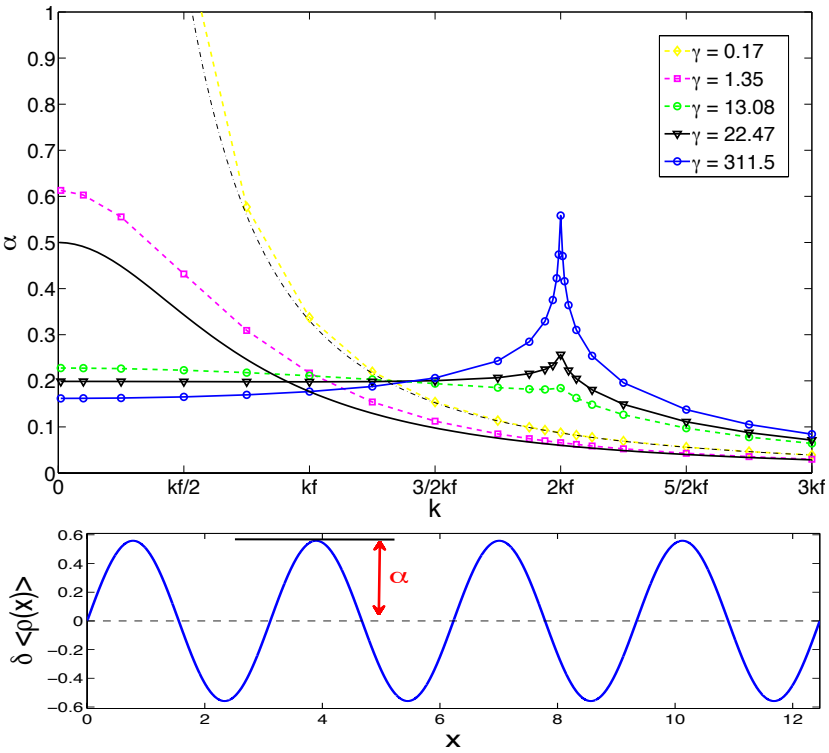

Figure 2.1: Top: The response amplitude for different values of $\gamma = g/\rho$ as a function of the momentum k. The dashed and solid line without markers are the classical Bogoliubov results for $\gamma = 0.17$ and $\gamma = 1.35$ respectively. Bottom: Density fluctuation at $\gamma = 311.5$ and $k = 2k_{\mathrm{F}}$. All calculations in both panels were done with cMPS bond dimension $D = 64$.

The matrix appearing on the right hand side of the above expression is (the momentum $\pm k$ block of) the Hessian of the energy functional $E(\overline{R}_0, \overline{Q}_0, R_0, Q_0) = \langle \Psi[\overline{Q}_0, \overline{R}_0] | \hat{H}_0 | \Psi[Q_0, R_0] \rangle$, whereas the inhomogeneous vector $\begin{bmatrix} v_1 & v_2 \end{bmatrix}$ contains the driving terms from $\hat{H}_1$. Note that Eq. (2.12) reduces to a normal eigenvalue problem when $\hat{H}_1 = 0$ and is related to the ansatz for excitations introduced in Ref. [31], which is capable of faithfully reproducing Type II Lieb-Liniger excitations.

As an application, we calculate the change in particle density on top of translation invariant Lieb Liniger solutions, for different values of the interaction strength g, and as a function of a small static ($\omega = 0$) perturbation with varying wave vector k. As can be observed from the results in Fig. 2.1, a strong response around $k = 2k_F$ is present for the case of strong interactions ($\gamma = g/\rho \gg 1$) which should be observable in experiments akin to those of Refs. [33, 35, 80]. This response cannot be explained using standard GPE, as interactions are a key ingredient for exciting Type II excitations.

2.4 Outlook and conclusion

We have developed a natural generalization of the GPE based on the formalism of cMPS suited for the study of one-dimensional quantum systems where entanglement plays an important role and the mean-field ansatz underlying the GPE is not justified. While it would be interesting to have a complete mathematical study of the existence, uniqueness (up to gauge transformations) and stability of the solutions of the QGPE for given boundary conditions, this is beyond the

goal and scope of this paper. It would also be enlightening to investigate whether there exist quantum generalization of certain exact solutions of the GPE, such as the dark soliton solution, and how they relate to the integrability of the full Lieb-Liniger Hamiltonian or to the topological excitations constructed using the related ansatz of Ref. [31]. Note that integrable matrix versions of the GPE were already formulated for the mean-field description of multicomponent Bose-Einstein condensates [115, 62, 1]. In addition, it would be instructive to compare the predictions of the QGPE to existing beyond-mean field studies such as e.g. Ref. [97].

As the cMPS ansatz is a versatile variational ansatz that can readily be extended to bosonic and fermionic systems with *e.g.* multiple particle species [48, 49, 98, 22], the QGPE equations generalize straightforwardly to such systems. Moreover, the approach described in this paper is in no way restricted to the Lieb-Liniger Hamiltonian, but is applicable to arbitrary Hamiltonians in one spatial dimension. cMPS methods have already been used to study (1+1) dimensional relativistic theories for fermions [48] and bosons [108] in a translationally invariant setting. Using the regularisation method described in Ref. [108], the derivation of the QGPE presented in this paper extends straightforwardly to such systems, enabling in principle the study of general bosonic non-linear σ-models with boundaries. Non-linear σ-models are of significant interest for the high energy physics community, for example, providing the underlying description of bosonic strings [37, 44] propagating on curved backgrounds. Given that cMPS methods are intrinsically non-perturbative, the approach of this paper has the potential to be particularly useful in the study of such models in the limit of large curvature, when perturbative quantization schemes fail. It is furthermore very encouraging that the implementation of Dirichlet and Neumann conditions in the quantum theory is straightforward, and we thus expect that the boundary condition implementation described in this paper can be used "as is" for the description of strings with either freely propagating endpoints, or with endpoints restricted to lie on D-branes [95, 96]. Finally, a challenging open problem would be to construct a higher-dimensional generalization of this QGPE. This would arise as the TDVP equation for the variational set of continuous projected-entangled pair states [66, 65], which are less well studied and understood.

2.5 Supplementary Material

2.5.1 Derivation of the quantum Gross-Pitaevskii equation

We start from the fully generic cMPS definition

$$|\Psi[Q,R,\boldsymbol{v}_1,\boldsymbol{v}_2]\rangle = \boldsymbol{v}_1^\dagger \mathcal{P}\mathrm{e}^{\int_{x_1}^{x_2} Q(x)\otimes\hat{1}+R(x)\otimes\hat{\psi}^\dagger(x)\,\mathrm{d}x}\boldsymbol{v}_2\,|\Omega\rangle \tag{2.13}$$

with virtual dimension D, and the Lieb-Liniger Hamiltonian

$$\hat{H} = \int_{x_1}^{x_2} \mathrm{d}x\, \frac{\mathrm{d}\hat{\psi}^\dagger}{\mathrm{d}x}(x)\frac{\mathrm{d}\hat{\psi}}{\mathrm{d}x}(x) + v(x)\hat{\psi}^\dagger(x)\hat{\psi}(x) + g\hat{\psi}^\dagger(x)\hat{\psi}^\dagger(x)\hat{\psi}(x)\hat{\psi}(x). \tag{2.14}$$

The energy expectation value was computed in Refs. [49, 119] and is given by

$$\begin{aligned}\langle\Psi|\hat{H}|\Psi\rangle = \int \mathrm{d}x\ \langle\rho_L(x)|&\mathcal{D}_x R(x)\otimes\overline{\mathcal{D}_x R(x)}\\ &+ v(x)R(x)\otimes\overline{R(x)} + gR(x)^2\otimes\overline{R(x)}^2\,|\rho_R(x)\rangle\end{aligned} \tag{2.15}$$

with the left and right density matrices $\rho_L(x)$ and $\rho_R(x)$ defined by

$$\rho_L(x_1) = \boldsymbol{v}_1\boldsymbol{v}_1^\dagger, \quad \frac{\mathrm{d}\rho_L}{\mathrm{d}x}(x) = Q(x)^\dagger\rho_L(x) + \rho_L(x)Q(x) + R(x)^\dagger\rho_L(x)R(x), \tag{2.16a}$$

$$\rho_R(x_2) = \boldsymbol{v}_2\boldsymbol{v}_2^\dagger, \quad \frac{\mathrm{d}\rho_R}{\mathrm{d}x}(x) = -[Q(x)\rho_R(x) + \rho_R(x)Q(x)^\dagger + R(x)\rho_R(x)R(x)^\dagger] \tag{2.16b}$$

and with

$$\mathcal{D}_x R(x) = \frac{\mathrm{d}R}{\mathrm{d}x}(x) + [Q(x), R(x)] \tag{2.17}$$

the spatial covariant derivative of R(x).

To facilitate the rest of the derivation, we also introduce the notation $\hat{M}(y,z) = \mathcal{P}\mathrm{e}^{\int_y^z \mathrm{d}x\, Q(x)\otimes\hat{1}+R(x)\otimes\hat{\psi}^\dagger(x)}$. A general tangent vector is obtained by computing the variation in the state $|\Psi[Q,R,\boldsymbol{v}_1,\boldsymbol{v}_2]\rangle$ under a generic variation $Q(x)\to Q(x)+\delta Q(x)$, $R(x)\to R(x)+\delta R(x)$, $\boldsymbol{v}_{1,2}\to\boldsymbol{v}_{1,2}+\delta\boldsymbol{v}_{1,2}$. The result is denoted as the state $|\Phi\rangle$ given by

$$\begin{aligned}|\Phi[\delta Q,\delta R,\delta\boldsymbol{v}_1,\delta\boldsymbol{v}_2]\rangle = \int_{x_1}^{x_2} &\boldsymbol{v}_1^\dagger\hat{M}(x_1,x)\big[\delta Q(x)\otimes\hat{1} + \delta R(x)\otimes\hat{\psi}^\dagger(x)\big]\hat{M}(x,x_2)\,|\Omega\rangle\ \mathrm{d}x\\ &+\delta\boldsymbol{v}_1^\dagger\hat{M}(x_1,x_2)\boldsymbol{v}_2\,|\Omega\rangle + \boldsymbol{v}_1^\dagger\hat{M}(x_1,x_2)\delta\boldsymbol{v}_2\,|\Omega\rangle\,.\end{aligned} \tag{2.18}$$

To properly deal with the boundary conditions, it is useful to derive the QGPE following the general recipe of the TDVP, i.e. as the Euler-Lagrange equations corresponding to extremizing the classical action

$$S[Q,R,\boldsymbol{v}_1,\boldsymbol{v}_2] = \int \mathrm{d}t \int_{x_1}^{x_2} \mathrm{d}x\ \langle\Psi[\overline{Q},\overline{R},\overline{\boldsymbol{v}}_1,\overline{\boldsymbol{v}}_2]|\mathrm{i}\frac{\mathrm{d}}{\mathrm{d}t} - \hat{H}|\Psi[Q,R,\boldsymbol{v}_1,\boldsymbol{v}_2]\rangle \tag{2.19}$$

We can easily derive the Euler-Lagrange equations by considering variations with respect to the complex conjugates of the variational parameters, which are treated as independent and appear only in the bra. Using our definition of tangent vectors, this immediately leads to the condition (using dots for time derivatives)

$$\mathrm{i}\,\langle\Phi[\overline{\delta Q},\overline{\delta R},\overline{\delta\boldsymbol{v}_1},\overline{\delta\boldsymbol{v}_2}]|\Phi[\dot{Q},\dot{R},\dot{\boldsymbol{v}}_1,\dot{\boldsymbol{v}}_2]\rangle = \langle\Phi[\overline{\delta Q},\overline{\delta R},\overline{\delta\boldsymbol{v}_1},\overline{\delta\boldsymbol{v}_2}]|\hat{H}|\Psi[Q,R,\boldsymbol{v}_1,\boldsymbol{v}_2]\rangle \tag{2.20}$$

for any possible variation. This is indeed equivalent to the geometric formulation of the TDVP in Eq. (3) of the main text. More generally, it tells us that we can find the tangent space projection $|\Phi[V, W, \boldsymbol{w}_1, \boldsymbol{w}_2]\rangle = \hat{P}_\Psi |\Theta\rangle$ of an arbitrary state $|\Theta\rangle$ —not necessarily $\hat{H}|\Psi[Q, R, \boldsymbol{v}_1, \boldsymbol{v}_2]\rangle$— by choosing $V(x)$, $W(x)$ and $\boldsymbol{w}_{1,2}$ such that

$$\langle \Phi[\overline{V}', \overline{W}', \overline{\boldsymbol{w}}_1', \overline{\boldsymbol{w}}_2']|\Phi[V, W, \boldsymbol{w}_1, \boldsymbol{w}_2]\rangle = \langle \Phi[\overline{V}', \overline{W}', \overline{\boldsymbol{w}}_1', \overline{\boldsymbol{w}}_2']|\Theta\rangle \tag{2.21}$$

for all possible $\overline{V}'(x) = \overline{\delta Q}(x)$, $\overline{W}'(x) = \overline{\delta R}(x)$ and $\overline{\boldsymbol{w}}_{1,2}' = \overline{\delta \boldsymbol{v}}_{1,2}$. The left hand side contains the overlap of two different tangent vectors and is given by

$$\begin{aligned}
\langle \Phi[V', W', \boldsymbol{w}_1', \boldsymbol{w}_2']|\Phi[V, W, \boldsymbol{w}_1, \boldsymbol{w}_2]\rangle = &\int_{x_1}^{x_2} \mathrm{d}x\ \langle \rho_L(x)|W(x) \otimes \overline{W}'(x)|\rho_R(x)\rangle \\
&+ \int_{x_1}^{x_2} \mathrm{d}x \int_x^{x_2} \mathrm{d}y\, \langle \rho_L(x)|\left(V(x) \otimes \mathbb{1} + W(x) \otimes \overline{R}(x)\right) E(x, y) \\
&\qquad \times \left(\mathbb{1} \otimes \overline{V}'(y) + R(y) \otimes \overline{W}'(y)\right)|\rho_R(y)\rangle \\
&+ \int_{x_1}^{x_2} \mathrm{d}x \int_{x_1}^{x} \mathrm{d}y\, \langle \rho_L(y)|\left(\mathbb{1} \otimes \overline{V}'(y) + R(y) \otimes \overline{W}'(y)\right) E(y, x) \\
&\qquad \times \left(V(x) \otimes \mathbb{1} + W(x) \otimes \overline{R}(x)\right)|\rho_R(x)\rangle \\
&+ \int_{x_1}^{x_2} \mathrm{d}x [\boldsymbol{v}_1^\dagger \otimes \overline{\boldsymbol{w}}_1'^\dagger] E(x_1, x)\left(V(x) \otimes \mathbb{1} + W(x) \otimes \overline{R}(x)\right)|\rho_R(x)\rangle \\
&+ \int_{x_1}^{x_2} \mathrm{d}x\, \langle \rho_L(x)|\left(V(x) \otimes \mathbb{1} + W(x) \otimes \overline{R}(x)\right) E(x, x_2)[\boldsymbol{v}_2 \otimes \overline{\boldsymbol{w}}_2'] \\
&+ \int_{x_1}^{x_2} \mathrm{d}x\, [\boldsymbol{w}_1^\dagger \otimes \overline{\boldsymbol{v}}_1^\dagger] E(x_1, x)\left(\mathbb{1} \otimes \overline{V}'(x) + R(x) \otimes \overline{W}'(x)\right)|\rho_R(x)\rangle \\
&+ [\boldsymbol{w}_1^\dagger \otimes \overline{\boldsymbol{w}}_1'^\dagger]\,|\rho_R(x_1)\rangle + [\boldsymbol{w}_1^\dagger \otimes \overline{\boldsymbol{v}}_1^\dagger] E(x_1, x_2)[\boldsymbol{v}_2 \otimes \overline{\boldsymbol{w}}_2'] \\
&+ \int_{x_1}^{x_2} \mathrm{d}x\ \langle \rho_L(x)|\left(\mathbb{1} \otimes \overline{V}'(x) + R(x) \otimes \overline{W}'(x)\right) E(x, x_2)[\boldsymbol{w}_2 \otimes \overline{\boldsymbol{v}}_2] \\
&+ \langle \rho_L(x_2)|\,[\boldsymbol{w}_2 \otimes \overline{\boldsymbol{w}}_2'] + [\boldsymbol{v}_1^\dagger \otimes \overline{\boldsymbol{w}}_1'^\dagger] E(x_1, x_2)[\boldsymbol{w}_2 \otimes \overline{\boldsymbol{v}}_2]
\end{aligned}$$

where the terms on the first 5 lines corresponds to all contributions of non-zero V and W, and the terms on lines 6 and 7 correspond to non-zero $\boldsymbol{w}_1$ and non-zero $\boldsymbol{w}_2$, respectively. Here, we have introduced a new notation

$$E(x, y) = \mathcal{P} \exp\left(\int_x^y Q(z) \otimes \mathbb{1} + \mathbb{1} \otimes \overline{Q}(z) + R(z) \otimes \overline{R}(z)\, \mathrm{d}z\right). \tag{2.22}$$

It is the continuum equivalent of the (product of) MPS transfer matrices and allows to *e.g.* write

$$\langle \rho_L(x)| = [\boldsymbol{v}_1^\dagger \otimes \overline{\boldsymbol{v}}_1^\dagger] E(x_1, x), \qquad |\rho_R(x)\rangle = E(x, x_2)[\boldsymbol{v}_2 \otimes \overline{\boldsymbol{v}}_2]. \tag{2.23}$$

Let us now first compute $\hat{H}|\Psi[Q, R, \boldsymbol{v}_1, \boldsymbol{v}_2]\rangle$ itself. Using the rules from Ref. [49] and by applying partial integration to the kinetic energy term, we obtain

$$\begin{aligned}
\hat{H}|\Psi[Q, R, \boldsymbol{v}_1, \boldsymbol{v}_2]\rangle = &\int_{x_1}^{x_2} \boldsymbol{v}_1^\dagger \hat{M}(x_1, x)\left(-\mathcal{D}_x^2 R(x) + v(x)R(x)\right) \otimes \hat{\psi}^\dagger(x) \hat{M}(x, x_2)\boldsymbol{v}_2\,|\Omega\rangle\ \mathrm{d}x \\
&+ \int_{x_1}^{x_2} \boldsymbol{v}_1^\dagger \hat{M}(x_1, x)\left(gR(x)^2 - [R(x), \mathcal{D}_x R(x)]\right) \otimes \left(\hat{\psi}^\dagger(x)\right)^2 \hat{M}(x, x_2)\boldsymbol{v}_2\,|\Omega\rangle\ \mathrm{d}x \\
&- \boldsymbol{v}_1^\dagger \mathcal{D}_x R(x_1) \otimes \psi^\dagger(x_1)\hat{M}(x_1, x_2)\boldsymbol{v}_2\,|\Omega\rangle + \boldsymbol{v}_1^\dagger \hat{M}(x_1, x_2)\mathcal{D}_x R(x_2) \otimes \psi^\dagger(x_2)\boldsymbol{v}_2\,|\Omega\rangle\,.
\end{aligned} \tag{2.24}$$

Given the linearity of the tangent space projector, we can compute the projection of the 4 different terms separately and add the result:

1. The first term of Eq. (2.24) is already in the explicit form of a tangent vector $|\Phi[V, W, \boldsymbol{w}_1, \boldsymbol{w}_2]\rangle$ with $W(x) = -\mathcal{D}_x^2 R(x) + v(x)R(x)$ and $V(x) = 0$, $\boldsymbol{w}_{1,2} = 0$. It does not need to be projected.

2. The second term is of the form $|\Theta\rangle = \int_{x_1}^{x_2} \boldsymbol{v}_1^\dagger \hat{M}(x_1, x) B(x) \otimes (\hat{\psi}^\dagger(x))^2 \hat{M}(x, x_2) \boldsymbol{v}_2 \, |\Omega\rangle \, \mathrm{d}x$, where $B(x) = gR(x)^2 - [R(x), \mathcal{D}_x R(x)]$. We obtain

$$
\begin{aligned}
&\langle \Phi[V', W', \boldsymbol{w}_1', \boldsymbol{w}_2'] | \Theta \rangle = \int_{x_1}^{x_2} \mathrm{d}x \, \langle \rho_L(x) | B(x) \otimes \big(\overline{R}(x) \overline{W}'(x) + \overline{W}'(x) \overline{R}(x) \big) | \rho_R(x) \rangle \\
&+ \int_{x_1}^{x_2} \mathrm{d}x \int_{x}^{x_2} \mathrm{d}y \, \langle \rho_L(x) | \big(B(x) \otimes \overline{R}(x)^2 \big) E(x, y) \big(\mathbb{1} \otimes \overline{V}'(y) + R(y) \otimes \overline{W}'(y) \big) | \rho_R(y) \rangle \\
&+ \int_{x_1}^{x_2} \mathrm{d}x \int_{x_1}^{x} \mathrm{d}y \, \langle \rho_L(y) | \big(\mathbb{1} \otimes \overline{V}'(y) + R(y) \otimes \overline{W}'(y) \big) E(y, x) \big(B(x) \otimes \overline{R}(x)^2 \big) | \rho_R(x) \rangle \\
&+ \int_{x_1}^{x_2} \mathrm{d}x [\boldsymbol{v}_1^\dagger \otimes \overline{\boldsymbol{w}}_1'^\dagger] E(x_1, x) \big(B(x) \otimes \overline{R}(x)^2 \big) \, | \rho_R(x) \rangle \\
&+ \int_{x_1}^{x_2} \mathrm{d}x \, \langle \rho_L(x) | \, \big(B(x) \otimes \overline{R}(x)^2 \big) E(x, x_2) [\boldsymbol{v}_2 \otimes \overline{\boldsymbol{w}}_2']
\end{aligned}
$$

   One can easily verify that by choosing

$$
\begin{aligned}
V(x) &= -\rho_L(x)^{-1} R(x)^\dagger \rho_L(x) B(x) \rho_R(x) R(x)^\dagger \rho_R(x)^{-1} \\
W(x) &= +\rho_L(x)^{-1} R(x)^\dagger \rho_L(x) B(x) + B(x) \rho_R(x) R(x)^\dagger \rho_R(x)^{-1} \\
\boldsymbol{w}_1^\dagger &= 0 \\
\boldsymbol{w}_2 &= 0
\end{aligned}
$$

   every single line of $\langle \Phi[V', W', \boldsymbol{w}_1', \boldsymbol{w}_2'] | \Theta \rangle$ matches with the corresponding line in the first lines of $\langle \Phi[V', W', \boldsymbol{w}_1', \boldsymbol{w}_2'] | \Phi[V, W, \boldsymbol{w}_1, \boldsymbol{w}_2] \rangle$, whereas the last two lines of the latter vanish because of the choice of $\boldsymbol{w}_{1,2} = 0$.

3. Next we deal with the third term $|\Theta\rangle = -\boldsymbol{v}_1^\dagger \mathcal{D}_x R(x_1) \otimes \psi^\dagger(x_1) \hat{M}(x_1, x_2) \boldsymbol{v}_2 \, |\Omega\rangle$, resulting in

$$
\begin{aligned}
&\langle \Phi[V', W', \boldsymbol{w}_1', \boldsymbol{w}_2'] | \Theta \rangle = -[\boldsymbol{v}_1^\dagger \otimes \overline{\boldsymbol{v}}_1^\dagger] \mathcal{D}_x R(x_1) \otimes \overline{W}'(x_1) \, | \rho_R(x_1) \rangle \\
&- \int_{x_1}^{x_2} \mathrm{d}y [\boldsymbol{v}_1^\dagger \otimes \overline{\boldsymbol{v}}_1^\dagger] \mathcal{D}_x R(x_1) \otimes \overline{R}(x_1) E(x_1, y) \big(\mathbb{1} \otimes \overline{V}'(y) + R(y) \otimes \overline{W}'(y) \big) \, | \rho_R(y) \rangle \\
&\qquad - [\boldsymbol{v}_1^\dagger \otimes \overline{\boldsymbol{w}}_1'^\dagger] \mathcal{D}_x R(x_1) \otimes \overline{R}(x_1) \, | \rho_R(x_1) \rangle \\
&\qquad\qquad - [\boldsymbol{v}_1^\dagger \otimes \overline{\boldsymbol{v}}_1^\dagger] \mathcal{D}_x R(x_1) \otimes \overline{R}(x_1) E(x_1, x_2) [\boldsymbol{v}_2 \otimes \overline{\boldsymbol{w}}_2']
\end{aligned}
$$

   Now we have to consider the effect of the boundary conditions. If $R(x_1)$ is fixed as $R(x_1) = a\mathbb{1}$ (Dirichlet condition), then the corresponding variation $\overline{W}'(x_1) = 0$ such that the first term vanishes and the remaining terms match the sixth line of $\langle \Phi[V', W', \boldsymbol{w}_1', \boldsymbol{w}_2'] | \Phi[V, W, \boldsymbol{w}_1, \boldsymbol{w}_2] \rangle$ by choosing

$$
V(x) = 0, \qquad W(x) = 0, \qquad \boldsymbol{w}_1^\dagger = -\overline{a} \boldsymbol{v}_1^\dagger \mathcal{D}_x R(x_1), \qquad \boldsymbol{w}_2 = 0.
$$

   Indeed, this boundary condition corresponds to fixing the value of the field operator $\hat{\psi}(x_1) = a$, so that $|\Theta\rangle$ can explicitly be rewritten as

$|\Theta\rangle = -\bar{a}\boldsymbol{v}_1^\dagger \mathcal{D}_x R(x_1)\hat{M}(x_1,x_2)\boldsymbol{v}_2 |\Omega\rangle$, which exactly equals the tangent vector $|\Phi[V,W,\boldsymbol{w}_1,\boldsymbol{w}_2]\rangle$ for this choice of the parameters.

Alternatively, if we do not fix $R(x_1)$, then the variation $\overline{W}'(x_1)$ automatically enforces the Neumann conditions $\boldsymbol{v}_1^\dagger \mathcal{D}_x R(x_1) = 0$ at any point in time, provided that $\rho_R(x_1)$ is full rank. Under this condition, we also obtain $|\Theta\rangle = 0$, which corresponds to inserting $\mathcal{D}_x R(x_1) = 0$ in the parameters above.

4. The last term of Eq. (2.24) can be dealt with similarly and is an explicit tangent vector corresponding to the choice

$$V(x) = 0, \qquad W(x) = 0, \qquad \boldsymbol{w}_1^\dagger = 0, \qquad \boldsymbol{w}_2 = \bar{b}\mathcal{D}_x R(x_2)\boldsymbol{v}_2.$$

in case of the Dirichlet condition $R(x_2) = b\mathbb{1}$. In the case of the Neumann condition, it is also zero.

Hence, for the boundary conditions here considered, only the second term of Eq. (2.24) needed to be projected onto the tangent space and, when considering the full Schrödinger equation, would be responsible for taking the exact evolution out of the manifold.

Grouping everything together gives rise to $|\Phi[V,W,\boldsymbol{w}_1,\boldsymbol{w}_2]\rangle = \hat{P}_\Psi \hat{H} |\Psi[Q,R,\boldsymbol{v}_1,\boldsymbol{v}_2]\rangle$ with

$$\begin{aligned}
V(x) =& -\rho_L(x)^{-1}R(x)^\dagger \rho_L(x)(gR(x)^2 - [R(x),\mathcal{D}_x R(x)])\rho_R(x)R(x)^\dagger \rho_R(x)^{-1} \\
W(x) =& -\mathcal{D}_x^2 R(x) + v(x)R(x) \\
&+ \rho_L(x)^{-1}R(x)^\dagger \rho_L(x)(gR(x)^2 - [R(x),\mathcal{D}_x R(x)]) \\
&+ (gR(x)^2 - [R(x),\mathcal{D}_x R(x)])\rho_R(x)R(x)^\dagger \rho_R(x)^{-1} \\
\boldsymbol{w}_1^\dagger =& -\bar{a}\boldsymbol{v}_1^\dagger \mathcal{D}_x R(x_1) \\
\boldsymbol{w}_2 =& +\bar{b}\mathcal{D}_x R(x_2)\boldsymbol{v}_2
\end{aligned}$$

which we have to equate to $\mathrm{i}\,|\Phi[\dot{Q},\dot{R},\dot{\boldsymbol{v}}_1,\dot{\boldsymbol{v}}_2]\rangle$. Matching the parameters as $\dot{Q} = V$ etc gives rise to the gauge covariatn QGPE of the main text for the specific choice of $P = 0$, though this choice is not unique. Indeed, one can note that the physical tangent vector $|\Phi[V,W,\boldsymbol{w}_1,\boldsymbol{w}_2]\rangle$ does not change under a substitution

$$\begin{aligned}
V(x) &\to V(x) + [P(x),Q(x)], & W(x) &\to W(x) + [P(x),R(x)], \\
\boldsymbol{w}_1^\dagger &\to \boldsymbol{w}_1^\dagger - \boldsymbol{v}_1^\dagger P(x_1), & \boldsymbol{w}_2 &\to \boldsymbol{w}_2 + P(x_2)\boldsymbol{v}_2,
\end{aligned} \tag{2.25}$$

which is how the fully gauge covariant formulation of the QGPE is obtained.

2.5.2 Derivation of the quantum Bogoliubov-de Gennes Equations

A stationary solution Q_0 and R_0 of the QGPE parameterizes a variationally optimal cMPS ground state approximation for a given Hamiltonian $\hat{H}_0$. Upon applying a perturbation $\hat{H}_1$ (possibly time-dependent), we can expand the QGPE to first order around Q_0 and R_0. In the following, we set $\hat{H}_0$ equal to the translation invariant Lieb-Liniger Hamiltonian ($v(x) = v_0 = -\mu$ with μ the chemical potential) in the thermodynamic limit, so that the stationary solution correspond to x (and t) independent matrices Q_0 and R_0, which we assume to be in the left-canonical form, i.e. $Q_0 + Q_0^\dagger + R_0^\dagger R_0 = 0$. Associated with this solution is a right density matrix $\rho_{R,0}$ satisfying

$$Q_0\rho_{R,0} + \rho_{R,0}Q_0^\dagger + R_0\rho_{R,0}R_0^\dagger = 0$$

and a matrix $P_0 = -\mathrm{i}R_0^\dagger[Q_0, R_0] + \mathrm{i}F_0$ where F_0 is the solution of the linear system

$$-Q_0^\dagger F_0 - F_0 Q_0 - R_0^\dagger F_0 R_0 = [Q_0, R_0]^\dagger[Q_0, R_0] - \mu R_0^\dagger R_0 + g(R_0^\dagger)^2 R_0^2.$$

We now consider a perturbation given by $\hat{H}_1(t) = \epsilon \int \mathrm{dx}\, \tilde{\mathrm{v}}(\mathrm{x},\mathrm{t})\hat{\psi}^\dagger(\mathrm{x})\hat{\psi}(\mathrm{x})$. The ansatz for the new solution of the QGPE is then given by

$$\begin{aligned} R(x,t) &= R_0 + \epsilon\tilde{R}(x,t), & Q(x,t) &= Q_0 + \epsilon\tilde{Q}(x,t), \\ \rho_{\mathrm{R}}(x,t) &= \rho_{\mathrm{R},0} + \epsilon\tilde{\rho}_{\mathrm{R}}(x,t), & \rho_{\mathrm{L}}(x,t) &= \mathbb{1} + \epsilon\tilde{\rho}_{\mathrm{L}}(x,t) \end{aligned} \tag{2.26}$$

where $\rho_{\mathrm{L,R}}(x,t)$ are the left and right density matrices. By expanding the relevant equations to first order in ϵ, we obtain

$$\begin{aligned} \partial_x\tilde{\rho}_{\mathrm{L}}(x,t) - Q_0^\dagger\tilde{\rho}_{\mathrm{L}}(x,t) + \tilde{\rho}_{\mathrm{L}}(x,t)Q_0 + R_0^\dagger\tilde{\rho}_{\mathrm{L}}(x,t)R_0 = \\ \tilde{Q}(x,t) + \tilde{Q}^\dagger(x,t) + R_0^\dagger\tilde{R}(x,t) + \tilde{R}^\dagger(x,t)R_0 \end{aligned} \tag{2.27}$$

$$\begin{aligned} \partial_x\tilde{\rho}_{\mathrm{R}}(x,t) + Q_0\tilde{\rho}_R(x,t) + \tilde{\rho}_R(x,t)Q_0^\dagger + R_0\tilde{\rho}_{\mathrm{R}}(x,t)R_0^\dagger = \\ -\left[\tilde{Q}(x,t)\rho_{\mathrm{R},0} + \rho_{\mathrm{R},0}\tilde{Q}^\dagger(x,t) + \tilde{R}(x,t)\rho_{\mathrm{R},0}R_0^\dagger + R_0\rho_{\mathrm{R},0}\tilde{R}^\dagger(x,t)\right] \end{aligned} \tag{2.28}$$

We furthermore choose

$$P(x,t) = P_0 + \epsilon\tilde{P}(x,t) = P_0 + \epsilon\big(-\mathrm{i}\tilde{R}^\dagger[Q_0,R_0] - \mathrm{i}R_0^\dagger\tilde{R}_{\mathrm{kin}}(x,t) + \mathrm{i}\tilde{F}(x,t)\big)$$

with $\tilde{R}_{\mathrm{kin}}(x,t) = [\tilde{Q}(x), R_0] + [Q_0, \tilde{R}(x)] + \partial_x\tilde{R}(x)$ and $\tilde{F}(x,t)$ the solution of

$$\begin{aligned} \partial_x\tilde{F} =& \tilde{F}Q_0 + F_0\tilde{Q} + \tilde{Q}^\dagger F_0 + Q_0^\dagger\tilde{F} + \tilde{R}^\dagger F_0 R_0 + R_0^\dagger\tilde{F}R_0 + R_0^\dagger F_0\tilde{R} \\ &+ [Q_0,R_0]^\dagger\tilde{R}_{\mathrm{kin}} + \tilde{R}_{\mathrm{kin}}^\dagger[Q_0,R_0] \\ &+ g\Big(\tilde{R}^\dagger R_0^\dagger R_0 R_0 + R_0^\dagger\tilde{R}^\dagger R_0 R_0 + R_0^\dagger R_0^\dagger\tilde{R}R_0 + R_0^\dagger R_0^\dagger R_0\tilde{R}\Big) \\ &+ v_0\tilde{R}^\dagger R_0 + v_0 R_0^\dagger\tilde{R} + \tilde{v}R_0^\dagger R_0, \end{aligned} \tag{2.29}$$

where we henceforth omit the (x,t) dependence of the $\tilde{\cdot}$ quantities. With this choice, we are assured that $\partial_t\tilde{Q} + R_0^\dagger\partial_t\tilde{R} = 0$ and, integrating this from the initial time when $\tilde{Q} = \tilde{R} = 0$, we obtain $\tilde{Q} + R_0^\dagger\tilde{R} = 0$. This equality assures that $Q(x)$ and $R(x)$ form a left canoncial representation to first order in ϵ. In particular, this makes the right hand side of Eq. (2.27) equal to zero, so that the solution of that equation is given by $\tilde{\rho}_{\mathrm{L}} = 0$.

The linearized QGPE itself is then given by

$$\begin{aligned} \mathrm{i}\partial_t\tilde{R}\,\rho_{\mathrm{R},0} =& -\partial_x^2\tilde{R}\rho_{\mathrm{R},0} - 2[Q_0,\partial_x\tilde{R}]\rho_{\mathrm{R},0} - [\partial_x\tilde{Q},R_0]\rho_{\mathrm{R},0} \\ &- [\tilde{Q},[Q_0,R_0]]\rho_{\mathrm{R},0} - [Q_0,[\tilde{Q},R_0]]\rho_{\mathrm{R},0} - [Q_0,[Q_0,\tilde{R}]]\rho_{\mathrm{R},0} - [Q_0,[Q_0,R_0]]\tilde{\rho}_{\mathrm{R}} \\ &+ g\Big((\tilde{R}^\dagger R_0^2 + R_0^\dagger\tilde{R}R_0 + R_0^\dagger R_0\tilde{R})\rho_{\mathrm{R},0} + R_0^\dagger R_0^2\tilde{\rho}_{\mathrm{R}} \\ &\qquad + \tilde{R}R_0\rho_{\mathrm{R},0}R_0^\dagger + R_0\tilde{R}\rho_{\mathrm{R},0}R_0^\dagger + R_0^2\tilde{\rho}_{\mathrm{R}}R_0^\dagger + R_0^2\rho_{\mathrm{R},0}\tilde{R}^\dagger\Big) \\ &+ v_0\tilde{R}\rho_{\mathrm{R},0} + v_0R_0\tilde{\rho}_{\mathrm{R}} + \tilde{v}R_0\rho_{\mathrm{R},0} \\ &+ [\tilde{R}_{\mathrm{kin}},R_0]\rho_{\mathrm{R},0}R_0^\dagger + [[Q_0,R_0],\tilde{R}]\rho_{\mathrm{R},0}R_0^\dagger \\ &\qquad + [[Q_0,R_0],R_0]\tilde{\rho}_{\mathrm{R}}R_0^\dagger + [[Q_0,R_0],R_0]\rho_{\mathrm{R},0}\tilde{R}^\dagger \\ &+ [\tilde{R},R_0^\dagger]\,[Q_0,R_0]\rho_{\mathrm{R},0} + [R_0,\tilde{R}^\dagger]\,[Q_0,R_0]\rho_{\mathrm{R},0} \\ &\qquad + [R_0,R_0^\dagger]\,\tilde{R}_{\mathrm{kin}}\rho_{\mathrm{R},0} + [R_0,R_0^\dagger]\,[Q_0,R_0]\tilde{\rho}_{\mathrm{R}} \\ &+ [\tilde{F},R_0]\rho_{\mathrm{R},0} + [F_0,\tilde{R}]\rho_{\mathrm{R},0} + [F_0,R_0]\tilde{\rho}_{\mathrm{R}} \end{aligned} \tag{2.30}$$

where we can further substitute $\tilde{Q} = -R_0^\dagger \tilde{R}$. Equations (2.28), (2.29) and (2.30) form a set of linear partial differential equations with as only source term the perturbed potential $\tilde{v}(x,t)$ and with mixing between $\tilde{R}$ and $\tilde{R}^\dagger$. Therefore, if $\tilde{v}(x,t) = \cos(kx - \omega t)$ for certain k and ω, we can make the ansatz

$$\tilde{R}(x) = e^{\mathrm{i}(kx-\omega t)} R_+ + e^{-\mathrm{i}(kx-\omega t)} R_-, \qquad \tilde{F}(x) = e^{\mathrm{i}(kx-\omega t)} F_+ + e^{-\mathrm{i}(kx-\omega t)} F_-,$$
$$\tilde{\rho}_{\mathrm{R}}(x) = e^{\mathrm{i}(kx-\omega t)} \rho_+ + e^{-\mathrm{i}(kx-\omega t)} \rho_- \ .$$

Note that both $\tilde{F}(x)$ and $\tilde{\rho}_{\mathrm{R}}(x)$ are hermitian matrices which means that $F_-^\dagger = F_+$ and $\rho_-^\dagger = \rho_+$. Inserting this ansatz into the relevant equations allows to express everything in terms of $R_\pm$ and finally gives rise to the quantum Bogoliubov-de Gennes equation [Eq. (2.12)] in the main text]. This equation can be iteratively solved at a computational cost of $\mathcal{O}(D^3)$. The same approach still works if $\tilde{v}(x,t)$ contains N different Fourier modes, where the complexity will increase linearly with N.

Chapter 3

Atomtronics: a continuous matrix product state approach

Synopsis:

We introduce a time evolution algorithm for one-dimensional quantum field theories with periodic boundary conditions. This is done by applying the Dirac-Frenkel time-dependent variational principle to the set of translational invariant continuous matrix product states with periodic boundary conditions. Moreover, the ansatz is accompanied with additional boundary degrees of freedom to study quantum impurity problems. The algorithm allows for a cutoff in the spectrum of the transfer matrix and thus has an efficient computational scaling. In particular we study the prototypical example of an atomtronic system - an interacting Bose gas rotating in a ring shaped trap in the presence of a localised barrier potential.

Based on:

D. Draxler, J. Haegeman , F. Verstraete , and M. Rizzi
e-print arXiv: 1609.09704, submitted to PRB

3.1 Introduction

The last decade has shown a tremendous development of tensor network based methods for studying strongly correlated quantum many-body systems [85]. More recently the scope of these methods was extended by introducing the variational class of continuous matrix product states (cMPS) [119, 49], which allows to simulate one dimensional (1D) quantum field theories directly in the continuum. Systems with continuous degrees of freedom such as superfluid atom circuits (i.e., cold atoms trapped in ring-shaped traps), have recently attracted a lot of attention as building blocks in the emerging field of *atomtronics* [33, 106, 56]. While (contact-)interacting quantum particles in the 1D continuum with periodic boundaries provide prototypical examples of integrable systems [75, 128, 69], the presence of controlled impurities to steer the atomtronic system often breaks the integrability conditions. Analytical solutions can thus only be found in special limits [60, 79], and even numerical studies do suffer from an intrinsic approximation as they always rely on discretised versions of the a priori continuous system [26].

In this paper we present a time evolution algorithm for translational invariant cMPS with periodic boundary conditions (pbc) which is perfectly well suited for the numerical study of atomtronic systems. The algorithm is based on the time-dependent variational principle (TDVP) [30, 38, 70], which was first introduced to the field of tensor network methods in Ref. [47] by applying it to the variational class of uniform matrix product states (MPS) in the thermodynamic limit and later to finite systems with open boundary conditions (obc) [51, 59]. Only recently TDVP was also applied to cMPS with obc [50, 31] (both for finite and infinite systems) but the extension of the algorithm to the pbc case has not been done so far neither for MPS nor for cMPS. The cMPS ansatz is further accompanied with additional boundary degrees of freedom to study Hamiltonians which contain local translational symmetry braking terms akin those in quantum impurity problems.

The difficulty in studying systems with pbc with tensor networks in general stems from the fact that contracting a tensor network with pbc is numerically much more costly than contracting one with obc. In the spirit of Refs. [122, 90, 92] it is however possible to overcome this difficulty by allowing effectively for a cutoff in the spectrum of the corresponding transfer matrix of the network. We present an analog of this procedure for uniform cMPS which makes our algorithm as efficient as conventional pbc DMRG methods [90]. Moreover we anticipate here that our method will not require the introduction of spatially dependent tensors, except for *one* variational boundary matrix at the impurity position, therefore providing an approach (almost) as cheap as translationally invariant cMPS algorithms.

The paper is organized as follows. In section 3.2 the algorithm is introduced and we explain the aforementioned cutoff procedure whereas in section 3.3 we define the Hamiltonian. In section 3.4 we present the results which are extensively benchmarked with DMRG based lattice simulations and classical Gross-Pitaevskii solutions.

3.2 Time-dependent variational principle

We start by defining a uniform cMPS with pbc and bond dimension D as

$$|\Psi[Q,R,B]\rangle = \mathrm{Tr}\Big[B\mathcal{P}\mathrm{e}^{\int_0^L Q\otimes\hat{1}+R\otimes\hat{\psi}^\dagger(x)\,\mathrm{d}x}\Big]\,|\Omega\rangle \tag{3.1}$$

with R, Q being matrices in $\mathbb{C}^{D\times D}$, $\mathcal{P}\mathrm{e}$ the path-ordering exponential, L the system size and $|\Omega\rangle$ the vacuum which is annihilated by the field operator $\hat{\psi}(x)$. The field operators are assumed

to be bosonic satisfying the commutation relation $[\hat{\psi}(x), \hat{\psi}^\dagger(y)] = \delta(x-y)$ and the boundary condition $\hat{\psi}(0) = \hat{\psi}(L)$. We also include the boundary matrix $B \in \mathbb{C}^{D\times D}$ to the variational space which accounts for the possibility of having a localised barrier at position $x = 0$ and for a possible phase twist in the boundary conditions. The invariance of a cMPS under multiplicative gauge transformations [49] of the form $R \to gRg^{-1}, Q \to gQg^{-1}, B \to gBg^{-1}$ with $g \in \mathrm{GL}(\mathbb{C}, D)$ allows to work with Q and R matrices s.t. $Q + Q^\dagger + R^\dagger R = 0$ which we refer to as the *left gauge condition*. This condition is always satisfied if we set $Q = -1/2R^\dagger R - \mathrm{i}K$ with K being a hermitian matrix.
The TDVP was originally formulated as an action principle [30, 38] over a given (complex) variational manifold giving rise to the Euler-Lagrange equations. However, TDVP can also be interpreted as a projected time-dependent Schrödinger equation $\mathrm{i}\frac{\mathrm{d}}{\mathrm{d}t}|\Psi\rangle = \hat{P}_\Psi \hat{H}|\Psi\rangle$, where $\hat{H}$ is a Hamiltonian and $\hat{P}_\Psi$ projects the r.h.s. to the tangent space of the variational manifold [52] at the point $|\Psi\rangle$. This projector guarantees that the state will never leave the variational manifold which can be seen as the guiding principle behind TDVP, i.e. finding the optimal approximation to the true time evolution within a certain variational manifold. In our setting the variational manifold is the set of cMPS with fixed bond dimension D and the tangent states spanning the corresponding tangent space are defined as

$$\begin{aligned}|\Phi[V,W,Y]\rangle &:= \left[Y\frac{\delta}{\delta B} + \int_0^{\mathrm{L}} \mathrm{d}x\ \left(V\frac{\delta}{\delta Q} + W\frac{\delta}{\delta R}\right)\right]|\Psi[Q,R,B]\rangle \\ &= \mathrm{Tr}\Big[Y\hat{M}(0,\mathrm{L})\Big] + \int_0^{\mathrm{L}} \mathrm{d}x\ \mathrm{Tr}\Big[B\hat{M}(0,x)\Big(V\otimes\hat{1} + W\otimes\hat{\Psi}^\dagger(x)\Big)\hat{M}(x,\mathrm{L})\Big] \end{aligned} \tag{3.2}$$

where W, V ane Y are variational matrices in $\mathbb{C}^{D\times D}$. We also introduced the notation $\hat{M}(x,y) = \mathcal{P}\mathrm{e}^{\int_x^y \mathrm{d}z Q\otimes\hat{1} + R\otimes\hat{\psi}^\dagger(z)}$.

Deriving the TDVP equations now amounts to finding the optimal tangent vector that the exact Schrödinger evolution is projected onto. By introducing a time-dependent parameterisation $(Q(t), R(t), B(t))$ we therefore have $|\Phi[\dot{Q},\dot{R},\dot{B}]\rangle = -\mathrm{i}\hat{P}_\Psi\hat{H}|\Psi[Q,R,B]\rangle$ and $|\Phi[\dot{Q},\dot{R},\dot{B}]\rangle$ is obtained by performing the minimisation

$$\min_{(V,W,Y)} \| \, |\Phi[V,W,Y]\rangle + \mathrm{i}\hat{H}|\Psi[Q,R,B]\rangle \, \| \ .$$

The solution to this minimisation problem is found to be

$$\mathrm{i}\begin{bmatrix}\dot{Q}\\ \dot{R}\\ \dot{B}\end{bmatrix} = G^{-1}\begin{bmatrix}g_1\\ g_2\\ g_3\end{bmatrix} \tag{3.3}$$

where the Gram matrix G and the vector $[g_1; g_2; g_3]$ are defined via

$$\langle\Phi[\overline{V},\overline{W},\overline{Y}]|\Phi[V,W,Y]\rangle = \left[V^\dagger W^\dagger Y^\dagger\right] G \begin{bmatrix}V\\ W\\ Y\end{bmatrix} \tag{3.4}$$

$$\langle\Phi[\overline{V},\overline{W},\overline{Y}]|\,\hat{H}\,|\Psi(Q,R,B)\rangle = \left[V^\dagger W^\dagger Y^\dagger\right]\begin{bmatrix}g_1\\ g_2\\ g_3\end{bmatrix}\ . \tag{3.5}$$

The square brackets are assumed to be vectors of length $3D^2$ and the Gram matrix G is a hermitian matrix of size $(3D^2 \times 3D^2)$. Further we will refer to the r.h.s. of Eq. (3.3) as

the gradient. It is important to note that G has a non-vanishing kernel of dimension D^2. This means that the inverse in Eq. (3.3) has to be understood as a pseudo-inverse acting solely on the orthogonal complement of the kernel of G. The existence of this kernel can be traced back to the fact that every tangent state $|\Phi[V,W,Y]\rangle$ is invariant under additive gauge transformations [49] of the form $W \to W + [X,R], V \to V + [X,Q]$ and $Y \to Y + [X,B]$ with some $X \in \mathbb{C}^{D\times D}$. From Eq. (3.4), and the fact that the tangent space is a linear vector space, as visible from Eq. (3.2), we can conclude that the states $|\Phi[[X,Q],[X,R],[X,B]]\rangle$ must have norm zero and the corresponding vectors $[[X,Q];[X,R];[X,B]]$ span the null space of G. It is convenient to work in a gauge s.t. $V = -R^\dagger W$ which eliminates all D^2 gauge degrees of freedom and thereby maps G to a $2D^2$-dimensional effective Gram matrix with full rank. Further, this choice of gauge allows for a *left gauge* conserving update procedure as we will not update Q but rather K as $\mathrm{i}\dot{K} = 1/2(R^\dagger\dot{R} - \dot{R}^\dagger R)$. This equation guarantees that K will stay hermitian to first order in dt and the corresponding $Q = -1/2R^\dagger R - \mathrm{i}K$ will thus satisfy the left gauge condition throughout the time evolution.

It is worth mentioning that in the context of TDVP the difference in the computational scaling between systems with obc and pbc is that for obc it is always possible, just like for standard MPS, to find a gauge such that $G = \mathbb{I}$, which drastically reduces the cost of solving Eq. (3.3), whereas for pbc in general such a gauge does not exist.

When solving Eq. (3.3) in imaginary time (to find an approximation to the ground state of some Hamiltonian) it is important to restrict to tangent states that are orthogonal to $|\Psi(Q,R,B)\rangle$, i.e. $\Big\langle \Phi[\overline{V},\overline{W},\overline{Y}] \Big| \Psi(Q,R,B)\Big\rangle = \Big[V^\dagger W^\dagger Y^\dagger\Big]\,[y_1;y_2;y_3] = 0$. This constrain is due to the fact that $|\Psi(Q,R,B)\rangle$ itself is an element of the tangent space as $|\Phi[\mathbb{I},0_{D\times D},0_{D\times D}]\rangle = \mathrm{L}\,|\Psi(Q,R,B)\rangle$. Hence, without imposing orthogonality the evolution would not preserve the norm of the state. Thus we not only have to project Eq. (3.3) onto the orthogonal compliment of the kernel of G but also to the subspace orthogonal to the vector $[y_1;y_2;y_3]$. Note that for real time evolution orthogonality does not have to be imposed, since then the TDVP equations are symplectic differential equations [70] and as such respect conservation of norm and energy.

In this paper we will only focus on ground state properties hence solving Eq. (3.3) in imaginary time. In the case of a simple Euler integration the imaginary time TDVP equations are equivalent to a steepest descend optimization where the cost function is the expectation value of the Hamiltonian, i.e., the energy of the state. Further improvement of the convergence properties can be achieved by applying a version of the non-linear conjugate gradient search on a curved manifold. This is a rather involved task as the energy has to be minimised along geodesics and the parallel transport of tangent states corresponding to different tangent spaces has to be calculated in general. However, for small enough time steps the parallel transport can be neglected [81] and the only ingredients needed for a non-linear CG search are then the gradient and the metric G defined in Eq. (3.3).

3.2.1 Cut off in the transfer matrix

We will now proceed by calculating the vector $[y_1;y_2;y_3]$ and thereby explain the neccessary *cut off* procedure to make the algorithm numerically efficient. By using standard cMPS calculus technics [49] we find that

$$\Big\langle \Phi[\overline{V},\overline{W},\overline{Y}] \Big| \Psi(Q,R,B)\Big\rangle = \int_0^{\mathrm{L}} \mathrm{d}x \mathrm{Tr}\Big[B\otimes\overline{B}\mathrm{e}^{xT}\Big(\mathbb{I}\otimes\overline{V} + R\otimes\overline{W}\Big)\mathrm{e}^{(\mathrm{L}-x)T}\Big] + \mathrm{Tr}\Big[B\otimes\overline{Y}\mathrm{e}^{\mathrm{L}T}\Big] \tag{3.6}$$

where $T = Q \otimes \mathbb{I} + \mathbb{I} \otimes \overline{Q} + R \otimes \overline{R}$ is the generator of the cMPS transfer matrix $E(x,y) = \mathrm{e}^{(y-x)T}$. The matrix T can always be rescaled to have one zero eigenvalue, with all other eigenvalues having non-positive real parts: we notice that this property is automatically fulfilled by virtue of the left gauge condition, $Q+Q^\dagger+R^\dagger R = 0$. We also assume that these eigenvalues are ordered with decreasing real part such that $|\mathrm{e}^{\lambda_1}| \geq |\mathrm{e}^{\lambda_2}| \geq \cdots \geq |\mathrm{e}^{\lambda_{D^2}}|$. If we insert a spectral decomposition of $T = \sum_{i=1}^{D^2} \lambda_i |r_i)(l_i|$, with $|r_i)$ and $(l_i|$ respectively the right and left eigenvectors corresponding to the eigenvalue λ_i, then Eq. (3.6) becomes

$$\begin{aligned}
&\Big\langle \Phi[\overline{V},\overline{W},\overline{Y}] \,\Big|\, \Psi(Q,R,B) \Big\rangle = \\
&\sum_{\mathrm{i}\neq k=1}^{D^2} \frac{\mathrm{e}^{\lambda_i \mathrm{L}} - \mathrm{e}^{\lambda_k \mathrm{L}}}{\lambda_i - \lambda_k} \mathrm{Tr}\Big[B \otimes \overline{B} |r_i)(l_i| \left(\mathbb{I} \otimes \overline{V} + R \otimes \overline{W}\right) |r_k)(l_k|\Big] \\
&+ \mathrm{L} \sum_{i=1}^{D^2} \mathrm{e}^{\lambda_i \mathrm{L}} \mathrm{Tr}\left[B \otimes \overline{B} |r_i)(l_i| \Big(\mathbb{I} \otimes \overline{V} + R \otimes \overline{W}\Big) |r_i)(l_i|\right] + \sum_{i=1}^{D^2} \mathrm{e}^{\lambda_i \mathrm{L}} \mathrm{Tr}\Big[B \otimes \overline{Y} |r_i)(l_i|\Big] \,,
\end{aligned} \tag{3.7}$$

where we neglected (accidental) degeneracies of the sub-dominant λ's (but a generalization thereto is straightforward). The vector $[y_1; y_2; y_3]$ is then immediately found by reshaping vectors to matrices according to $a \otimes \bar{b}|x) \rightarrow axb^\dagger$. However, in order to have an overall computational cost of $\mathcal{O}(D^3)$ we can not compute the whole spectrum of T as the cost of this would be of $\mathcal{O}(D^6)$. The situation can be remedied by introducing a cutoff in the spectrum of T and only calculating the leading m_1 eigenvalues. The cutoff is chosen in such a way that $\forall i > m_1$, $|\mathrm{e}^{\mathrm{L}\lambda_i}| < tol$ for some predefined tolerance tol and we can set $\mathrm{e}^{\mathrm{L}\lambda_i} = 0$. For large enough L it can happen that the factor $\mathrm{L}\mathrm{e}^{\mathrm{L}\lambda_i}$ might again be above the tolerance and hence another cutoff at $m_2 \geq m_1$ needs to be taken into account. As long as m_2 is not too large this can be done with an iterative eigenvalue solver at a cost of $\mathcal{O}(D^3)$. The tolerance was chosen to be $tol = 10^{-9}$ in all simulations which roughly corresponds to $m_2 \approx 30$ for the largest bond dimension used in this paper. The final expression of Eq. (3.6) with these approximations can be found in the Supplement Section (3.6.1). It is however important to mention that this expression will contain the matrix $(\tilde{T}_i^{m_1})^{\mathrm{p}} := \Big[\lambda_i(\mathbb{I} - \sum_{k=1}^{m_1} |r_k)(l_k|) - (T - \sum_{k=1}^{m_1} \lambda_k |r_k)(l_k|)\Big]^{\mathrm{p}}$ where the notation p stands for the pseudo-inverse of a matrix with non vanishing null space (see Supplement Section (3.6.1) for more details). At first glance it might seem that we still have to compute the whole spectrum of T in order to calculate the pseudo-inverse of the matrix $\tilde{T}_i^{m_1}$. This however is not true since we only need to know how $\tilde{T}_i^{m_1}$ acts on a vector, for which it is sufficient to know only the first m_1 eigenvalues and eigenvectors. This allows us to use an iterative solver to compute the action of $\tilde{T}_i^{m_1}$ on a vector with a cost of $\mathcal{O}(D^3)$. The calculation of the Gram matrix G and the vector $[g_1; g_2; g_3]$ in Eq. (3.3) follows along the same lines but is very lengthy and the explicit calculation can also be found in the Supplement Section (3.6.1). Note that we actually never have to calculate the full matrix G but again only need to know how it acts on a vector. This can also be done with an iterative solver which means that the overall cost of the algorithm remains of $\mathcal{O}(D^3)$.

3.3 The model

The system we aim to study consists of an interacting Bose gas loaded in a ring shaped trap of length L which is interrupted by a localised barrier rotating at constant velocity. In the rotating frame the Hamiltonian describing this system reads

$$\hat{H} = \int_0^{\mathrm{L}} \mathrm{d}x \left[\left(\partial_x \hat{\psi}^\dagger + \mathrm{i}\frac{2\pi\Omega}{\mathrm{L}}\hat{\psi}^\dagger \right) \left(\partial_x \hat{\psi} - \mathrm{i}\frac{2\pi\Omega}{\mathrm{L}}\hat{\psi} \right) + c\hat{\psi}^\dagger\hat{\psi}^\dagger\hat{\psi}\hat{\psi} + U_0\delta(x)\hat{\psi}^\dagger\hat{\psi} - \mu\hat{\psi}^\dagger\hat{\psi} \right] \tag{3.8}$$

with $c > 0$ being the interaction strength, U_0 the barrier strength, $\mu > 0$ the chemical potential and Ω the Coriolis flux. The spatial dependence of the operators $\hat{\psi}(x)$ has been omitted for the sake of brevity and we have set $\hbar = 1$ and the mass $m = 1/2$. An essential feature of the ground state physics of $\hat{H}$ is the periodicity of its ground state energy as a function of Ω with period 1 for all values of c and U_0. This can be appreciated by performing the canonical transformation $\hat{\psi}(x) \to \mathrm{e}^{\mathrm{i}\frac{2\pi n}{L}x}\hat{\psi}(x)$ which shifts $\Omega \to \Omega - n$ and preserves the periodic boundary conditions $\psi(0) = \psi(L)$ for integer values n. More generally, by using a non-integer value $n = \Omega$, the model is mapped to a standard Lieb-Liniger type Hamiltonian [75], with the addition of a barrier where the field operators also obey twisted boundary conditions $\hat{\psi}(L) = \mathrm{e}^{\mathrm{i}2\pi\Omega}\hat{\psi}(0)$. At this point it seems that there are two strategies to proceed: one can either simulate the Hamiltonian in (3.8) where the field operators obey periodic boundary conditions or one can study the Lieb-Liniger type Hamiltonian with twisted boundary conditions. In both cases the cMPS wave function has to obey a certain regularity condition [49] to have a well defined kinetic energy at position $x = 0$. For a system with pbc this regularity condition reads $BR - RB = 0$ whereas for twisted boundary conditions it reads $BR - \mathrm{e}^{\mathrm{i}2\pi\Omega}RB = 0$. Both of these conditions impose a certain parametrisation on R and B. We have observed that either parametrisation of R and B negatively affects the numerical stability of the Gram matrix G, even for small values of the bond dimension D.

Therefore, we have chosen a third strategy, which produces a regularised Hamiltonian $\hat{H}_\epsilon$ in terms a cut-off length ϵ *only* around the barrier, where the twisted boundary conditions have not to be enforced explicitly but rather emerge from a (divergent) boundary term in the Hamiltonian. In order to construct it, we pass through a discretization on a lattice with $N_\mathrm{s} = L/\epsilon$ sites and lattice spacing ϵ, where each site j accommodates modes $\tilde{a}_j = \sqrt{\epsilon}\,\mathrm{e}^{\mathrm{i}\frac{2\pi\Omega}{\mathrm{L}}(j-1/2)\epsilon}\,\hat{\psi}\left((j-1/2)\epsilon\right)$. This is very similar to the above mentioned lattice version commonly used for standard MPS (see e.g. Ref. [26]), apart from a slightly more convenient choice about the barrier delta function, $\delta(x) = \lim_{\epsilon\to 0}\left(\delta(x-\epsilon/2) + \delta(x+\epsilon/2)\right)/2$. We expand the Hamiltonian (3.8) to the lowest relevant order in ϵ as

$$\begin{aligned}\hat{H}_{\mathrm{Lattice}} = &\sum_{j=1}^{N_\mathrm{s}-1} \frac{1}{\epsilon^2}\left[\tilde{a}_{j+1}^\dagger - \tilde{a}_j^\dagger\right]\left[\tilde{a}_{j+1} - \tilde{a}_j\right] + \frac{1}{\epsilon^2}\left[\tilde{a}_1^\dagger - \mathrm{e}^{-\mathrm{i}2\pi\Omega}\tilde{a}_{N_\mathrm{s}}^\dagger\right]\left[\tilde{a}_1 - \mathrm{e}^{\mathrm{i}2\pi\Omega}\tilde{a}_{N_\mathrm{s}}\right] \\ &+ \sum_{j=1}^{N_\mathrm{s}}\left[\frac{c}{\epsilon}\tilde{a}_{j+1}^\dagger\tilde{a}_j^\dagger\tilde{a}_j\tilde{a}_{j+1} - \mu\tilde{a}_j^\dagger\tilde{a}_j\right] + \frac{U_0}{2\epsilon}\left[\tilde{a}_1^\dagger\tilde{a}_1 + \tilde{a}_{N_\mathrm{s}}^\dagger\tilde{a}_{N_\mathrm{s}}\right] .\end{aligned} \tag{3.9}$$

We notice that all complex phases have cancelled in the bulk of the system and Ω only appears in the hopping across the boundary, thus making the periodicity 1 in Ω manifest. By taking again the continuum limit and reintroducing the field derivatives, we get

$$\begin{aligned}\hat{H}_\epsilon = \int_0^{\mathrm{L}} \mathrm{d}x \ \Big[\partial_x\hat{\psi}^\dagger\partial_x\hat{\psi} + c\hat{\psi}^\dagger\hat{\psi}^\dagger\hat{\psi}\hat{\psi} - \mu\hat{\psi}^\dagger\hat{\psi}\Big] + \frac{U_0}{2}\big(\hat{\psi}^\dagger(0)\hat{\psi}(0) + \hat{\psi}^\dagger(L)\hat{\psi}(L)\big) \\ + \frac{1}{\epsilon}\big(\hat{\psi}^\dagger(0) - \mathrm{e}^{-\mathrm{i}2\pi\Omega}\hat{\psi}^\dagger(L)\big)\big(\hat{\psi}(0) - \mathrm{e}^{\mathrm{i}2\pi\Omega}\hat{\psi}(L)\big) \\ + \frac{1}{2}\big(\hat{\psi}^\dagger(0) - \mathrm{e}^{-\mathrm{i}2\pi\Omega}\hat{\psi}^\dagger(L)\big)\big(\partial_x\hat{\psi}(0) + \mathrm{e}^{\mathrm{i}2\pi\Omega}\partial_x\hat{\psi}(L)\big) \\ + \frac{1}{2}\big(\partial_x\hat{\psi}^\dagger(0) + \mathrm{e}^{-\mathrm{i}2\pi\Omega}\partial_x\hat{\psi}^\dagger(L)\big)\big(\hat{\psi}(0) - \mathrm{e}^{\mathrm{i}2\pi\Omega}\hat{\psi}(L)\big) \\ + \mathcal{O}(\epsilon)\ . \end{aligned} \tag{3.10}$$

While in this regularized Hamiltonian $\hat{H}_\epsilon$ the field operators in Eq. (3.10) are assumed to obey pbc but the matrices R and B are now completely free, and we can thus circumvent the Gram matrix instability. This introduces a competition between minimizing the first line in (3.10) thus the energy and minimizing the remaining two lines which try to enforce the boundary condition, via a diverging weight. A detailed study of the energy scaling w.r.t ϵ is given in the Supplement Section (3.6.2) and unless otherwise stated we will set $\epsilon = 2.5 \times 1\mathrm{e}^{-3}$ for the remaining part of the paper.

3.4 Results

In the absence of a barrier the system is a perfect superfluid and its ground state energy is given by a series of intersecting parabolas due to Galilean invariance [9]. The corresponding persistent current $I(\Omega)$ is thus a perfect sawtooth in the rotating frame and it is related to the ground state energy $E(\Omega)$ via

$$I(\Omega) = -\frac{1}{2\pi}\frac{\partial E(\Omega)}{\partial\Omega}\ . \tag{3.11}$$

If the barrier is turned on rotational symmetry is broken and the persistent current changes its shape from a smeared sawtooth (weak barrier) to a sinusoid (large barrier) (see Fig. 3.1). The rich interplay between quantum fluctuations, interactions and statistics manifests itself in the intriguing behaviour of the persistent currents amplitude α. The dependence of the amplitude on both the dimensionless interaction strength $\gamma = c/\rho$ (ρ being the ground state density) and on the barrier height $\lambda = mU_0L/\pi$ was recently thoroughly studied by some of us [26]. There it was found that the amplitude displays a maximum at intermediate interactions for all values of λ. In the following we will give numerical evidence that the cMPS not only displays the correct density profiles for the whole parameter range of γ and λ but also perfectly well captures the non monotonicity of the function $\alpha(\gamma)$. The numerical results are compared to DMRG based lattice simulations and to exact results from a classical Gross-Pitaevskii analysis at weak interactions.

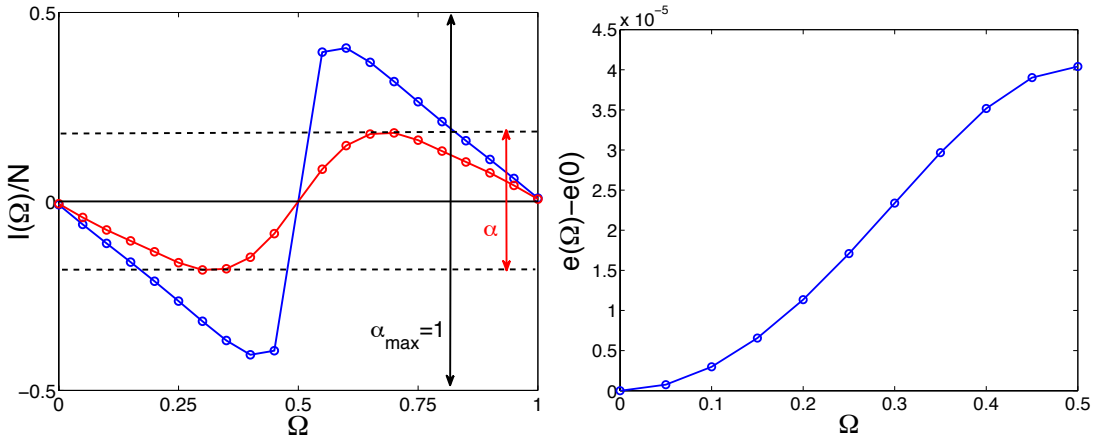

Figure 3.1: Left: Persistent current in units of $I_0 = 2\pi/mL^2$ for $\lambda = 9.5$ (blue, D=10) and $\lambda = 38.2$ (red, D=10) both at $\gamma = 2.33$. Right: Energy density difference at $\lambda = 38.2$ and $\gamma = 33$ at $D = 12$. The other parameters in both panels are $L = 120$ and $N = 18$.

3.4.1 Density profiles

In Fig. 3.2 several density profiles are shown for different values of γ and barrier height λ. At small γ little entanglement is present in the system and the ground state is well described by a dark soliton solution of the classical Gross-Pitaevskii (GP) equation [26]. Hence, the cMPS ansatz already converged to this solution at a very small bond dimension of $D = 4$ as can be seen from the inset of panel (a) in Fig. 3.2. The condition number of the Gram matrix in Eq. (3.3) is in general negatively affected by small eigenvalues of the fix point of the transfer matrix T. This fact in practice upper bounds the largest possible bond dimension which explains the rather small values of D in the limit of weak interaction or little entanglement. With increasing γ the width of the central depletion around $x = 0$ decreases as the barrier effectively gets screened by a decaying healing length $\xi = 1/\sqrt{4mc\rho}$. At large γ Friedel oscillations start to build up as the density profiles and the energy of the system start to resemble those of free fermions. The inset of panel (c) in Fig. 3.2 compares the cMPS result for large γ with the DMRG data from Ref. [26] and shows perfect agreement of the density profiles even at moderate values of D.

The cMPS ansatz also allows to study in principle arbitrary large (or small) densities where it is not possible anymore to describe the system with a low filling lattice approximation. This methodological advantage can be exploited to study e.g. the full width at half maximum of the central depletion, a quantity which could be measured in experiments akin those in Ref. [33]. We find that the width is decaying algebraically with the average number of particles when all other parameters are kept fixed as is shown in panel (d) of Fig. 3.2. Note that the density profiles in general converge from inside to the outside as the effective cMPS correlation length increases with increasing D. In the plots of panel (d) the effective correlation length has not fully converged as the Friedel oscillations are too strongly suppressed when compared to results from Luttinger liquid theory [15]. However, the profile of the central depletion and its vicinity and thus the width have already converged which was further checked by a finite D scaling as is shown in the Supplement Section (3.6.2) of this paper.

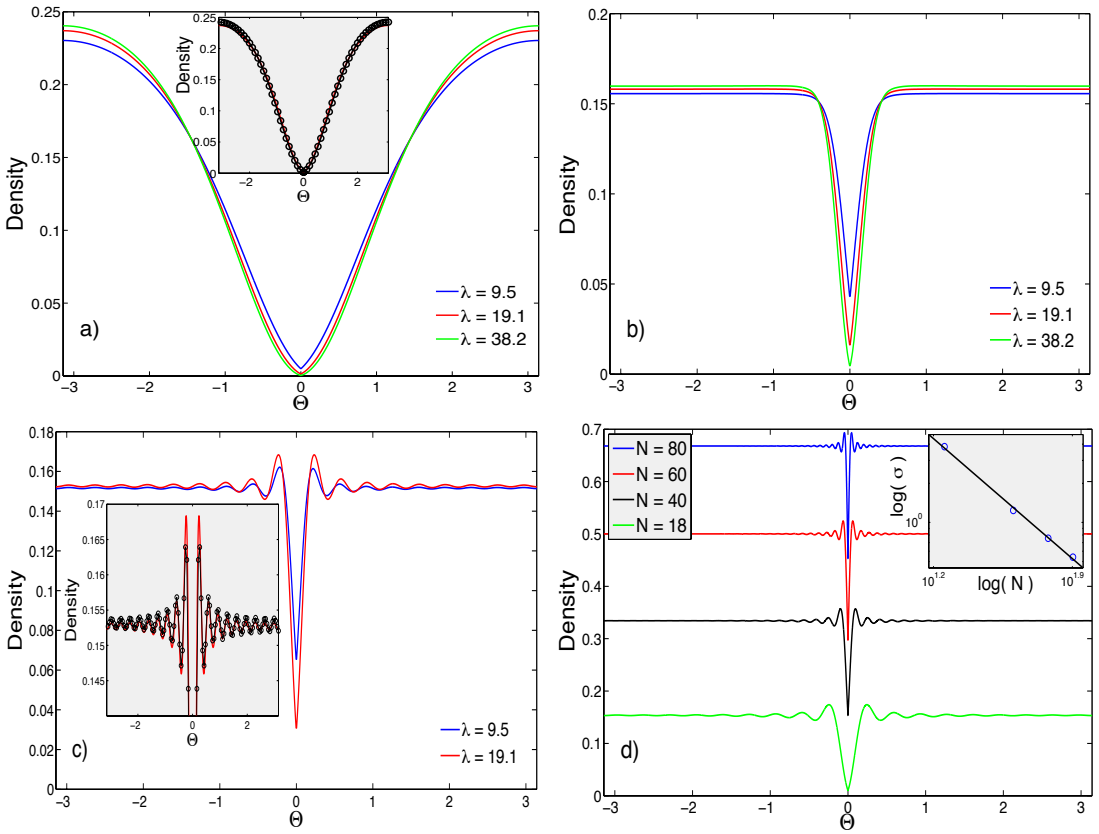

Figure 3.2: Density profiles vs angular coordinate $\Theta = \frac{2\pi}{L}x$ at $L = 120$ and $\Omega = 0$ for different values of the interaction γ and the barrier height λ. (a) Weak interaction at $\gamma = 0.03$, $N = 18$ and $D = 4$. Inset: GP solution (black dots) and cMPS result (red) at $\lambda = 19.1$ (b) Intermediate interaction at $\gamma = 2.33$, $N = 18$ and $D = 10$. (c) Strong interaction at $\gamma = 33$, $N = 18$ and $D = 12$. Inset: DMRG data (black dots) compared to cMPS results (red) at $\lambda = 19.1$. (d) Density profile at fixed $\gamma = 33$, $\lambda = 19.1$ and $L = 120$ but for different particle number $N = 80(D = 18), N = 60(D = 18), N = 40(D = 16)$ and $N = 18(D = 12)$. Inset: loglog plot of the width σ (blue dots) of the central depletion around $\Theta = 0$ as a function of N. The black line is a linear fit indicating an algebraic decay of $\sigma(N)$.

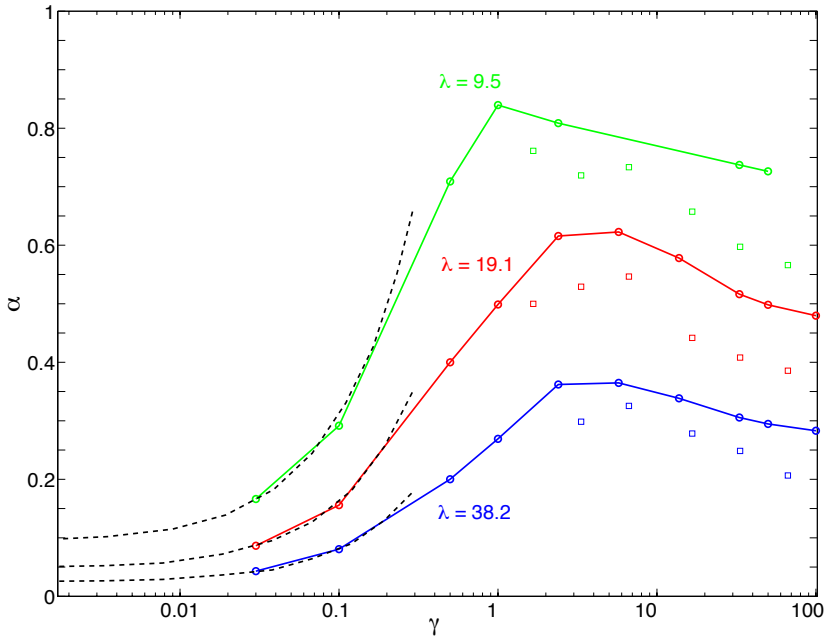

Figure 3.3: Persistent current amplitude in units of $I_0 = 2\pi/mL^2$ as a function of γ for several values of λ at $L = 120$ and $N = 18$. Three different approaches were used: cMPS (dots), DMRG (squares) at $D_{\mathrm{MPS}} = 20$ (and unitary lattice spacing $a = 1$) and GP (black dashed line). The bond dimension increases from $D = 4$ at $\gamma = 0.03$ up to $D = 14$ for $\gamma \geq 5$.

3.4.2 Persistent current amplitude

We will now study the behaviour of the persistent current amplitude as a function of λ and γ. The results presented in Fig. 3.3 are compared to a DMRG based MPS simulation for intermediate and large γ and a classical GP calculation at small γ. It is worth mentioning that the DMRG based lattice approximation is not applicable in the limit of small γ or large densities. In this limit increasing quantum density fluctuations demand for a large occupation number of the local Hilbert basis on the lattice thus making the DMRG simulation computationally inefficient. Moreover, the cosine form of the single particle dispersion relation on the lattice is only at small densities a reasonable approximation of the parabolic dispersion in the continuum. The cMPS itself however is per definition a superposition of states with different particle number and as thus captures the correct physics even at small γ. In fact, the cMPS approach perfectly well describes the non monotonic behaviour of α for the whole range of γ and λ. With increasing γ the bond dimension D has to be increased, since the state gets more and more correlated and sensibly departs from the nearly product state at $\gamma \simeq 0$. The fixed point of T has a fairly large spectral support, and at $\gamma \gg 1$ the largest possible value of D ($D = 20$ in Fig. 3.4) is dictated rather by the computational resources at hand than by the condition number of G. The cMPS ansatz hence interpolates between the classical mean-field solution at small γ and the strongly correlated quantum regime at large γ. This beautifully illustrates the fact that the TDVP equations for cMPS do collapse to the classical GP-equation at $D = 1$ which was recently shown in Ref. [50].

3.4.3 Thermodynamic limit

We are now interested in approaching the thermodynamic limit s.t. both $N, L \to \infty$ at fixed density $\rho = N/L$. It is well known [75] that the ground state energy of the Lieb-Liniger Hamiltonian scales as $E_0^{\mathrm{LL}} = N\rho^2 e(\gamma) = L\rho^3 e(\gamma)$ with e being a dimensionless function depending only on γ. In the presence of a barrier such a scaling is a bit cumbersome as the barrier height $\lambda = mUL/\pi$ itself also depends on L. We will therefore propose a different definition of the barrier height given by

$$\Lambda \equiv mU_0 \frac{L}{N} = \frac{\pi\lambda}{N} \,. \tag{3.12}$$

This definition also holds in the thermodynamic limit and it is easy to see that under the scaling transformation $x \to 1/\rho x$ the ground state energy of (3.8) scales as $E = N\rho^2 f(\gamma, \Lambda)$ with f being now dimensionless as well. Note that the energy dependence on Ω has dropped since the corresponding contributions are only of $\mathcal{O}(1/L)$. In Fig. 3.4 the thermodynamic limit scaling of the ground state energy density is shown at $\gamma = 80, \Lambda = 4$ and $\rho = 0.125$. The cMPS results are further compared to a Tree-Tensor Network (TTN) [39] based lattice simulation. The TTN approach is based on a lattice discretization of the Hamiltonian given in Eq. (3.8), just like the one used for the MPS/DMRG simulations reported above, while the tensor-network structure is taken to be hierarchical: different length-scales in the system are accounted for by different layers of renormalizing tensors. The loop-free topology of this network allows to drastically reduce the computational cost of pbc simulations by exploiting the internal gauge degrees of freedom. It is thus possible to work with much larger bond dimensions similar to those of obc simulations. We find that both cMPS and TTN give the same result for the asymptotic value of the energy density up to an error due to the absence of a finite D scaling. Note that all TTN results were calculated in the continuum limit by considering $\lim_{a\to 0} E(a)$ with a being the lattice spacing in the TTN simulation. It is further instructive to compare the number of variational parameters used in both approaches. In a TTN simulation the number of variational parameters is $(N_{\mathrm{sites}}(d-1)D_{\mathrm{TTN}}^2)$ where d is the local Hilbert space dimension (bosonic occupation $0 \ldots (d-1)$) in the TTN calculation ($d \approx 4$ in all simulations). In comparison, the number of variational parameters in the cMPS is only $(2D^2)$ which is several orders of magnitude smaller compared to the TTN approach for the bond dimensions and system sizes used in Fig. 3.4. To give an example we calculate the energy density at $L = 256$, $\Omega = 0$, $\rho = 0.125$, $\gamma = 80$ and $\Lambda = 4$. The cMPS result at $D = 16$ equal $E/L = 0.0063305(\pm 1\mathrm{e}{-7})$ while the TTN at $D_{\mathrm{TTN}} = 96$ gives $E/L = 0.00632(\pm 1\mathrm{e}{-5})$ (with the cMPS error bar coming from a finite $\epsilon > 0$ as explained in the Supplement Section (3.6.2) and the error in the TTN energy stemming from taking the continuum limit). Quite remarkably, both energies are well compatible even though in the former case only 512 variational parameters had to be optimized while for the latter as much as 28 millions (at $d = 4$ and $a = 1/4$) were taken into account. This a clear advantage of the cMPS ansatz itself independent of the possible variational optimization procedures at hand.

3.5 Outlook and Conclusion

We have developed a time evolution algorithm for uniform cMPS with periodic boundary conditions. The translational invariance of the ansatz is slightly broken as the algorithm also allows for local degrees of freedom encoded in a cMPS boundary matrix. The method is then used to study a rotating bose gas at all interactions which is interrupted by a localised barrier. The results are carefully benchmarked against lattice simulations and classical GP calculations

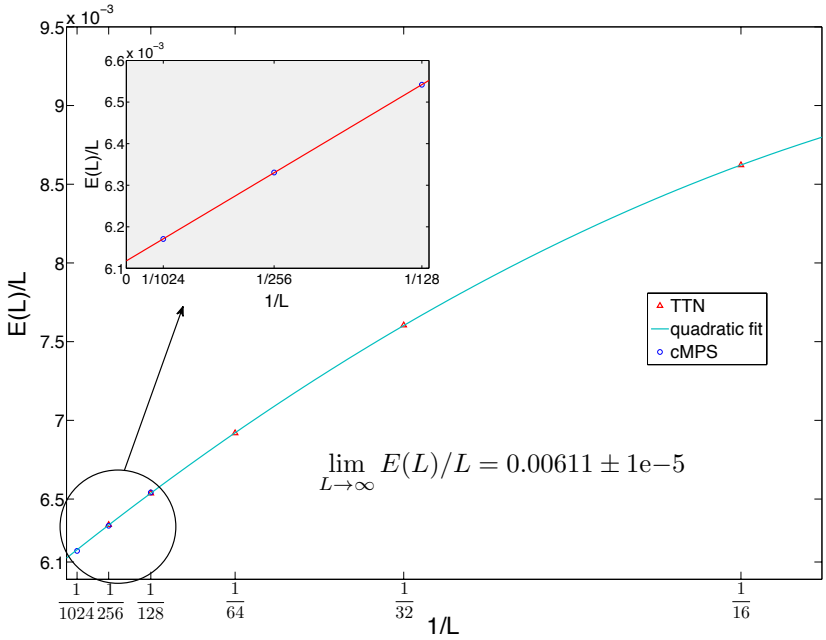

Figure 3.4: Energy density for different system sizes. The TTN simulation (red triangles) was performed at $D_{\mathrm{TTN}} = 96$ while the largest value for the cMPS simulations (blue circles) was $D = 20$ at $L = 1024$. Inset: Linear fit of the cMPS data. All simulations were done at $\Omega = 0$, $\rho = 0.125$, $\gamma = 80$ and $\Lambda = 4$.

showing very good agreement for all interactions. The study of real-time evolution would have gone beyond the scope of this paper but the algorithm is perfectly well suited for dynamical problems as well. Indeed, it is in principle not only possible to study the dynamics of global quenches but also the ones of local quenches in the barrier strength. Moreover, it is possible to generalize the method to case of multiple species or fermions to study e.g. spin currents or spinor condensates which have been recently experimentally realised [7]. Another direction of future research would be to extend the recently introduced cMPS ansatz for low lying excitations [31] to the pbc setting, which would build upon the technics presented in this paper.

3.6 Supplementary Material

3.6.1 Calculation of the Gram matrix and the gradient

We start by calculating the overlap of two tangent vectors which defines the Gram matrix G via Eq. (3.4) in the main text

$$\begin{aligned}
&\langle \Phi[\overline{V},\overline{W},\overline{Y}]\,|\Phi[V,W,Y]\rangle = \\
&\int_0^{\mathrm{L}}\mathrm{d}x\int_x^{\mathrm{L}}\mathrm{d}y\ \mathrm{Tr}\Big[B\otimes\overline{B}\mathrm{e}^{xT}\Big(V\otimes\mathbb{I}+W\otimes\overline{R}\Big)\mathrm{e}^{(y-x)T}\Big(\mathbb{I}\otimes\overline{V}+R\otimes\overline{W}\Big)\mathrm{e}^{(\mathrm{L}-y)T} \\
&\qquad\qquad + B\otimes\overline{B}\mathrm{e}^{xT}\Big(\mathbb{I}\otimes\overline{V}+R\otimes\overline{W}\Big)\mathrm{e}^{(y-x)T}\Big(V\otimes\mathbb{I}+W\otimes\overline{R}\Big)\mathrm{e}^{(\mathrm{L}-y)T}\Big] \\
&+\int_0^{\mathrm{L}}\mathrm{d}x\ \mathrm{Tr}\Big[B\otimes\overline{B}\mathrm{e}^{xT}W\otimes\overline{W}\mathrm{e}^{(\mathrm{L}-x)T}\Big] \\
&+\int_0^{\mathrm{L}}\mathrm{d}x\ \mathrm{Tr}\Big[B\otimes\overline{Y}\mathrm{e}^{xT}\Big(V\otimes\mathbb{I}+W\otimes\overline{R}\Big)\mathrm{e}^{(\mathrm{L}-x)T}\Big] \\
&+\int_0^{\mathrm{L}}\mathrm{d}x\ \mathrm{Tr}\Big[Y\otimes\overline{B}\mathrm{e}^{xT}\Big(\mathbb{I}\otimes\overline{V}+R\otimes\overline{W}\Big)\mathrm{e}^{(\mathrm{L}-x)T}\Big]+\mathrm{Tr}\Big[Y\otimes\overline{Y}\mathrm{e}^{LT}\Big]\,. \qquad (3.13)
\end{aligned}$$

To compute these integrals we insert a spectral decomposition of the transfer matrix T and further define

$$\tilde{T}_i^{m_j}\Big|_{i=1}^{m_j} := \sum_{k=m_j+1}^{D^2}(\lambda_i-\lambda_k)|r_k)(l_k| = \Big[\lambda_i(\mathbb{I}-\sum_{k=1}^{m_j}|r_k)(l_k|)-(T-\sum_{k=1}^{m_j}\lambda_k|r_k)(l_k|)\Big] \quad (3.14)$$

and $\hat{T}_i^{m_j} := \Big(\tilde{T}_i^{m_j}\Big)^2$ where $|r_k)(l_k|$ is the projector on the eigenspace with eigenvalue λ_k of T (we assume that the eigenvalues are non-degenerate) and the integers $m_j < D^2$ being the cut-off. The pseudo inverse of these matrices is denoted by $\Big(\tilde{T}_i^{m_j}\Big)^{\mathrm{p}} = \sum_{k=m_j+1}^{D^2}\frac{1}{(\lambda_i-\lambda_k)}|r_k)(l_k|$ whose action on a vector can be iteratively computed at a computational cost $\mathcal{O}(D^3+m_jD^2)$ by making use of the r.h.s. of Eq. (3.14). We also introduce a third cutoff m_3 such that $\forall i > m_3$, $\mathrm{L}^2/2|\mathrm{e}^{\mathrm{L}\lambda_i}| < tol$. With this definitions the overlap is then found to be as follows.

$$\begin{aligned}
&\langle \Phi[\overline{V},\overline{W},\overline{Y}]\,|\Phi[V,W,Y]\rangle \approx \qquad (3.15)\\
&\Big\{\sum_{i\neq j\neq k=1}^{m_1}\frac{(\lambda_i-\lambda_k)(\mathrm{e}^{\lambda_i\mathrm{L}}-\mathrm{e}^{\lambda_j\mathrm{L}})-(\lambda_i-\lambda_j)(\mathrm{e}^{\lambda_i\mathrm{L}}-\mathrm{e}^{\lambda_k\mathrm{L}})}{(\lambda_i-\lambda_j)(\lambda_i-\lambda_k)(\lambda_j-\lambda_k)}\times \\
&\qquad\qquad \mathrm{Tr}\Big[B\otimes\overline{B}|r_i)(l_i|\Big(V\otimes\mathbb{I}+W\otimes\overline{R}\Big)|r_j)(l_j|\Big(\mathbb{I}\otimes\overline{V}+R\otimes\overline{W}\Big)|r_k)(l_k|\Big] \\
&+\left(\sum_{i\neq j=1}^{m_2}\frac{\mathrm{L}\mathrm{e}^{\lambda_j\mathrm{L}}}{(\lambda_j-\lambda_i)}+\sum_{i\neq j=1}^{m_1}\frac{\mathrm{e}^{\lambda_i\mathrm{L}}-\mathrm{e}^{\lambda_j\mathrm{L}}}{(\lambda_j-\lambda_i)^2}\right)\times \\
&\qquad\qquad \mathrm{Tr}\Big[B\otimes\overline{B}|r_i)(l_i|\Big(V\otimes\mathbb{I}+W\otimes\overline{R}\Big)|r_j)(l_j|\Big(\mathbb{I}\otimes\overline{V}+R\otimes\overline{W}\Big)|r_j)(l_j| \\
&\qquad\qquad\quad + B\otimes\overline{B}|r_j)(l_j|\Big(V\otimes\mathbb{I}+W\otimes\overline{R}\Big)|r_i)(l_i|\Big(\mathbb{I}\otimes\overline{V}+R\otimes\overline{W}\Big)|r_j)(l_j| \\
&\qquad\qquad\quad + B\otimes\overline{B}|r_j)(l_j|\Big(V\otimes\mathbb{I}+W\otimes\overline{R}\Big)|r_j)(l_j|\Big(\mathbb{I}\otimes\overline{V}+R\otimes\overline{W}\Big)|r_i)(l_i|\Big] \\
&+\frac{\mathrm{L}^2}{2}\sum_{i=1}^{m3}\mathrm{e}^{\lambda_i\mathrm{L}}\mathrm{Tr}\Big[B\otimes\overline{B}|r_i)(l_i|\Big(V\otimes\mathbb{I}+W\otimes\overline{R}\Big)|r_i)(l_i|\Big(\mathbb{I}\otimes\overline{V}+R\otimes\overline{W}\Big)|r_i)(l_i|\Big]
\end{aligned}$$

$$
\begin{aligned}
&+\sum_{i\neq j=1}^{m_1}\mathrm{Tr}\Big[B\otimes\overline{B}|r_i)(l_i|\Big(V\otimes\mathbb{I}+W\otimes\overline{R}\Big)|r_j)(l_j|\Big(\mathbb{I}\otimes\overline{V}+R\otimes\overline{W}\Big)\times\\
&\qquad\Big(\frac{\mathrm{e}^{\lambda_i\mathrm{L}}}{(\lambda_i-\lambda_j)}\Big(\tilde{T}_i^{m_1}\Big)^{\mathrm{p}}-\frac{\mathrm{e}^{\lambda_j\mathrm{L}}}{(\lambda_i-\lambda_j)}\Big(\tilde{T}_j^{m_1}\Big)^{\mathrm{p}}\Big)\\
&+\sum_{i\neq k=1}^{m_1}\mathrm{Tr}\Big[B\otimes\overline{B}|r_i)(l_i|\Big(V\otimes\mathbb{I}+W\otimes\overline{R}\Big)\times\\
&\qquad\Big(\frac{\mathrm{e}^{\lambda_i\mathrm{L}}}{(\lambda_i-\lambda_k)}\Big(\tilde{T}_i^{m_1}\Big)^{\mathrm{p}}-\frac{\mathrm{e}^{\lambda_k\mathrm{L}}}{(\lambda_i-\lambda_k)}\Big(\tilde{T}_k^{m_1}\Big)^{\mathrm{p}}\Big)\Big(\mathbb{I}\otimes\overline{V}+R\otimes\overline{W}\Big)|r_k)(l_k|\Big]\\
&+\sum_{j\neq k=1}^{m_1}\mathrm{Tr}\Big[B\otimes\overline{B}\Big(\frac{\mathrm{e}^{\lambda_j\mathrm{L}}}{(\lambda_j-\lambda_k)}\Big(\tilde{T}_j^{m_1}\Big)^{\mathrm{p}}-\frac{\mathrm{e}^{\lambda_k\mathrm{L}}}{(\lambda_j-\lambda_k)}\Big(\tilde{T}_k^{m_1}\Big)^{\mathrm{p}}\Big)\times\\
&\qquad\Big(V\otimes\mathbb{I}+W\otimes\overline{R}\Big)|r_j)(l_j|\Big(\mathbb{I}\otimes\overline{V}+R\otimes\overline{W}\Big)|r_k)(l_k|\Big]
\end{aligned}
$$

$$
\begin{aligned}
&+\sum_{i=1}^{m_1}\mathrm{e}^{\lambda_i\mathrm{L}}\mathrm{Tr}\Big[B\otimes\overline{B}|r_i)(l_i|\Big(V\otimes\mathbb{I}+W\otimes\overline{R}\Big)\Big(\tilde{T}_i^{m_1}\Big)^{\mathrm{p}}\Big(\mathbb{I}\otimes\overline{V}+R\otimes\overline{W}\Big)\Big(\tilde{T}_i^{m_1}\Big)^{\mathrm{p}}\Big]\\
&+\sum_{j=1}^{m_1}\mathrm{e}^{\lambda_j\mathrm{L}}\mathrm{Tr}\Big[B\otimes\overline{B}\Big(\tilde{T}_j^{m_1}\Big)^{\mathrm{p}}\Big(V\otimes\mathbb{I}+W\otimes\overline{R}\Big)|r_j)(l_j|\Big(\mathbb{I}\otimes\overline{V}+R\otimes\overline{W}\Big)\Big(\tilde{T}_j^{m_1}\Big)^{\mathrm{p}}\Big]\\
&+\sum_{k=1}^{m_1}\mathrm{e}^{\lambda_k\mathrm{L}}\mathrm{Tr}\Big[B\otimes\overline{B}\Big(\tilde{T}_k^{m_1}\Big)^{\mathrm{p}}\Big(V\otimes\mathbb{I}+W\otimes\overline{R}\Big)\Big(\tilde{T}_k^{m_1}\Big)^{\mathrm{p}}\Big(\mathbb{I}\otimes\overline{V}+R\otimes\overline{W}\Big)|r_k)(l_k|\Big]
\end{aligned}
$$

$$
\begin{aligned}
&-\sum_{i=1}^{m_1}\mathrm{e}^{\lambda_i\mathrm{L}}\mathrm{Tr}\Big[B\otimes\overline{B}\Big(\hat{T}_i^{m_1}\Big)^{\mathrm{p}}\Big(V\otimes\mathbb{I}+W\otimes\overline{R}\Big)|r_i)(l_i|\Big(\mathbb{I}\otimes\overline{V}+R\otimes\overline{W}\Big)|r_i)(l_i|\Big]\\
&-\sum_{i=1}^{m_1}\mathrm{e}^{\lambda_i\mathrm{L}}\mathrm{Tr}\Big[B\otimes\overline{B}|r_i)(l_i|\Big(V\otimes\mathbb{I}+W\otimes\overline{R}\Big)\Big(\hat{T}_i^{m_1}\Big)^{\mathrm{p}}\Big(\mathbb{I}\otimes\overline{V}+R\otimes\overline{W}\Big)|r_i)(l_i|\Big]\\
&-\sum_{i=1}^{m_1}\mathrm{e}^{\lambda_i\mathrm{L}}\mathrm{Tr}\Big[B\otimes\overline{B}|r_i)(l_i|\Big(V\otimes\mathbb{I}+W\otimes\overline{R}\Big)|r_i)(l_i|\Big(\mathbb{I}\otimes\overline{V}+R\otimes\overline{W}\Big)\Big(\hat{T}_i^{m_1}\Big)^{\mathrm{p}}\Big]
\end{aligned}
$$

$$
\begin{aligned}
&+\mathrm{L}\sum_{i=1}^{m_2}\mathrm{e}^{\lambda_i\mathrm{L}}\mathrm{Tr}\Big[B\otimes\overline{B}\Big(\tilde{T}_i^{m_2}\Big)^{\mathrm{p}}\Big(V\otimes\mathbb{I}+W\otimes\overline{R}\Big)|r_i)(l_i|\Big(\mathbb{I}\otimes\overline{V}+R\otimes\overline{W}\Big)|r_i)(l_i|\Big]\\
&+\mathrm{L}\sum_{i=1}^{m_2}\mathrm{e}^{\lambda_i\mathrm{L}}\mathrm{Tr}\Big[B\otimes\overline{B}|r_i)(l_i|\Big(V\otimes\mathbb{I}+W\otimes\overline{R}\Big)\Big(\tilde{T}_i^{m_2}\Big)^{\mathrm{p}}\Big(\mathbb{I}\otimes\overline{V}+R\otimes\overline{W}\Big)|r_i)(l_i|\Big]\\
&+\mathrm{L}\sum_{i=1}^{m_2}\mathrm{e}^{\lambda_i\mathrm{L}}\mathrm{Tr}\Big[B\otimes\overline{B}|r_i)(l_i|\Big(V\otimes\mathbb{I}+W\otimes\overline{R}\Big)|r_i)(l_i|\Big(\mathbb{I}\otimes\overline{V}+R\otimes\overline{W}\Big)\Big(\tilde{T}_i^{m_2}\Big)^{\mathrm{p}}\Big]\\
&+\Big(V\otimes\mathbb{I}+W\otimes\overline{R}\Big)\leftrightarrow\Big(\mathbb{I}\otimes\overline{V}+R\otimes\overline{W}\Big)\Big\}\\
&+\sum_{i\neq j=1}^{m_1}\frac{\mathrm{e}^{\lambda_i\mathrm{L}}-\mathrm{e}^{\lambda_j\mathrm{L}}}{(\lambda_i-\lambda_j)}\mathrm{Tr}\Big[B\otimes\overline{B}|r_i)(l_i|W\otimes\overline{W}|r_j)(l_j|\Big]
\end{aligned}
$$

$$
\begin{aligned}
&+\mathrm{L}\sum_{i=1}^{m_2}\mathrm{e}^{\lambda_i \mathrm{L}}\mathrm{Tr}\Big[B\otimes\overline{B}|r_i)(l_i|W\otimes\overline{W}|r_i)(l_i|\Big]\\
&+\sum_{i=1}^{m_1}\mathrm{e}^{\lambda_i \mathrm{L}}\mathrm{Tr}\Big[B\otimes\overline{B}|r_i)(l_i|W\otimes\overline{W}\Big(\tilde{T}_i^{m_1}\Big)^{\mathrm{p}}+B\otimes\overline{B}\Big(\tilde{T}_i^{m_1}\Big)^{\mathrm{p}}W\otimes\overline{W}|r_i)(l_i|\Big]\\
&+\sum_{i\neq j=1}^{m_1}\frac{\mathrm{e}^{\lambda_i \mathrm{L}}-\mathrm{e}^{\lambda_j \mathrm{L}}}{(\lambda_i-\lambda_j)}\Big(\mathrm{Tr}\Big[B\otimes\overline{Y}|r_i)(l_i|\Big(V\otimes\mathbb{I}+W\otimes\overline{R}\Big)|r_j)(l_j|\Big]\\
&\qquad\qquad+\mathrm{Tr}\Big[Y\otimes\overline{B}|r_i)(l_i|\Big(\mathbb{I}\otimes\overline{V}+R\otimes\overline{W}\Big)|r_j)(l_j|\Big]\Big)\\
&+\sum_{i=1}^{m_1}\mathrm{e}^{\lambda_i \mathrm{L}}\mathrm{Tr}\Big[B\otimes\overline{Y}|r_i)(l_i|\Big(V\otimes\mathbb{I}+W\otimes\overline{R}\Big)\Big(\tilde{T}_i^{m_1}\Big)^{\mathrm{p}}\\
&\qquad\qquad+B\otimes\overline{Y}\Big(\tilde{T}_i^{m_1}\Big)^{\mathrm{p}}\Big(V\otimes\mathbb{I}+W\otimes\overline{R}\Big)|r_i)(l_i|\Big]\\
&+\sum_{i=1}^{m_1}\mathrm{e}^{\lambda_i \mathrm{L}}\mathrm{Tr}\Big[Y\otimes\overline{B}|r_i)(l_i|\Big(\mathbb{I}\otimes\overline{V}+R\otimes\overline{W}\Big)\Big(\tilde{T}_i^{m_1}\Big)^{\mathrm{p}}\\
&\qquad\qquad+Y\otimes\overline{B}\Big(\tilde{T}_i^{m_1}\Big)^{\mathrm{p}}\Big(\mathbb{I}\otimes\overline{V}+R\otimes\overline{W}\Big)|r_i)(l_i|\Big]\\
&+\mathrm{L}\sum_{i=1}^{m_2}\mathrm{e}^{\lambda_i \mathrm{L}}\Big(\mathrm{Tr}\Big[B\otimes\overline{Y}|r_i)(l_i|\Big(V\otimes\mathbb{I}+W\otimes\overline{R}\Big)|r_i)(l_i|\Big]\\
&\qquad\qquad+\mathrm{Tr}\Big[Y\otimes\overline{B}|r_i)(l_i|\Big(\mathbb{I}\otimes\overline{V}+R\otimes\overline{W}\Big)|r_i)(l_i|\Big]\Big)\\
&+\sum_{i=1}^{m1}\mathrm{e}^{\lambda_i \mathrm{L}}\mathrm{Tr}\Big[Y\otimes\overline{Y}|r_i)(l_i|\Big]\ .
\end{aligned}
\tag{3.16}
$$

The terms in the above expression are ordered as follows. The curly brackets include those terms where three transfer matrices had to be computed giving rise to threefold indexed expressions. Lines $1-5$ have contributions of all three indices being smaller than the corresponding cutoffs m_1, m_2 or m_3. In the very first line all three indices are unequal whereas from line 2 to 4 two of them are equal and in the fifth line all three indices are equal to each other. Lines 6-8 are derived from line 1 but where one index exceeds the cut-off. The next block of lines 9-11 contains the sum of terms from line1 where two indices exceed the cutoff plus the terms from lines 2-4 where the index pair which is equal to each other exceeds the cutoff. The last two blocks of lines 12-14 and 15-17 within the curly brackets are derived from lines 2-4 but where the one index which is unequal to the others exceeds the cutoff. The notation in line 18 is an abbreviation for terms which are the same as the ones inside the curly brackets but where $\Big(V\otimes\mathbb{I}+W\otimes\overline{R}\Big)$ and $\Big(\mathbb{I}\otimes\overline{V}+R\otimes\overline{W}\Big)$ exchange places. Finally, the last seven lines in the whole expression are terms which include only two transfer matrices and the distinction of cases goes along the same lines.

We will now proceed by calculating the *gradient* defined in Eq. (3.5) of the main text for the Hamiltonian $\hat{H}_\epsilon$ defined in the paper. We again refer to [49, 31] for details on cMPS calculus involving a Hamiltonian. The gradient is then defined via the following expression

$$
\begin{aligned}
&\langle\Phi[\overline{V},\overline{W},\overline{Y}]|\,\hat{H}_\epsilon\,|\Psi(Q,R,B)\rangle = \\
&\int_0^{\mathrm{L}}\mathrm{d}x\int_x^{\mathrm{L}}\mathrm{d}y\;\mathrm{Tr}\Big[B\otimes\overline{B}\mathrm{e}^{xT}\Big([Q,R]\otimes[\overline{Q},\overline{R}]+cR^2\otimes\overline{R}^2-\mu R\otimes\overline{R}\Big)\times \\
&\qquad\qquad\qquad\qquad\qquad\qquad\qquad\qquad\mathrm{e}^{(y-x)T}\Big(\mathbb{I}\otimes\overline{V}+R\otimes\overline{W}\Big)\mathrm{e}^{(\mathrm{L}-y)T} \\
&\qquad\qquad+B\otimes\overline{B}\mathrm{e}^{xT}\Big(\mathbb{I}\otimes\overline{V}+R\otimes\overline{W}\Big)\times \\
&\qquad\qquad\qquad\qquad\mathrm{e}^{(y-x)T}\Big([Q,R]\otimes[\overline{Q},\overline{R}]+cR^2\otimes\overline{R}^2-\mu R\otimes\overline{R}\Big)\mathrm{e}^{(\mathrm{L}-y)T}\Big] \\
&+\int_0^{\mathrm{L}}\mathrm{d}x\;\mathrm{Tr}\Big[B\otimes\overline{B}\mathrm{e}^{xT}\Big([Q,R]\otimes([\overline{Q},\overline{W}]+[\overline{V},\overline{R}]) \\
&\qquad\qquad\qquad\qquad+cR^2\otimes(\overline{RW}+\overline{WR})-\mu R\otimes\overline{W}\Big)\mathrm{e}^{(\mathrm{L}-x)T}\Big] \\
&+\frac{U_0}{2}\int_0^{\mathrm{L}}\mathrm{d}x\;\mathrm{Tr}\Big[\Big(BR\otimes\overline{BR}+RB\otimes\overline{RB}\Big)\mathrm{e}^{xT}\Big(\mathbb{I}\otimes\overline{V}+R\otimes\overline{W}\Big)\mathrm{e}^{(\mathrm{L}-x)T}\Big] \\
&+\frac{U_0}{2}\mathrm{Tr}\Big[\Big(BR\otimes\overline{BW}+RB\otimes\overline{WB}\Big)\mathrm{e}^{\mathrm{L}T}\Big] \\
&+\int_0^{\mathrm{L}}\mathrm{d}x\;\mathrm{Tr}\Big[B\otimes\overline{Y}\mathrm{e}^{xT}\Big([Q,R]\otimes[\overline{Q},\overline{R}]+cR^2\otimes\overline{R}^2-\mu R\otimes\overline{R}\Big)\mathrm{e}^{(\mathrm{L}-x)T}\Big] \\
&+\frac{U_0}{2}\mathrm{Tr}\Big[\Big(BR\otimes\overline{YR}+RB\otimes\overline{RY}\Big)\mathrm{e}^{\mathrm{L}T}\Big] \\
&+\int_0^{\mathrm{L}}\mathrm{d}x\;\mathrm{Tr}\Big[\Big\{\frac{1}{\epsilon}\Big(BR-\mathrm{e}^{\mathrm{i}2\pi\Omega}RB\Big)\otimes\Big(\overline{BR}-\mathrm{e}^{-\mathrm{i}2\pi\Omega}\overline{RB}\Big) \\
&\quad+\frac{1}{2}\Big(B[Q,R]+\mathrm{e}^{\mathrm{i}2\pi\Omega}[Q,R]B\Big)\otimes\Big(\overline{BR}-\mathrm{e}^{-\mathrm{i}2\pi\Omega}\overline{RB}\Big) \\
&\quad+\frac{1}{2}\Big(BR-\mathrm{e}^{\mathrm{i}2\pi\Omega}RB\Big)\otimes\Big(\overline{B[Q,R]}+\mathrm{e}^{-\mathrm{i}2\pi\Omega}\overline{[Q,R]B}\Big)\Big\}\mathrm{e}^{xT}\Big(\mathbb{I}\otimes\overline{V}+R\otimes\overline{W}\Big)\mathrm{e}^{(\mathrm{L}-x)T}\Big] \\
&+\frac{1}{\epsilon}\mathrm{Tr}\Big[\Big(BR-\mathrm{e}^{\mathrm{i}2\pi\Omega}RB\Big)\otimes\Big\{\Big(\overline{BW}-\mathrm{e}^{-\mathrm{i}2\pi\Omega}\overline{WB}\Big)+\Big(\overline{YR}-\mathrm{e}^{-\mathrm{i}2\pi\Omega}\overline{RY}\Big)\Big\}\mathrm{e}^{\mathrm{L}T}\Big] \\
&+\frac{1}{2}\mathrm{Tr}\Big[\Big(B[Q,R]+\mathrm{e}^{\mathrm{i}2\pi\Omega}[Q,R]B\Big)\otimes\Big\{\Big(\overline{BW}-\mathrm{e}^{-\mathrm{i}2\pi\Omega}\overline{WB}\Big)+\Big(\overline{YR}-\mathrm{e}^{-\mathrm{i}2\pi\Omega}\overline{RY}\Big)\Big\}\mathrm{e}^{\mathrm{L}T}\Big] \\
&+\frac{1}{2}\mathrm{Tr}\Big[\Big(BR-\mathrm{e}^{\mathrm{i}2\pi\Omega}RB\Big)\otimes\Big\{\Big(\overline{B[Q,W]}+\mathrm{e}^{-\mathrm{i}2\pi\Omega}\overline{[Q,W]B}\Big) \\
&\qquad\qquad+\Big(\overline{B[V,R]}+\mathrm{e}^{-\mathrm{i}2\pi\Omega}\overline{[V,R]B}\Big)+\Big(\overline{Y[Q,R]}+\mathrm{e}^{-\mathrm{i}2\pi\Omega}\overline{[Q,R]Y}\Big)\Big\}\mathrm{e}^{\mathrm{L}T}\Big]\,.
\end{aligned}
\tag{3.17}
$$

The integrals can again be computed in the same way as for the Gram matrix by inserting a spectral decomposition of T giving rise to

$$
\begin{aligned}
&\langle\Phi[\overline{V},\overline{W},\overline{Y}]|\,\hat{H}_\epsilon\,|\Psi(Q,R,B)\rangle \approx \\
&\Big\{\sum_{i\neq j\neq k=1}^{m_1}\frac{(\lambda_i-\lambda_k)(\mathrm{e}^{\lambda_i\mathrm{L}}-\mathrm{e}^{\lambda_j\mathrm{L}})-(\lambda_i-\lambda_j)(\mathrm{e}^{\lambda_i\mathrm{L}}-\mathrm{e}^{\lambda_k\mathrm{L}})}{(\lambda_i-\lambda_j)(\lambda_i-\lambda_k)(\lambda_j-\lambda_k)}\times \\
&\mathrm{Tr}\Big[B\otimes\overline{B}|r_i)(l_i|\Big([Q,R]\otimes[\overline{Q},\overline{R}] \\
&\qquad\qquad+cR^2\otimes\overline{R}^2-\mu R\otimes\overline{R}\Big)|r_j)(l_j|\Big(\mathbb{I}\otimes\overline{V}+R\otimes\overline{W}\Big)|r_k)(l_k|\Big]
\end{aligned}
$$

$$
\begin{aligned}
&+\left(\sum_{i\neq j=1}^{m_2}\frac{\mathrm{L}\mathrm{e}^{\lambda_j \mathrm{L}}}{(\lambda_j-\lambda_i)}+\sum_{i\neq j=1}^{m_1}\frac{\mathrm{e}^{\lambda_i \mathrm{L}}-\mathrm{e}^{\lambda_j \mathrm{L}}}{(\lambda_j-\lambda_i)^2}\right)\times\\
&\mathrm{Tr}\Big[B\otimes\overline{B}|r_i)(l_i|\Big([Q,R]\otimes[\overline{Q},\overline{R}]+cR^2\otimes\overline{R}^2-\mu R\otimes\overline{R}\Big)|r_j)(l_j|\Big(\mathbb{I}\otimes\overline{V}+R\otimes\overline{W}\Big)|r_j)(l_j|\\
&+B\otimes\overline{B}|r_j)(l_j|\Big([Q,R]\otimes[\overline{Q},\overline{R}]+cR^2\otimes\overline{R}^2-\mu R\otimes\overline{R}\Big)|r_i)(l_i|\Big(\mathbb{I}\otimes\overline{V}+R\otimes\overline{W}\Big)|r_j)(l_j|\\
&+B\otimes\overline{B}|r_j)(l_j|\Big([Q,R]\otimes[\overline{Q},\overline{R}]+cR^2\otimes\overline{R}^2-\mu R\otimes\overline{R}\Big)|r_j)(l_j|\Big(\mathbb{I}\otimes\overline{V}+R\otimes\overline{W}\Big)|r_i)(l_i|\Big]\\
&+\frac{\mathrm{L}^2}{2}\sum_{i=1}^{m3}\mathrm{e}^{\lambda_i \mathrm{L}}\mathrm{Tr}\Big[B\otimes\overline{B}|r_i)(l_i|\Big([Q,R]\otimes[\overline{Q},\overline{R}]\\
&\qquad\qquad+cR^2\otimes\overline{R}^2-\mu R\otimes\overline{R}\Big)|r_i)(l_i|\Big(\mathbb{I}\otimes\overline{V}+R\otimes\overline{W}\Big)|r_i)(l_i|\Big]\\
&+\sum_{i\neq j=1}^{m_1}\mathrm{Tr}\Big[B\otimes\overline{B}|r_i)(l_i|\Big([Q,R]\otimes[\overline{Q},\overline{R}]+cR^2\otimes\overline{R}^2-\mu R\otimes\overline{R}\Big)|r_j)(l_j|\\
&\qquad\qquad\times\Big(\mathbb{I}\otimes\overline{V}+R\otimes\overline{W}\Big)\Big(\frac{\mathrm{e}^{\lambda_i \mathrm{L}}}{(\lambda_i-\lambda_j)}\Big(\tilde{T}_i^{m_1}\Big)^{\mathrm{p}}-\frac{\mathrm{e}^{\lambda_j \mathrm{L}}}{(\lambda_i-\lambda_j)}\Big(\tilde{T}_j^{m_1}\Big)^{\mathrm{p}}\Big)\\
&+\sum_{i\neq k=1}^{m_1}\mathrm{Tr}\Big[B\otimes\overline{B}|r_i)(l_i|\Big([Q,R]\otimes[\overline{Q},\overline{R}]+cR^2\otimes\overline{R}^2-\mu R\otimes\overline{R}\Big)\\
&\qquad\qquad\times\Big(\frac{\mathrm{e}^{\lambda_i \mathrm{L}}}{(\lambda_i-\lambda_k)}\Big(\tilde{T}_i^{m_1}\Big)^{\mathrm{p}}-\frac{\mathrm{e}^{\lambda_k \mathrm{L}}}{(\lambda_i-\lambda_k)}\Big(\tilde{T}_k^{m_1}\Big)^{\mathrm{p}}\Big)\Big(\mathbb{I}\otimes\overline{V}+R\otimes\overline{W}\Big)|r_k)(l_k|\Big]\\
&+\sum_{j\neq k=1}^{m_1}\mathrm{Tr}\Big[B\otimes\overline{B}\Big(\frac{\mathrm{e}^{\lambda_j \mathrm{L}}}{(\lambda_j-\lambda_k)}\Big(\tilde{T}_j^{m_1}\Big)^{\mathrm{p}}-\frac{\mathrm{e}^{\lambda_k \mathrm{L}}}{(\lambda_j-\lambda_k)}\Big(\tilde{T}_k^{m_1}\Big)^{\mathrm{p}}\Big)\\
&\qquad\qquad\times\Big([Q,R]\otimes[\overline{Q},\overline{R}]+cR^2\otimes\overline{R}^2-\mu R\otimes\overline{R}\Big)|r_j)(l_j|\Big(\mathbb{I}\otimes\overline{V}+R\otimes\overline{W}\Big)|r_k)(l_k|\Big]\\
&+\sum_{i=1}^{m_1}\mathrm{e}^{\lambda_i \mathrm{L}}\mathrm{Tr}\Big[B\otimes\overline{B}|r_i)(l_i|\Big([Q,R]\otimes[\overline{Q},\overline{R}]+cR^2\otimes\overline{R}^2-\mu R\otimes\overline{R}\Big)\Big(\tilde{T}_i^{m_1}\Big)^{\mathrm{p}}\\
&\qquad\qquad\times\Big(\mathbb{I}\otimes\overline{V}+R\otimes\overline{W}\Big)\Big(\tilde{T}_i^{m_1}\Big)^{\mathrm{p}}\Big]\\
&+\sum_{j=1}^{m_1}\mathrm{e}^{\lambda_j \mathrm{L}}\mathrm{Tr}\Big[B\otimes\overline{B}\Big(\tilde{T}_j^{m_1}\Big)^{\mathrm{p}}\Big([Q,R]\otimes[\overline{Q},\overline{R}]+cR^2\otimes\overline{R}^2-\mu R\otimes\overline{R}\Big)|r_j)(l_j|\\
&\qquad\qquad\times\Big(\mathbb{I}\otimes\overline{V}+R\otimes\overline{W}\Big)\Big(\tilde{T}_j^{m_1}\Big)^{\mathrm{p}}\Big]\\
&+\sum_{k=1}^{m_1}\mathrm{e}^{\lambda_k \mathrm{L}}\mathrm{Tr}\Big[B\otimes\overline{B}\Big(\tilde{T}_k^{m_1}\Big)^{\mathrm{p}}\Big([Q,R]\otimes[\overline{Q},\overline{R}]+cR^2\otimes\overline{R}^2-\mu R\otimes\overline{R}\Big)\Big(\tilde{T}_k^{m_1}\Big)^{\mathrm{p}}\\
&\qquad\qquad\times\Big(\mathbb{I}\otimes\overline{V}+R\otimes\overline{W}\Big)|r_k)(l_k|\Big]\\
&-\sum_{i=1}^{m_1}\mathrm{e}^{\lambda_i \mathrm{L}}\mathrm{Tr}\Big[B\otimes\overline{B}\Big(\hat{T}_i^{m_1}\Big)^{\mathrm{p}}\Big([Q,R]\otimes[\overline{Q},\overline{R}]+cR^2\otimes\overline{R}^2-\mu R\otimes\overline{R}\Big)|r_i)(l_i|\\
&\qquad\qquad\times\Big(\mathbb{I}\otimes\overline{V}+R\otimes\overline{W}\Big)|r_i)(l_i|\Big]
\end{aligned}
$$

$$
\begin{aligned}
&- \sum_{i=1}^{m_1} \mathrm{e}^{\lambda_i \mathrm{L}} \mathrm{Tr}\Big[B \otimes \overline{B} | r_i)(l_i | \Big([Q,R] \otimes [\overline{Q},\overline{R}] + cR^2 \otimes \overline{R}^2 - \mu R \otimes \overline{R} \Big) \Big(\hat{T}_i^{m_1} \Big)^{\mathrm{p}} \\
&\qquad\qquad \times \Big(\mathbb{I} \otimes \overline{V} + R \otimes \overline{W} \Big) | r_i)(l_i | \Big] \\
&- \sum_{i=1}^{m_1} \mathrm{e}^{\lambda_i \mathrm{L}} \mathrm{Tr}\Big[B \otimes \overline{B} | r_i)(l_i | \Big([Q,R] \otimes [\overline{Q},\overline{R}] + cR^2 \otimes \overline{R}^2 - \mu R \otimes \overline{R} \Big) | r_i)(l_i | \\
&\qquad\qquad \times \Big(\mathbb{I} \otimes \overline{V} + R \otimes \overline{W} \Big) \Big(\hat{T}_i^{m_1} \Big)^{\mathrm{p}} \Big] \\
&+ \mathrm{L} \sum_{i=1}^{m_2} \mathrm{e}^{\lambda_i \mathrm{L}} \mathrm{Tr}\Big[B \otimes \overline{B} \Big(\tilde{T}_i^{m_2} \Big)^{\mathrm{p}} \Big([Q,R] \otimes [\overline{Q},\overline{R}] + cR^2 \otimes \overline{R}^2 - \mu R \otimes \overline{R} \Big) | r_i)(l_i | \\
&\qquad\qquad \times \Big(\mathbb{I} \otimes \overline{V} + R \otimes \overline{W} \Big) | r_i)(l_i | \Big] \\
&+ \mathrm{L} \sum_{i=1}^{m_2} \mathrm{e}^{\lambda_i \mathrm{L}} \mathrm{Tr}\Big[B \otimes \overline{B} | r_i)(l_i | \Big([Q,R] \otimes [\overline{Q},\overline{R}] + cR^2 \otimes \overline{R}^2 - \mu R \otimes \overline{R} \Big) \Big(\tilde{T}_i^{m_2} \Big)^{\mathrm{p}} \\
&\qquad\qquad \times \Big(\mathbb{I} \otimes \overline{V} + R \otimes \overline{W} \Big) | r_i)(l_i | \Big] \\
&+ \mathrm{L} \sum_{i=1}^{m_2} \mathrm{e}^{\lambda_i \mathrm{L}} \mathrm{Tr}\Big[B \otimes \overline{B} | r_i)(l_i | \Big([Q,R] \otimes [\overline{Q},\overline{R}] + cR^2 \otimes \overline{R}^2 - \mu R \otimes \overline{R} \Big) | r_i)(l_i | \\
&\qquad\qquad \times \Big(\mathbb{I} \otimes \overline{V} + R \otimes \overline{W} \Big) \Big(\tilde{T}_i^{m_2} \Big)^{\mathrm{p}} \Big] \\
&+ \Big([Q,R] \otimes [\overline{Q},\overline{R}] + cR^2 \otimes \overline{R}^2 - \mu R \otimes \overline{R} \Big) \leftrightarrow \Big(\mathbb{I} \otimes \overline{V} + R \otimes \overline{W} \Big) \Big\} \\
&+ \sum_{i \neq j=1}^{m_1} \frac{\mathrm{e}^{\lambda_i \mathrm{L}} - \mathrm{e}^{\lambda_j \mathrm{L}}}{(\lambda_i - \lambda_j)} \mathrm{Tr}\Big[B \otimes \overline{B} | r_i)(l_i | \Big([Q,R] \otimes ([\overline{Q},\overline{W}] + [\overline{V},\overline{R}]) \\
&\qquad\qquad + cR^2 \otimes (\overline{RW} + \overline{WR}) - \mu R \otimes \overline{W} \Big) | r_j)(l_j | \Big] \\
&+ \sum_{i=1}^{m_1} \mathrm{e}^{\lambda_i \mathrm{L}} \mathrm{Tr}\Big[B \otimes \overline{B} | r_i)(l_i | \Big([Q,R] \otimes ([\overline{Q},\overline{W}] + [\overline{V},\overline{R}]) \\
&\qquad\qquad + cR^2 \otimes (\overline{RW} + \overline{WR}) - \mu R \otimes \overline{W} \Big) \Big(\tilde{T}_i^{m_1} \Big)^{\mathrm{p}} \\
&\qquad + B \otimes \overline{B} \Big(\tilde{T}_i^{m_1} \Big)^{\mathrm{p}} \Big([Q,R] \otimes ([\overline{Q},\overline{W}] + [\overline{V},\overline{R}]) \\
&\qquad\qquad + cR^2 \otimes (\overline{RW} + \overline{WR}) - \mu R \otimes \overline{W} \Big) | r_i)(l_i | \Big] \\
&+ \mathrm{L} \sum_{i=1}^{m_2} \mathrm{e}^{\lambda_i \mathrm{L}} \mathrm{Tr}\Big[B \otimes \overline{B} | r_i)(l_i | \Big([Q,R] \otimes ([\overline{Q},\overline{W}] + [\overline{V},\overline{R}]) \\
&\qquad\qquad + cR^2 \otimes (\overline{RW} + \overline{WR}) - \mu R \otimes \overline{W} \Big) | r_i)(l_i | \Big] \\
&+ \frac{U_0}{2} \sum_{i \neq j=1}^{m_1} \frac{\mathrm{e}^{\lambda_i \mathrm{L}} - \mathrm{e}^{\lambda_j \mathrm{L}}}{(\lambda_i - \lambda_j)} \mathrm{Tr}\Big[\Big(BR \otimes \overline{BR} + RB \otimes \overline{RB} \Big) | r_i)(l_i | \Big(\mathbb{I} \otimes \overline{V} + R \otimes \overline{W} \Big) | r_j)(l_j | \Big] \\
&+ \frac{U_0}{2} \sum_{i=1}^{m_1} \mathrm{e}^{\lambda_i \mathrm{L}} \mathrm{Tr}\Big[\Big(BR \otimes \overline{BR} + RB \otimes \overline{RB} \Big) | r_i)(l_i | \Big(\mathbb{I} \otimes \overline{V} + R \otimes \overline{W} \Big) \Big(\tilde{T}_i^{m_1} \Big)^{\mathrm{p}}
\end{aligned}
$$

$$
\begin{aligned}
&\quad + \Big(BR\otimes\overline{BR} + RB\otimes\overline{RB}\Big)\Big(\tilde{T}_i^{m_1}\Big)^{\mathrm{p}}\Big(\mathbb{I}\otimes\overline{V} + R\otimes\overline{W}\Big)|r_i)(l_i|\Big] \\
&+ \mathrm{L}\frac{U_0}{2}\sum_{i=1}^{m_2}\mathrm{e}^{\lambda_i \mathrm{L}}\mathrm{Tr}\Big[\Big(BR\otimes\overline{BR} + RB\otimes\overline{RB}\Big)|r_i)(l_i|\Big(\mathbb{I}\otimes\overline{V} + R\otimes\overline{W}\Big)|r_i)(l_i|\Big] \\
&+ \frac{U_0}{2}\sum_{i=1}^{m_1}\mathrm{e}^{\lambda_i \mathrm{L}}\mathrm{Tr}\Big[\Big(BR\otimes\overline{BW} + RB\otimes\overline{WB}\Big)|r_i)(l_i|\Big] \\
&+ \sum_{i\neq j=1}^{m_1}\frac{\mathrm{e}^{\lambda_i \mathrm{L}} - \mathrm{e}^{\lambda_j \mathrm{L}}}{(\lambda_i-\lambda_j)}\mathrm{Tr}\Big[B\otimes\overline{Y}|r_i)(l_i|\Big([Q,R]\otimes[\overline{Q},\overline{R}] + cR^2\otimes\overline{R}^2 - \mu R\otimes\overline{R}\Big)|r_j)(l_j|\Big] \\
&+ \sum_{i=1}^{m_1}\mathrm{e}^{\lambda_i \mathrm{L}}\mathrm{Tr}\Big[B\otimes\overline{Y}|r_i)(l_i|\Big([Q,R]\otimes[\overline{Q},\overline{R}] + cR^2\otimes\overline{R}^2 - \mu R\otimes\overline{R}\Big)\Big(\tilde{T}_i^{m_1}\Big)^{\mathrm{p}} \\
&\qquad + B\otimes\overline{Y}\Big(\tilde{T}_i^{m_1}\Big)^{\mathrm{p}}\Big([Q,R]\otimes[\overline{Q},\overline{R}] + cR^2\otimes\overline{R}^2 - \mu R\otimes\overline{R}\Big)|r_i)(l_i|\Big] \\
&+ \frac{U_0}{2}\sum_{i=1}^{m_1}\mathrm{e}^{\lambda_i \mathrm{L}}\mathrm{Tr}\Big[\Big(BR\otimes\overline{YR} + RB\otimes\overline{RY}\Big)|r_i)(l_i|\Big] \\
&+ \sum_{i\neq j=1}^{m_1}\frac{\mathrm{e}^{\lambda_i \mathrm{L}} - \mathrm{e}^{\lambda_j \mathrm{L}}}{(\lambda_i-\lambda_j)}\mathrm{Tr}\Big[\Big\{\frac{1}{\epsilon}\Big(BR - \mathrm{e}^{\mathrm{i}2\pi\Omega}RB\Big)\otimes\Big(\overline{BR} - \mathrm{e}^{-\mathrm{i}2\pi\Omega}\overline{RB}\Big) \\
&\qquad + \frac{1}{2}\Big(B[Q,R] + \mathrm{e}^{\mathrm{i}2\pi\Omega}[Q,R]B\Big)\otimes\Big(\overline{BR} - \mathrm{e}^{-\mathrm{i}2\pi\Omega}\overline{RB}\Big) \\
&\qquad + \frac{1}{2}\Big(BR - \mathrm{e}^{\mathrm{i}2\pi\Omega}RB\Big)\otimes\Big(\overline{B[Q,R]} + \mathrm{e}^{-\mathrm{i}2\pi\Omega}\overline{[Q,R]B}\Big)\Big\} \\
&\qquad\qquad \times |r_i)(l_i|\Big(\mathbb{I}\otimes\overline{V} + R\otimes\overline{W}\Big)|r_j)(l_j|\Big] \\
&+ \sum_{i=1}^{m_1}\mathrm{e}^{\lambda_i \mathrm{L}}\mathrm{Tr}\Big[\Big\{\frac{1}{\epsilon}\Big(BR - \mathrm{e}^{\mathrm{i}2\pi\Omega}RB\Big)\otimes\Big(\overline{BR} - \mathrm{e}^{-\mathrm{i}2\pi\Omega}\overline{RB}\Big) \\
&\qquad + \frac{1}{2}\Big(B[Q,R] + \mathrm{e}^{\mathrm{i}2\pi\Omega}[Q,R]B\Big)\otimes\Big(\overline{BR} - \mathrm{e}^{-\mathrm{i}2\pi\Omega}\overline{RB}\Big) \\
&\qquad + \frac{1}{2}\Big(BR - \mathrm{e}^{\mathrm{i}2\pi\Omega}RB\Big)\otimes\Big(\overline{B[Q,R]} + \mathrm{e}^{-\mathrm{i}2\pi\Omega}\overline{[Q,R]B}\Big)\Big\} \\
&\qquad\qquad \times \Big\{|r_i)(l_i|\Big(\mathbb{I}\otimes\overline{V} + R\otimes\overline{W}\Big)\Big(\tilde{T}_i^{m_1}\Big)^{\mathrm{p}} \\
&\qquad\qquad + \Big(\tilde{T}_i^{m_1}\Big)^{\mathrm{p}}\Big(\mathbb{I}\otimes\overline{V} + R\otimes\overline{W}\Big)|r_i)(l_i|\Big\}\Big] \\
&+ \mathrm{L}\sum_{i=1}^{m_2}\mathrm{e}^{\lambda_i \mathrm{L}}\mathrm{Tr}\Big[\Big\{\frac{1}{\epsilon}\Big(BR - \mathrm{e}^{\mathrm{i}2\pi\Omega}RB\Big)\otimes\Big(\overline{BR} - \mathrm{e}^{-\mathrm{i}2\pi\Omega}\overline{RB}\Big) \\
&\qquad + \frac{1}{2}\Big(B[Q,R] + \mathrm{e}^{\mathrm{i}2\pi\Omega}[Q,R]B\Big)\otimes\Big(\overline{BR} - \mathrm{e}^{-\mathrm{i}2\pi\Omega}\overline{RB}\Big) \\
&\qquad + \frac{1}{2}\Big(BR - \mathrm{e}^{\mathrm{i}2\pi\Omega}RB\Big)\otimes\Big(\overline{B[Q,R]} + \mathrm{e}^{-\mathrm{i}2\pi\Omega}\overline{[Q,R]B}\Big)\Big\} \\
&\qquad\qquad \times |r_i)(l_i|\Big(\mathbb{I}\otimes\overline{V} + R\otimes\overline{W}\Big)|r_i)(l_i|\Big] \\
&+ \sum_{i=1}^{m_1}\mathrm{e}^{\lambda_i \mathrm{L}}\frac{1}{\epsilon}\mathrm{Tr}\Big[\Big(BR - \mathrm{e}^{\mathrm{i}2\pi\Omega}RB\Big)\otimes\Big\{\Big(\overline{BW} - \mathrm{e}^{-\mathrm{i}2\pi\Omega}\overline{WB}\Big) \\
&\qquad\qquad + \Big(\overline{YR} - \mathrm{e}^{-\mathrm{i}2\pi\Omega}\overline{RY}\Big)\Big\}|r_i)(l_i|\Big]
\end{aligned}
$$

$$+\sum_{i=1}^{m_1} \mathrm{e}^{\lambda_i \mathrm{L}} \frac{1}{2} \mathrm{Tr}\Big[\Big(B[Q,R] + \mathrm{e}^{\mathrm{i}2\pi\Omega}[Q,R]B\Big) \otimes \Big\{\Big(\overline{BW} - \mathrm{e}^{-\mathrm{i}2\pi\Omega}\overline{WB}\Big) + \Big(\overline{YR} - \mathrm{e}^{-\mathrm{i}2\pi\Omega}\overline{RY}\Big)\Big\}|r_i)(l_i|\Big]$$

$$+\sum_{i=1}^{m_1} \mathrm{e}^{\lambda_i \mathrm{L}} \frac{1}{2} \mathrm{Tr}\Big[\Big(BR - \mathrm{e}^{\mathrm{i}2\pi\Omega}RB\Big) \otimes \Big\{\Big(\overline{B[Q,W]} + \mathrm{e}^{-\mathrm{i}2\pi\Omega}\overline{[Q,W]B}\Big) + \Big(\overline{B[V,R]} + \mathrm{e}^{-\mathrm{i}2\pi\Omega}\overline{[V,R]B}\Big) + \Big(\overline{Y[Q,R]} + \mathrm{e}^{-\mathrm{i}2\pi\Omega}\overline{[Q,R]Y}\Big)\Big\}|r_i)(l_i|\Big] . \tag{3.18}$$

The ordering of the terms in the above expression goes along the same lines as for the calculation of the Gram matrix. Moreover, the abbreviation $(...) \leftrightarrow (...)$ has to be understood as the sum of all the terms inside the corresponding curly brackets but with the two brackets exchanged. Note that in principle one can choose a different (smaller) *tol* in the computation of the gradient as for the computation of the Gram matrix which leads to different (larger) integers m_1, m_2 and m_3 respectively.

To conclude, we will calculate the vector $[y_1; y_2; y_3]$ which was introduced in section 3.2 of the main paper. The calculation goes along the same lines as for the Gram matrix and the gradient and we find that Eq. (3.6) can be approximated by

$$\Big\langle \Phi[\overline{V},\overline{W},\overline{Y}] \,\Big|\, \Psi(Q,R,B) \Big\rangle \approx$$

$$\sum_{i=1}^{m_1} \mathrm{e}^{\lambda_i \mathrm{L}} \mathrm{Tr}\Big[B \otimes \overline{B} (\tilde{T}_i^{m_1})^{\mathrm{p}} \Big(\mathbb{I} \otimes \overline{V} + R \otimes \overline{W}\Big) |r_i)(l_i| + |r_i)(l_i| \Big(\mathbb{I} \otimes \overline{V} + R \otimes \overline{W}\Big) (\tilde{T}_i^{m_1})^{\mathrm{p}} B \otimes \overline{B}\Big] \tag{3.19}$$

$$+ \sum_{\mathrm{i}\neq k=1}^{m_1} \frac{\mathrm{e}^{\lambda_i \mathrm{L}} - \mathrm{e}^{\lambda_k \mathrm{L}}}{\lambda_i - \lambda_k} \mathrm{Tr}\Big[B \otimes \overline{B} |r_i)(l_i| \Big(\mathbb{I} \otimes \overline{V} + R \otimes \overline{W}\Big) |r_k)(l_k|\Big] \tag{3.20}$$

$$+ \mathrm{L} \sum_{i=1}^{m_2} \mathrm{e}^{\lambda_i \mathrm{L}} \mathrm{Tr}\Big[B \otimes \overline{B} |r_i)(l_i| \Big(\mathbb{I} \otimes \overline{V} + R \otimes \overline{W}\Big) |r_i)(l_i|\Big] . \tag{3.21}$$

3.6.2 Scaling behaviour of the ground state energy and finite D scaling of the density profiles

Next we will discus the dependence of the ground state energy of Hamiltonian (3.10) on the cutoff ϵ around position $x = 0$. The Hamiltonain is thus split into two parts, $\hat{H}_\epsilon = \hat{H}_{\mathrm{bulk}} + \hat{H}_{\mathrm{boundary}}$, where the *bulk* part equals to the first line in (3.10) and the *boundary* term consists of the remaining three lines in (3.10). We are interested in the scaling of the respective ground state energies $E_{\mathrm{bulk}}(\epsilon)$ and $E_{\mathrm{boundary}}(\epsilon)$ at a fixed bond dimension D. Fig.(3.5) shows that both converge linearly with ϵ, with quadratic corrections in $E_{\mathrm{bulk}}(\epsilon)$ (left panel) not visible in the plotted region for $E_{\mathrm{boundary}}(\epsilon)$ (right panel). The asymptotic value $\lim_{\epsilon\to 0} E_{\mathrm{boundary}}(\epsilon)$ decreases with increasing D and is found to be $\mathcal{O}(10^{-6})$ already at $D = 16$. In the main text we have chosen $\epsilon = 2.5 \times 10^{-3}$ which corresponds to an error in the energy density of the bulk of roughly 10^{-8} (in comparison to $\lim_{\epsilon\to 0} E_{\mathrm{bulk}}(\epsilon)/L$). A sensitive measure for how well the twisted boundary conditions are imposed is given by $||BR - \mathrm{e}^{\mathrm{i}2\pi\Omega}RB||_{\mathrm{cMPS}}$, where

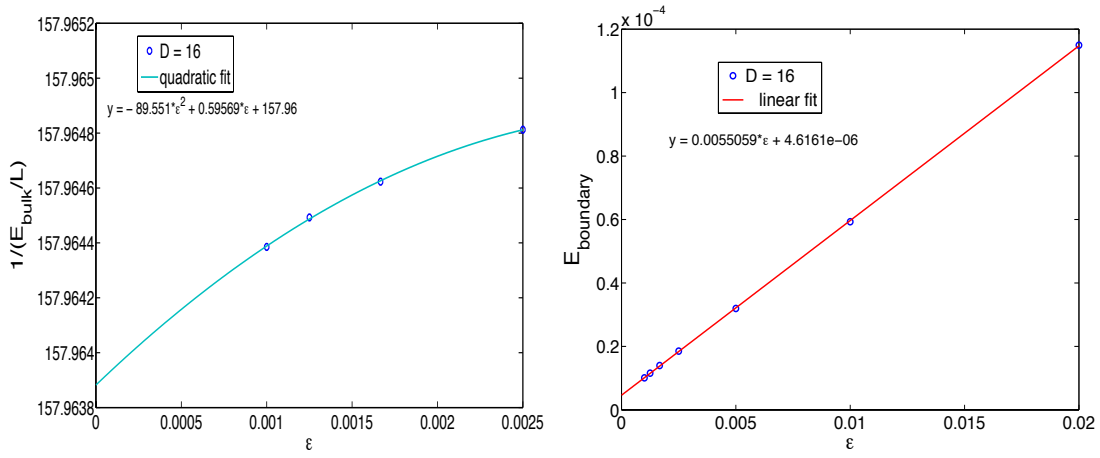

Figure 3.5: Left: Inverse ground state energy density of the bulk as a function of the cutoff ϵ. Right: Ground state expectation value of the boundary terms in Hamiltonain (3.10) for several values of ϵ. The other parameters in both panels are $D = 16$, $L = 256$, $N = 32$, $\gamma = 80$, $\Lambda = 4$ and $\Omega = 0$.

the norm $||.||_{\mathrm{cMPS}}$ is weighted by the proper cMPS metric given by $\mathrm{e}^{\mathrm{L}T}$. This is precisely the cMPS expectation value of $(\psi(0) - \mathrm{e}^{\mathrm{i}2\pi\Omega}\psi(\mathrm{L}))^\dagger(\psi(0) - \mathrm{e}^{\mathrm{i}2\pi\Omega}\psi(\mathrm{L}))$ and thus has to decrease linearly for small enough ϵ as can be seen from the right panel of Fig.(3.5). In fact this value is $\mathcal{O}(10^{-8})$ for $\epsilon = 2.5 \times 10^{-3}$ indicating that the twisted boundary conditions are very well approximated even for relatively large $\epsilon > 0$. To conclude, it is perfectly well justified to consider only $E_{\mathrm{bulk}}(\epsilon)$ as the true approximation to the exact ground state energy as long as ϵ is chosen small enough.

Finally, we are interested in the convergence behaviour of the density profiles with increasing bond dimension. In Fig.(3.6) we show density profiles for three different values of D while having all other parameters fixed. As mentioned in section 3.4 we observe that the profiles converge from inside to the outside as the effective cMPS correlation length increases. The central depletion has already almost converged at the lowest value of D while for this value the behaviour in the bulk is still pretty off as can be seen from the strongly damped Friedel oscillations in the inset of Fig.(3.6) in comparison to predictions of Luttinger liquid theory for the Lieb-Liniger model with obc [15].

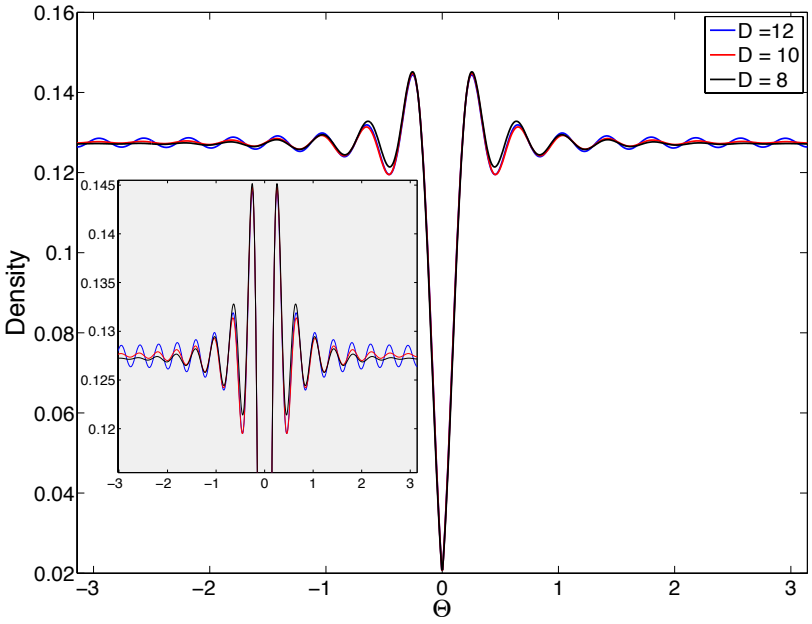

Figure 3.6: Density profile for three different values of D at $L = 128$, $N = 16$, $\gamma = 80$, $\Lambda = 4$ and $\Omega = 0$. The inset shows a zoom around the bulk value of the density.

Conclusions and Outlook

In conclusion, we have presented several variational optimization methods and time evolution algorithms for the class of continuous Matrix Product States. In particular, we generalized the well known Gross-Pitaevskii equation (GPE) to the one dimensional case where quantum correlations and entanglement prevent the application of mean-field theories. The methods are thoroughly benchmarked against exact results and other numerical methods, thereby providing evidence for their excellent description of strongly correlated one dimensional quantum field theories. These methods also significantly contribute to the methodological toolbox for cMPS.

More specifically, in chapter 1 we introduced a variational method to calculate low lying excitations of extended one dimensional quantum field theories. This method is based upon applying the Rayleigh-Ritz principle to the class of uniform cMPS in the thermodynamic limit. The method is benchmark against the Lieb-Liniger model and we find perfect agreement between the numerical results and the exact solutions. More specifically, Lieb's Type I and Type II excitations are revealed as topological excitations within our ansatz and we identify clear solitonic signatures in the latter for weak interactions. Moreover, a non-integrable version of the Lieb-Liniger model is studied and it was possible to identify non trivial bound states in the spectrum of this model.

In chapter 2 we applied the time-dependent variational principle to the class of non-uniform cMPS with open boundary conditions. The resulting equations generalize the GPE to the one dimensional case by including quantum correlations. Linearizing these quantum Gross-Pitaevskii equations (qGPE) gives rise to a quantum version of the Bogoliubov de-Gennes equations. These equations are then used to calculate the response of the Lieb-Liniger ground state against weak external perturbations at all interactions.

Furthermore, in chapter 3 we have extended the time evolution algorithm of chapter 2 to the case of uniform cMPS with periodic boundary conditions. The cMPS is however not completely uniform as additional boundary degrees of freedom are included that allow to study quantum impurity problems. Systems with ring shaped geometries became recently more and more important as they constitute the building blocks in the emerging field of atomtronics. Here, we focused on the typical example of an atomtronic system, i.e a rotating Bose Gas loaded in a ring shaped trap that is interrupted by a localised barrier. We studied density profiles and the persistent current's amplitude as a function of both the interaction and the barrier height. The cMPS results were thoroughly benchmarked against classical GP calculations for weak interactions and DMRG (or TTN) based lattice simulations at large interactions. We find that the cMPS ansatz interpolates between these two regimes and gives the correct result at all interactions.

The algorithms presented in chapter 1 and 3 can be in principle applied to a plethora of different problems, without the need of further substantial methodological improvements, as none of these methods is restricted to a specific model. Despite some efforts, we were however not able to develop a well suited numerical integration scheme for the full qGPE presented in chapter 2. This is certainly a drawback of this method but it should not be (miss-) interpreted as the ultima ratio but rather as the state of the art of an ongoing research project. Indeed, even the GPE itself is still an object of intense research even though it first appeared already 70 years ago. Moreover, we developed a perturbative approach (in the external potential) to solve the qGPE. This already allows the study of many important problems without having to address the qGPE in the most general case.

Bibliography

[1] D. A. TAKAHASHI, *One-dimensional integrable spinor becs mapped to matrix nonlinear schrödinger equation and solution of bogoliubov equation in these systems*, Journal of the Physical Society of Japan, 80 (2010), p. 015002.

[2] M. J. ABLOWITZ, *Nonlinear Dispersive Waves: Asymptotic Analysis and Solitons*, Cambridge University Press, 2011.

[3] I. AFFLECK, T. KENNEDY, E. H. LIEB, AND H. TASAKI, *Rigorous results on valence-bond ground states in antiferromagnets*, Phys. Rev. Lett., 59 (1987), pp. 799–802.

[4] G. E. ASTRAKHARCHIK AND L. P. PITAEVSKII, *Lieb's soliton-like excitations in harmonic trap*, ArXiv e-prints: 1210.8337, (2012).

[5] V. BAGNATO AND D. KLEPPNER, *Bose-einstein condensation in low-dimensional traps*, Phys. Rev. A, 44 (1991), pp. 7439–7441.

[6] W. BAO, D. JAKSCH, AND P. A. MARKOWICH, *Numerical solution of the gross-pitaevskii equation for bose-einstein condensation*, Journal of Computational Physics, 187 (2003), pp. 318–342.

[7] S. BEATTIE, S. MOULDER, R. J. FLETCHER, AND Z. HADZIBABIC, *Persistent currents in spinor condensates*, Phys. Rev. Lett., 110 (2013), p. 025301.

[8] C. BECKER, S. STELLMER, P. SOLTAN-PANAHI, S. DÖRSCHER, M. BAUMERT, E.-M. RICHTER, J. KRONJÄGER, K. BONGS, AND K. SENGSTOCK, *Oscillations and interactions of dark and dark bright solitons in Bose Einstein condensates*, Nature Physics, 4 (2008), pp. 496–501.

[9] F. BLOCH, *Superfluidity in a ring*, Phys. Rev. A, 7 (1973), pp. 2187–2191.

[10] N. N. BOGOLYUBOV, *On the theory of superfluidity*, J. Phys.(USSR), 11 (1947), pp. 23–32. [Izv. Akad. Nauk Ser. Fiz.11,77(1947)].

[11] S. BURGER, K. BONGS, S. DETTMER, W. ERTMER, K. SENGSTOCK, A. SANPERA, G. V. SHLYAPNIKOV, AND M. LEWENSTEIN, *Dark solitons in bose-einstein condensates*, Phys. Rev. Lett., 83 (1999).

[12] V. BUSLAEV AND G. PERELMAN, *On the stability of solitary waves for nonlinear schrodinger equations*, Translations of the American Mathematical Society-Series 2, 164 (1995), pp. 75–98.

[13] Y. CASTIN AND R. DUM, *Low-temperature bose-einstein condensates in time-dependent traps: Beyond the $u(1)$ symmetry-breaking approach*, Phys. Rev. A, 57 (1998), pp. 3008–3021.

[14] J.-S. CAUX AND P. CALABRESE, *Dynamical density-density correlations in the one-dimensional bose gas*, Phys. Rev. A, 74 (2006), p. 031605.

[15] M. A. CAZALILLA, *Bosonizing one-dimensional cold atomic gases*, Journal of Physics B: Atomic, Molecular and Optical Physics, 37 (2004), p. S1.

[16] M. A. CAZALILLA, R. CITRO, T. GIAMARCHI, E. ORIGNAC, AND M. RIGOL, *One dimensional bosons: From condensed matter systems to ultracold gases*, Rev. Mod. Phys., 83 (2011), pp. 1405–1466.

[17] M. A. CAZALILLA AND A. F. HO, *Instabilities in binary mixtures of one-dimensional quantum degenerate gases*, Phys. Rev. Lett., 91 (2003), p. 150403.

[18] X. CHEN, Z.-C. GU, Z.-X. LIU, AND X.-G. WEN, *Symmetry protected topological orders and the group cohomology of their symmetry group*, Phys. Rev. B, 87 (2013), p. 155114.

[19] X. CHEN, Z.-C. GU, AND X.-G. WEN, *Classification of gapped symmetric phases in one-dimensional spin systems*, Phys. Rev. B, 83 (2011), p. 035107.

[20] A. Y. CHERNY AND J. BRAND, *Approximate expression for the dynamic structure factor in the lieb-liniger model*, Journal of Physics: Conference Series, 129 (2008), p. 012051.

[21] A. Y. CHERNY AND J. BRAND, *Dynamic and static density-density correlations in the one-dimensional bose gas: Exact results and approximations*, Phys. Rev. A, 79 (2009), p. 043607.

[22] S. S. CHUNG, K. SUN, AND C. J. BOLECH, *On the matrix product ansatz for fermi fields in one-dimension*, ArXiv e-prints: 1501.00228, (2015).

[23] J. I. CIRAC AND F. VERSTRAETE, *Renormalization and tensor product states in spin chains and lattices*, Journal of Physics A: Mathematical and Theoretical, 42 (2009), p. 504004.

[24] V. COFFMAN, J. KUNDU, AND W. K. WOOTTERS, *Distributed entanglement*, Phys. Rev. A, 61 (2000), p. 052306.

[25] D. COHEN, E. HAIRER, AND C. LUBICH, *Conservation of energy, momentum and actions in numerical discretizations of non-linear wave equations*, Numerische Mathematik, 110 (2008), pp. 113–143.

[26] M. COMINOTTI, D. ROSSINI, M. RIZZI, F. HEKKING, AND A. MINGUZZI, *Optimal persistent currents for interacting bosons on a ring with a gauge field*, Phys. Rev. Lett., 113 (2014), p. 025301.

[27] J. CRANK AND P. NICOLSON, *A practical method for numerical evaluation of solutions of partial differential equations of the heat-conduction type*, in Mathematical Proceedings of the Cambridge Philosophical Society, vol. 43, Cambridge Univ Press, 1947, pp. 50–67.

[28] F. DALFOVO, S. GIORGINI, L. P. PITAEVSKII, AND S. STRINGARI, *Theory of bose-einstein condensation in trapped gases*, Reviews of Modern Physics, 71 (1999), p. 463.

[29] S. DETTMER, D. HELLWEG, P. RYYTTY, J. J. ARLT, W. ERTMER, K. SENGSTOCK, D. S. PETROV, G. V. SHLYAPNIKOV, H. KREUTZMANN, L. SANTOS, AND M. LEWENSTEIN, *Observation of phase fluctuations in elongated bose-einstein condensates*, Phys. Rev. Lett., 87 (2001), p. 160406.

[30] P. A. M. DIRAC, *On the Annihilation of Electrons and Protons*, Mathematical Proceedings of the Cambridge Philosophical Society, 26 (1930), p. 376.

[31] D. DRAXLER, J. HAEGEMAN, T. J. OSBORNE, V. STOJEVIC, L. VANDERSTRAETEN, AND F. VERSTRAETE, *Particles, holes, and solitons: A matrix product state approach*, Physical Review Letters, 111 (2013), p. 020402.

[32] V. DUNJKO, V. LORENT, AND M. OLSHANII, *Bosons in cigar-shaped traps: Thomas-fermi regime, tonks-girardeau regime, and in between*, Phys. Rev. Lett., 86 (2001), pp. 5413–5416.

[33] S. ECKEL, J. G. LEE, F. JENDRZEJEWSKI, N. MURRAY, C. W. CLARK, C. J. LOBB, W. D. PHILLIPS, M. EDWARDS, AND G. K. CAMPBELL, *Hysteresis in a quantized superfluid /'atomtronic/' circuit*, Nature, 506 (2014), pp. 200–203.

[34] J. ESTEVE, J.-B. TREBBIA, T. SCHUMM, A. ASPECT, C. I. WESTBROOK, AND I. BOUCHOULE, *Observations of density fluctuations in an elongated bose gas: Ideal gas and quasicondensate regimes*, Phys. Rev. Lett., 96 (2006).

[35] N. FABBRI, M. PANFIL, D. CLÉMENT, L. FALLANI, M. INGUSCIO, C. FORT, AND J.-S. CAUX, *Dynamical structure factor of one-dimensional bose gases: Experimental signatures of beyond-luttinger-liquid physics*, Phys. Rev. A, 91 (2015), p. 043617.

[36] M. FANNES, B. NACHTERGAELE, AND R. WERNER, *Finitely correlated states on quantum spin chains*, Comm. Math. Phys., 144 (1992), pp. 443–490.

[37] E. FRADKIN AND A. TSEYTLIN, *Quantum string theory effective action*, Nuclear Physics B, 261 (1985), pp. 1–27.

[38] J. FRENKEL, *Wave Mechanics, Advanced General Theory*, Oxford, 1934.

[39] M. GERSTER, P. SILVI, M. RIZZI, R. FAZIO, T. CALARCO, AND S. MONTANGERO, *Unconstrained tree tensor network: An adaptive gauge picture for enhanced performance*, Phys. Rev. B, 90 (2014), p. 125154.

[40] T. GIAMARCHI, *Quantum Physics in One Dimension*, Clarendon Press - Oxford, 2003.

[41] M. GIRARDEAU, *Relationship between Systems of Impenetrable Bosons and Fermions in One Dimension*, Journal of Mathematical Physics, 1 (1960), pp. 516–523.

[42] M. GIRARDEAU, *Relationship between systems of impenetrable bosons and fermions in one dimension*, Journal of Mathematical Physics, 1 (1960), pp. 516–523.

[43] A. GÖRLITZ, J. M. VOGELS, A. E. LEANHARDT, C. RAMAN, T. L. GUSTAVSON, J. R. ABO-SHAEER, A. P. CHIKKATUR, S. GUPTA, S. INOUYE, T. ROSENBAND, AND W. KETTERLE, *Realization of bose-einstein condensates in lower dimensions*, Phys. Rev. Lett., 87 (2001), p. 130402.

[44] M. B. GREEN, J. H. SCHWARZ, AND E. WITTEN, *Superstring theory*, vol. 469, Cambridge University Press, 1987.

[45] E. P. GROSS, *Structure of a quantized vortex in boson systems*, Il Nuovo Cimento, 20 (1961), p. 454.

[46] E. P. GROSS, *Hydrodynamics of a superfluid condensate*, Journal of Mathematical Physics, 4 (1963), pp. 195–207.

[47] J. HAEGEMAN, J. I. CIRAC, T. J. OSBORNE, I. PIŽORN, H. VERSCHELDE, AND F. VERSTRAETE, *Time-dependent variational principle for quantum lattices*, Phys. Rev. Lett., 107 (2011), p. 070601.

[48] J. HAEGEMAN, J. I. CIRAC, T. J. OSBORNE, H. VERSCHELDE, AND F. VERSTRAETE, *Applying the variational principle to (1+1)-dimensional quantum field theories*, Phys. Rev. Lett., 105 (2010), p. 251601.

[49] J. HAEGEMAN, J. I. CIRAC, T. J. OSBORNE, AND F. VERSTRAETE, *Calculus of continuous matrix product states*, Phys. Rev. B, 88 (2013), p. 085118.

[50] J. HAEGEMAN, D. DRAXLER, V. STOJEVIC, J. I. CIRAC, T. J. OSBORNE, AND F. VERSTRAETE, *Quantum gross-pitaevskii equation*, arXiv: 150.06575, (2015).

[51] J. HAEGEMAN, C. LUBICH, I. OSELEDETS, B. VANDEREYCKEN, AND F. VERSTRAETE, *Unifying time evolution and optimization with matrix product states*, ArXiv e-prints: 1408.5056, (2014).

[52] J. HAEGEMAN, M. MARIEN, T. J. OSBORNE, AND F. VERSTRAETE, *Geometry of matrix product states: Metric, parallel transport, and curvature*, J. Math. Phys., 55 (2014), p. 021902.

[53] J. HAEGEMAN, S. MICHALAKIS, B. NACHTERGAELE, T. J. OSBORNE, N. SCHUCH, AND F. VERSTRAETE, *Elementary excitations in gapped quantum spin systems*, Phys. Rev. Lett., 111 (2013), p. 080401.

[54] J. HAEGEMAN, B. PIRVU, D. J. WEIR, J. I. CIRAC, T. J. OSBORNE, H. VERSCHELDE, AND F. VERSTRAETE, *Variational matrix product ansatz for dispersion relations*, Phys. Rev. B, 85 (2012).

[55] F. D. M. HALDANE, *Luttinger liquid theory of one-dimensional quantum fluids. i. properties of the luttinger model and their extension to the general 1d interacting spinless fermi gas*, Journal of Physics C: Solid State Physics, 14 (1981), p. 2585.

[56] D. W. HALLWOOD, T. ERNST, AND J. BRAND, *Robust mesoscopic superposition of strongly correlated ultracold atoms*, Phys. Rev. A, 82 (2010), p. 063623.

[57] R. HARDIN AND F. TAPPERT, *Applications of the split-step fourier method to the numerical solution of nonlinear and variable coefficient wave equations*, Siam Rev, 15 (1973), p. 423.

[58] M. B. HASTINGS, *An area law for one-dimensional quantum systems*, Journal of Statistical Mechanics: Theory and Experiment, 2007 (2007), p. P08024.

[59] P. HAUKE AND L. TAGLIACOZZO, *Spread of correlations in long-range interacting quantum systems*, Phys. Rev. Lett., 111 (2013), p. 207202.

[60] F. W. J. HEKKING AND L. I. GLAZMAN, *Quantum fluctuations in the equilibrium state of a thin superconducting loop*, Phys. Rev. B, 55 (1997), pp. 6551–6558.

[61] S. HOFFERBERTH, I. LESANOVSKY, B. FISCHER, T. SCHUMM, AND J. SCHMIEDMAYER, *Non-equilibrium coherence dynamics in one-dimensional bose gases*, Nature, 449 (2007), pp. 324–327.

[62] J. IEDA, T. MIYAKAWA, AND M. WADATI, *Exact analysis of soliton dynamics in spinor bose-einstein condensates*, Phys. Rev. Lett., 93 (2004), p. 194102.

[63] A. IMAMBEKOV AND L. I. GLAZMAN, *Exact exponents of edge singularities in dynamic correlation functions of 1d bose gas*, Phys. Rev. Lett., 100 (2008), p. 206805.

[64] M. ISHIKAWA AND H. TAKAYAMA, *Solitons in a one-dimensional bose system with the repulsive delta-function interaction*, J. Phys. Soc. Jpn., 49 (1980).

[65] D. JENNINGS, C. BROCKT, J. HAEGEMAN, T. J. OSBORNE, AND F. VERSTRAETE, *Continuum tensor network field states, path integral representations and spatial symmetries*, New Journal of Physics, 17 (2015), p. 063039.

[66] D. JENNINGS, J. HAEGEMAN, T. J. OSBORNE, AND F. VERSTRAETE, *Variational quantum field states with symmetry: The continuum limit of a projected entangled pair state*, ArXiv e-prints: 1212.3833, (2012).

[67] T. KINOSHITA, T. WENGER, AND D. S. WEISS, *Observation of a one-dimensional tonks-girardeau gas*, Science, 305 (2004), pp. 1125–1128.

[68] T. KINOSHITA, T. WENGER, AND D. S. WEISS, *Local pair correlations in one-dimensional bose gases*, Phys. Rev. Lett., 95 (2005).

[69] V. KOREPIN, N. BOGOLIUBOV, AND A. IZERGIN, *Quantum Inverse Scattering Method and Correlation Functions*, Cambridge University Press, 1997.

[70] P. KRAMER AND M. SARACENO, *Geometry of the Time-Dependent Variational Principle in Quantum Mechanics*, vol. 140 of Lecture Notes in Physics, Springer, 1981.

[71] P. KRÜGER, S. HOFFERBERTH, I. E. MAZETS, I. LESANOVSKY, AND J. SCHMIEDMAYER, *Weakly interacting bose gas in the one-dimensional limit*, Phys. Rev. Lett., 105 (2010).

[72] P. P. KULISH, S. V. MANAKOV, AND L. D. FADDEEV, *Comparison of the exact quantum and quasiclassical results for a nonlinear Schrödinger equation*, Theoretical and Mathematical Physics, 28 (1976), pp. 615–620.

[73] A. J. LEGGETT, *Bose-einstein condensation in the alkali gases: Some fundamental concepts*, Rev. Mod. Phys., 73 (2001), pp. 307–356.

[74] E. H. LIEB, *Exact analysis of an interacting bose gas. ii. the excitation spectrum*, Phys. Rev., 130 (1963), pp. 1616–1624.

[75] E. H. LIEB AND W. LINIGER, *Exact analysis of an interacting bose gas. i. the general solution and the ground state*, Phys. Rev., 130 (1963).

[76] E. H. LIEB, R. SEIRINGER, J. P. SOLOVEJ, AND J. YNGVASON, *The Mathematics of the Bose Gas and its Condensation: Series: Oberwolfach Seminars*, vol. 34, Birkhäuser Verlag GmbH, 2005.

[77] E. H. LIEB, R. SEIRINGER, AND J. YNGVASON, *One-dimensional behavior of dilute, trapped bose gases*, Commun. Math. Phys., 244 (2004), pp. 347–393.

[78] C. LUBICH, *On splitting methods for schrödinger - poisson and cubic nonlinear schrödinger equations*, Mathematics of computation, 77 (2008), pp. 2141–2153.

[79] K. A. MATVEEV, A. I. LARKIN, AND L. I. GLAZMAN, *Persistent current in superconducting nanorings*, Phys. Rev. Lett., 89 (2002), p. 096802.

[80] F. MEINERT, M. PANFIL, M. J. MARK, K. LAUBER, J.-S. CAUX, AND H.-C. NÄGERL, *Probing the excitations of a lieb-liniger gas from weak to strong coupling*, Phys. Rev. Lett., 115 (2015), p. 085301.

[81] A. MILSTED, J. HAEGEMAN, AND T. J. OSBORNE, *Matrix product states and variational methods applied to critical quantum field theory*, Phys. Rev. D, 88 (2013), p. 085030.

[82] H. MORITZ, T. STÖFERLE, M. KÖHL, AND T. ESSLINGER, *Exciting collective oscillations in a trapped 1d gas*, Phys. Rev. Lett., 91 (2003), p. 250402.

[83] V. MURG, F. VERSTRAETE, O. LEGEZA, AND R. M. NOACK, *Simulating strongly correlated quantum systems with tree tensor networks*, Phys. Rev. B, 82 (2010), p. 205105.

[84] M. OLSHANII, *Atomic scattering in the presence of an external confinement and a gas of impenetrable bosons*, Phys. Rev. Lett., 81 (1998), pp. 938–941.

[85] R. ORUS, *A practical introduction to tensor networks: Matrix product states and projected entangled pair states*, ArXiv e-prints: 13062164, (2013).

[86] T. J. OSBORNE, J. EISERT, AND F. VERSTRAETE, *Holographic quantum states*, Phys. Rev. Lett., 105 (2010).

[87] S. ÖSTLUND AND S. ROMMER, *Thermodynamic limit of density matrix renormalization*, Phys. Rev. Lett., 75 (1995), pp. 3537–3540.

[88] B. PAREDES, A. WIDERA, V. MURG, O. MANDEL, S. FOLLING, I. CIRAC, G. V. SHLYAPNIKOV, T. W. HANSCH, AND I. BLOCH, *Tonks-girardeau gas of ultracold atoms in an optical lattice*, Nature, 429 (2004), pp. 277–281.

[89] D. S. PETROV, G. V. SHLYAPNIKOV, AND J. T. M. WALRAVEN, *Regimes of quantum degeneracy in trapped 1d gases*, Phys. Rev. Lett., 85 (2000), pp. 3745–3749.

[90] P. PIPPAN, S. R. WHITE, AND H. G. EVERTZ, *Efficient matrix-product state method for periodic boundary conditions*, Phys. Rev. B, 81 (2010), p. 081103.

[91] B. PIRVU, J. HAEGEMAN, AND F. VERSTRAETE, *Matrix product state based algorithm for determining dispersion relations of quantum spin chains with periodic boundary conditions*, Phys. Rev. B, 85 (2012).

[92] B. PIRVU, F. VERSTRAETE, AND G. VIDAL, *Exploiting translational invariance in matrix product state simulations of spin chains with periodic boundary conditions*, Phys. Rev. B, 83 (2011), p. 125104.

[93] L. P. PITAEVSKII, *Vortex Lines in an Imperfect Bose Gas*, Soviet Journal of Experimental and Theoretical Physics, 13 (1961), p. 451.

[94] L. P. PITAEVSKII AND S. STRINGARI, *Bose-Einstein Condensation*, Oxford University Press, 2003.

[95] J. POLCHINSKI, *Dirichlet branes and ramond-ramond charges*, Physical Review Letters, 75 (1995), p. 4724.

[96] J. POLCHINSKI, *String theory. Vol. 1: An introduction to the bosonic string*, vol. 402, Cambridge University Press, 1998.

[97] U. V. POULSEN AND K. MØLMER, *Quantum states of bose-einstein condensates formed by molecular dissociation*, Phys. Rev. A, 63 (2001), p. 023604.

[98] F. QUIJANDRÍA, J. J. GARCÍA-RIPOLL, AND D. ZUECO, *Continuous matrix product states for coupled fields: Application to luttinger liquids and quantum simulators*, Phys. Rev. B, 90 (2014), p. 235142.

[99] F. QUIJANDRÍA, J. J. GARCÍA-RIPOLL, AND D. ZUECO, *Continuous matrix product states for coupled fields: Application to luttinger liquids and quantum simulators*, Phys. Rev. B, 90 (2014), p. 235142.

[100] F. QUIJANDRÍA AND D. ZUECO, *Continuous-matrix-product-state solution for the mixing-demixing transition in one-dimensional quantum fields*, Phys. Rev. A, 92 (2015), p. 043629.

[101] J. SATO, R. KANAMOTO, E. KAMINISHI, AND T. DEGUCHI, *Quantum dark solitons in the 1D Bose gas and the superfluid velocity*, ArXiv e-prints: 1204.3960, (2012).

[102] U. SCHOLLWÖCK, *The density-matrix renormalization group in the age of matrix product states*, Annals of Physics, 326 (2011), pp. 96–192.

[103] N. SCHUCH, I. CIRAC, AND D. PÉREZ-GARCÍA, *{PEPS} as ground states: Degeneracy and topology*, Annals of Physics, 325 (2010), pp. 2153 – 2192.

[104] N. SCHUCH, D. PÉREZ-GARCÍA, AND I. CIRAC, *Classifying quantum phases using matrix product states and projected entangled pair states*, Phys. Rev. B, 84 (2011), p. 165139.

[105] T. SCHWEIGLER, V. KASPER, S. ERNE, B. RAUER, T. LANGEN, T. GASENZER, J. BERGES, AND J. SCHMIEDMAYER, *On solving the quantum many-body problem*, ArXiv e-prints: 1505.03126, (2015).

[106] B. T. SEAMAN, M. KRÄMER, D. Z. ANDERSON, AND M. J. HOLLAND, *Atomtronics: Ultracold-atom analogs of electronic devices*, Phys. Rev. A, 75 (2007), p. 023615.

[107] S. STELLMER, C. BECKER, P. SOLTAN-PANAHI, E.-M. RICHTER, S. DÖRSCHER, M. BAUMERT, J. KRONJÄGER, K. BONGS, AND K. SENGSTOCK, *Collisions of dark solitons in elongated bose-einstein condensates*, Phys. Rev. Lett., 101 (2008).

[108] V. STOJEVIC, J. HAEGEMAN, I. P. MCCULLOCH, L. TAGLIACOZZO, AND F. VERSTRAETE, *Conformal data from finite entanglement scaling*, Phys. Rev. B, 91 (2015), p. 035120.

[109] C. SULEM AND P.-L. SULEM, *The Nonlinear Schrödinger Equation*, Springer, 1999.

[110] L. TAGLIACOZZO, A. CELI, AND M. LEWENSTEIN, *Tensor networks for lattice gauge theories with continuous groups*, Phys. Rev. X, 4 (2014), p. 041024.

[111] T. R. TAHA AND M. I. ABLOWITZ, *Analytical and numerical aspects of certain nonlinear evolution equations. ii. numerical, nonlinear schrödinger equation*, Journal of Computational Physics, 55 (1984), pp. 203–230.

[112] B. TERHAL, *Is entanglement monogamous?*, ArXiv e-prints: 0307120, (2003).

[113] M. THALHAMMER, M. CALIARI, AND C. NEUHAUSER, *High-order time-splitting hermite and fourier spectral methods*, Journal of Computational Physics, 228 (2009), pp. 822–832.

[114] S. TRULLINGER, V. E. ZAKHAROV, AND V. L. POKROVSKY, *Solitons*, Elsevier, 1986.

[115] T. TSUCHIDA AND M. WADATI, *The coupled modified korteweg-de vries equations*, Journal of the Physical Society of Japan, 67 (1998), pp. 1175–1187.

[116] T. TSUZUKI, *Nonlinear waves in the Pitaevskii-Gross equation*, Journal of Low Temperature Physics, 4 (1971), pp. 441–457.

[117] A. M. TURNER, F. POLLMANN, AND E. BERG, *Topological phases of one-dimensional fermions: An entanglement point of view*, Phys. Rev. B, 83 (2011), p. 075102.

[118] L. VANDERSTRAETEN, F. VERSTRAETE, AND J. HAEGEMAN, *Scattering particles in quantum spin chains*, Phys. Rev. B, 92 (2015), p. 125136.

[119] F. VERSTRAETE AND J. I. CIRAC, *Continuous matrix product states for quantum fields*, Phys. Rev. Lett., 104 (2010).

[120] F. VERSTRAETE, J. J. GARCÍA-RIPOLL, AND J. I. CIRAC, *Matrix product density operators: Simulation of finite-temperature and dissipative systems*, Phys. Rev. Lett., 93 (2004).

[121] F. VERSTRAETE, V. MURG, AND J. CIRAC, *Matrix product states, projected entangled pair states, and variational renormalization group methods for quantum spin systems*, Advances in Physics, 57 (2008), pp. 143–224.

[122] F. VERSTRAETE, D. PORRAS, AND J. I. CIRAC, *Density matrix renormalization group and periodic boundary conditions: A quantum information perspective*, Phys. Rev. Lett., 93 (2004), p. 227205.

[123] G. VIDAL, *Efficient simulation of one-dimensional quantum many-body systems*, Phys. Rev. Lett., 93 (2004), p. 040502.

[124] G. VIDAL, *Class of quantum many-body states that can be efficiently simulated*, Phys. Rev. Lett., 101 (2008), p. 110501.

[125] M. WEINSTEIN, *The nonlinear schrödinger equation—singularity formation, stability and dispersion*, Contemp. Math, 99 (1989), pp. 213–232.

[126] A. WELLER, J. P. RONZHEIMER, C. GROSS, J. ESTEVE, M. K. OBERTHALER, D. J. FRANTZESKAKIS, G. THEOCHARIS, AND P. G. KEVREKIDIS, *Experimental observation of oscillating and interacting matter wave dark solitons*, Phys. Rev. Lett., 101 (2008).

[127] S. R. WHITE, *Density matrix formulation for quantum renormalization groups*, Phys. Rev. Lett., 69 (1992), pp. 2863–2866.

[128] C.-N. YANG AND C. YANG, *Thermodynamics of a one-dimensional system of bosons with repulsive delta-function interaction*, Journal of Mathematical Physics, 10 (1969), pp. 1115–1122.

[129] V. E. ZAKHAROV AND S. V. MANAKOV, *On the complete integrability of a nonlinear schrödinger equation*, Theoretical and Mathematical Physics, 19 (1974), pp. 551–559.

[130] M. ZWOLAK AND G. VIDAL, *Mixed-state dynamics in one-dimensional quantum lattice systems: A time-dependent superoperator renormalization algorithm*, Phys. Rev. Lett., 93 (2004).

Appendices

Appendix A

Some remarks on dynamical correlation functions

In this chapter we will try to answer the question to what extent the ansatz for excitations introduced in chapter 1 can be used to compute dynamical correlation functions of $(1+1)$-dimensional quantum field theories directly in the thermodynamic limit. The system of interest is again the Lieb-Liniger model (eq. 1.6) and we are in particular interested in the zero temperature dynamical structure factor (DSF)

$$S(p,\omega) = \int dt e^{i\omega t} \langle \psi | \hat{n}(-p) e^{-i(\hat{H}-E_0)t} \hat{n}(p) | \psi \rangle \tag{A.1}$$

with $|\psi\rangle$ being the ground state with corresponding energy E_0 and
$\hat{n}(p) = \int_{-\infty}^{\infty} dx e^{ipx} \psi^\dagger(x)\psi(x)$. Inserting a resolution of the identity given by the eigenvectors of the Hamiltonian $\hat{H}$ and performing the time integration leads to the *Lehmann series representation* of $S(p,\omega)$,

$$S(p,\omega) = \sum_m |\langle m|\hat{n}(p)|\psi\rangle|^2 \delta(\omega - E_m + E_0), \tag{A.2}$$

where $|m\rangle$ are assumed to be eigenstates of $\hat{H}$. This representation suggests a natural interpretation of the DSF as being proportional to the probability of creating a collective excitation with momentum p and energy ω (in units of $\hbar = 1$). The coefficients $|\langle m|\hat{n}(p)|\psi\rangle|^2$ in this sum are called *form factors*. For generic Hamiltonians it is very difficult to calculate the form factors since in general the exact eigenvectors are not known. This can be a hard task even for integrable systems. However, in the case of the LL Hamiltonian the DSF has been calculated numerically by means of the Algebraic Bethe Ansatz [14]. Moreover several approximate analytical expressions for the DSF have been derived [20, 21] and it is known [63] that the DSF exhibits a power-law behaviour near the enclosing dispersion curves, and that the corresponding exponents are known exactly [63].

In order to approximate the exact eigenstates $|m\rangle$ we will use the trivial excitations defined in equations (1.2) - (1.4). This will yield at each momentum, a D^2-dimensional orthonormal basis of approximated energy eigenstates. The form factors in this basis can be calculated along the lines of section 1.5 and are given by

$$\langle \Phi_k^n | \hat{n}(p) | \psi \rangle = \delta(p-k) \Big[\langle l | R \otimes \overline{W}_n | r \rangle + \langle l | R \otimes \overline{R} \Big(-T + \mathrm{i}k \Big)^{\mathsf{P}} \Big(1 \otimes \overline{V}_n + R \otimes \overline{W}_n \Big) | r \rangle \Big], \tag{A.3}$$

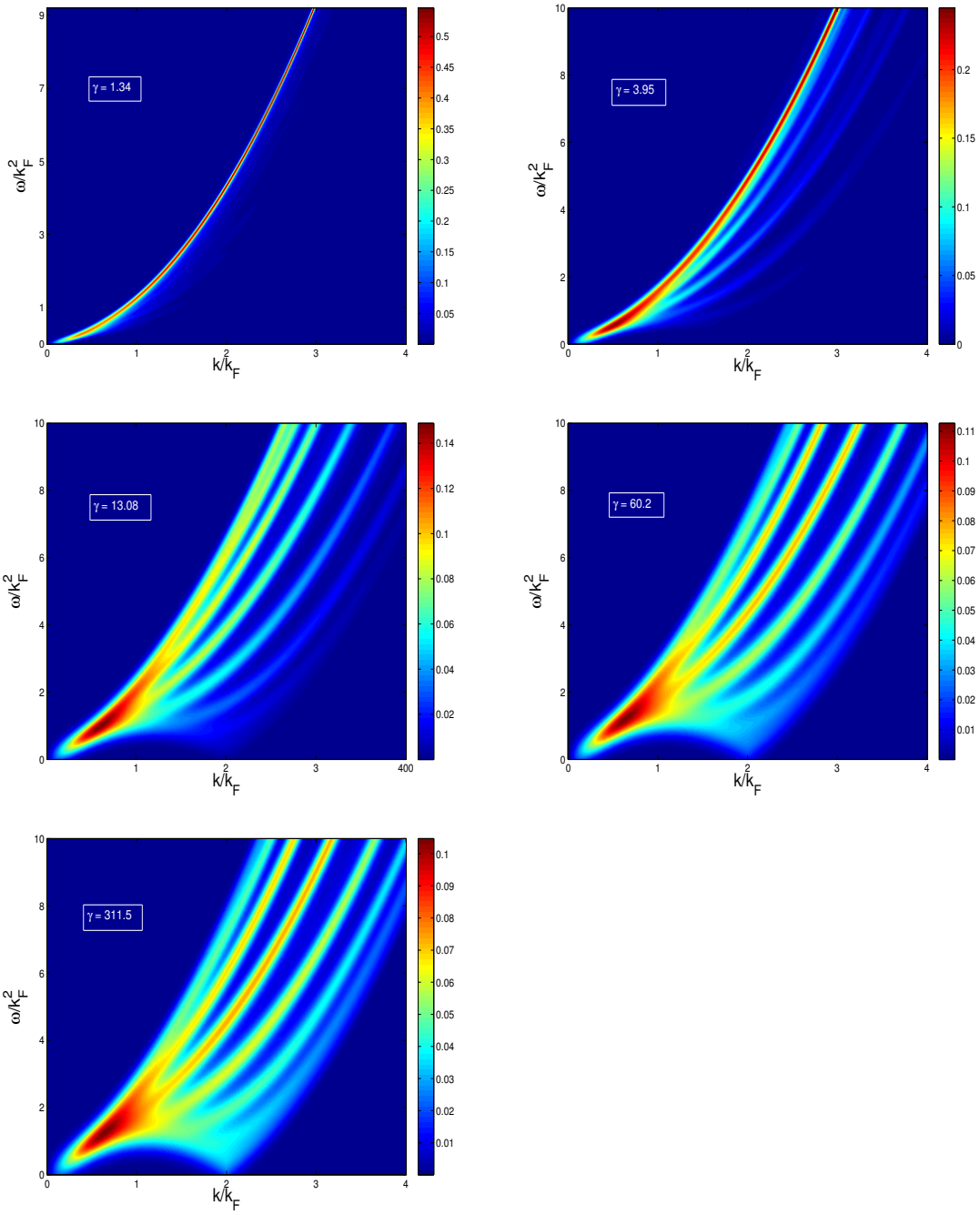

Figure A.1: Density plots of the Dynamical structure factor at $D = 64$ for several values of the effective interaction γ (from left top to bottom: γ = 1.34, 3.95, 13.08, 60.2, 311.5). The horizontal axis is the momentum up to $4k_{\mathrm{F}}$ and the vertical axis is the energy.

where the index n labels the D^2 excitations at momentum k and thus runs from 1 to D^2. Note that we also made use of the gauge condition given in eq. (1.15) to arrive at this expression.

In [14] it was shown that for small interaction strength the DSF has a sharp peak at Lieb's Type I branch while as γ increases this peak spreads out and forms a plateau between the Type II and Type I branch. For general momentum the signal lies strictly above the Type II branch modulo $2k_{\mathrm{F}} = 2\pi\rho$ with ρ being the ground state density. The Type I branch however is not a strict upper bound and the DSF has a small power law decaying tail inside the high energy (multi-particle) continuum [63].

In Figure A.1 we show density plots of the DSF at $D = 64$ for several values of γ ranging through the whole parameter regime from weak to strong interactions. To obtain these plots we convoluted the delta-function in eq. (A.2) with a gaussian of width 0.3. The qualitative dependence on γ as described above is very well captured within the topologically trivial excitation ansatz. For small γ the DSF only has support near the Type I branch while for larger γ the signal spreads out as expected. It is quite remarkable that the signal shows the correct power law behaviour above the Type I branch. Indeed, almost all of the D^2 excitations have an energy much larger than this branch (as can be seen e.g. from Fig. 1.2) but do not contribute to the DSF. This result can also be used to extract some information about the power law exponents [63], however with an accuracy strongly depending on γ and the momentum.

Apart from the correct overall dependence on γ and the good approximation near the limiting dispersion branches our approximation does not give the correct results in between these branches. Instead, our approximation leads to oscillations in the DSF with several strongly distinct branches already at intermediate γ. These oscillations do not have a counterpart in the exact result and might be interpreted as artificial bound states or multi particle-hole excitations where the quasi particles (holes) have momentum close to each other. Such excitations can be energetically favourable given the local nature of our ansatz for excitations (1.2). The amplitude of these oscillations slowly decreases with increasing D if the convolution width is kept fixed. In principle it is thus possible to extract the exact result by a finite D scaling but this would demand much higher bond dimensions than $D = 64$ of Fig. A.1.

To state this in a different manner, the ansatz for excitations of chapter 1 is very well suited to extract information about the energies of low lying excitations but it suffers in describing other properties of the corresponding states due to the intrincisally local nature of the ansatz. Indeed, since the excitations defined in (1.2) are elements of a linear vector space one can safely add two or more elementary excitations to form a multi component excitation with an energy being the sum of the energies of its individual components. While the energies just add up the correlation properties of such a multi component state are however very much different compared to theire elementary counterparts as the non local nature of such excitations and microscopic effects like scattering have to be taken into account.

As an outlook we would like to point out that recently an ansatz for such multi component scattering states was introduced in [118] for the variational class of MPS in the context of quantum spin chains. In principle it should be possible to extend this ansatz to the class of cMPS, thus allowing for a more systematic and complete study of dynamical correlation functions in one dimensional quantum field theories. Another possibility would be to use the qBdG equations from chapter 2 to calculate the response of a uniform system against weak time dependent damped external density perturbations. It is well known [94] that the imaginary part of the response function under such a perturbation is equal to the DSF. The intuition as to why this might give better results than the ones obtained from the single tangent plan ansatz is that the qBdG equations contain information from the double tangent plane as well (this information is encoded in the off-diagonal blocks of the matrix in eq. 2.12).

Appendix B

The two component Bose gas

In this chapter we introduce a cMPS ansatz for a non-relativistic two component bose-bose mixture in the thermodynamic limit and we will derive the corresponding TDVP equations. The system can be interpreted as bosons with "spin $1/2$" and the Hamiltonain reads

$$\hat{H} = \sum_{\alpha=1}^{2} \int_{-\infty}^{+\infty} \left[\frac{\mathrm{d}\hat{\psi}_\alpha^\dagger}{\mathrm{d}x} \frac{\mathrm{d}\hat{\psi}_\alpha}{\mathrm{d}x} - \mu_\alpha \hat{\psi}_\alpha^\dagger \hat{\psi}_\alpha + \sum_{\beta=1}^{2} g_{\alpha\beta} \hat{\psi}_\alpha^\dagger \hat{\psi}_\beta^\dagger \hat{\psi}_\beta \hat{\psi}_\alpha \right] \mathrm{d}x \tag{B.1}$$

with inter-interactions g_{ij} and intra-interactions g_{ii} and μ_α are the chemical potentials for each flavour (note that the argument of the field operators has been omitted for the sake of brevity). A bose-bose mixture exhibits a rich phase diagram ranging from a mixing-demixing transition if $g_{12} > 0$ to a possible collapse of the system if $g_{12} < 0$ [94, 17]. Furthermore, this system is in general not integrable but allows for an exact Bethe ansatz solution only at the special point of equal inter- and intra-interactions. From now on we will only consider positive symmetric interactions, i.e. $g_{11} = g_{22} = c > 0$ and $g_{12} = g_{21} = g/2 > 0$ and equal ground state densities $\rho_{01} = \rho_{02} = \rho_0$. With this restriction the two flavours start to demix once $g > 2c$ and a phase separation occurs [17].

The cMPS ansatz for such a system is given by

$$|\Psi(Q, R_1, R_2)\rangle = v_L^\dagger \left(\mathcal{P} \mathrm{e}^{\int_{-\infty}^{\infty} \mathrm{d}x \, [Q \otimes \mathbb{1} + R_1 \otimes \hat{\psi}_1^\dagger(x) + R_2 \otimes \hat{\psi}_2^\dagger(x)]} \right) v_R |\Omega\rangle \tag{B.2}$$

where the field operators satisfy the commutation relation $[\hat{\psi}_i(x), \hat{\psi}_j^\dagger(y)] = \delta_{i,j}\delta(x-y)$. The difficulty in studying systems with different species of particles with cMPS stems from the fact that the cMPS matrices must fulfil the same commutation relations as the particles themselves which is a consequence of the regularity requirements for a cMPS [49]. Hence, the matrices R_i have to fulfil

$$\Big[R_i, R_j \Big] = 0 \, . \tag{B.3}$$

We propose the following parametrization

$$\begin{aligned} R_1 &= G^{-1} D_1 G \\ R_2 &= G^{-1} D_2 G \end{aligned} \tag{B.4}$$

where D_1 and D_2 are diagonal $(D \times D)$-dimensional matrices and G is an invertible matrix of the same dimension. Further we will work in left gauge by setting $Q = -1/2 R_1^\dagger R_1 - 1/2 R_2^\dagger R_2 - \mathrm{i}K$ with K being hermitian. In this gauge the transfer matrix $T = Q \otimes \mathbb{I} + \mathbb{I} \otimes$

$\overline{Q} + R_1 \otimes \overline{R}_1 + R_2 \otimes \overline{R}_2$ has one zero eigenvalue with corresponding right $|r\rangle$ and left $\langle\mathbb{I}|$ eigenvector and the remaining spectrum has negative real part.

The tangent states are given by

$$|\Phi(V, W_1, W_2)\rangle := \int_{-\infty}^{\infty} \mathrm{d}x \; v_L^\dagger \hat{U}(-\infty, x)\Big(V\otimes\mathbb{1} + W_1\otimes\hat{\psi}_1^\dagger(x) + W_2\otimes\hat{\psi}_2^\dagger(x)\Big)\hat{U}(x,\infty)v_R|\Omega\rangle \tag{B.5}$$

with $U(x,y) = \mathrm{e}^{\int_x^y \mathrm{d}z\,[Q\otimes\mathbb{1} + R_1\otimes\hat{\psi}_1^\dagger(z) + R_2\otimes\hat{\psi}_2^\dagger(z)]}$. These states are invariant under additive gauge transformations [49] of the form $V \to V + [Q, X]$, $W_1 \to W_1 + [R_1, X]$, $W_2 \to W_2 + [R_2, X]$ where X is a D-dimensional matrix. The commonly used *left gauge* condition is enforced by demanding

$$V + R_1^\dagger W_1 + R_2^\dagger W_2 = 0 \tag{B.6}$$

which can always be achieved by an appropriate choice of X.

To derive the TDVP equations on has to find the optimal matrices $(V, W_1, W_2) = (\dot{Q}, \dot{R}_1, \dot{R}_2)$ that minimise the cost function $\| \, |\Phi[V, W_1, W_2]\rangle + \mathrm{i}\hat{H}\,|\Psi[Q, R_1, R_2]\rangle \, \|$. This amounts to calculating the Gram matrix, defined as an overlap between two tangent states, and the energy gradient. To compute these quantities we proceed in a similar way as in section 1.5.

The overlap of two tangent vectors is given by

$$\langle\Phi[\overline{V}, \overline{W}_1, \overline{W}_2]|\Phi[V, W_1, W_2]\rangle = 2\pi\delta(0)\,\langle\mathbb{I}|\,\Big(W_1\otimes\overline{W}_1 + W_2\otimes\overline{W}_2\Big)\,|r\rangle \tag{B.7}$$

and the energy gradient is defined via

$$\begin{aligned}
&\langle\Phi[\overline{V}, \overline{W}_1, \overline{W}_2]|\,\hat{H}\,|\Psi(Q, R_1, R_2)\rangle = 2\pi\delta(0)\\
&\times\Big[\,\langle\mathbb{I}|\,\Big([Q, R_1]\otimes[\overline{Q}, \overline{R_1}] + [Q, R_2]\otimes[\overline{Q}, \overline{R_2}] - \mu_1 R_1\otimes\overline{R}_1 - \mu_2 R_2\otimes\overline{R}_2 +\\
&\qquad + c(R_1^2\otimes\overline{R}_1^2 + R_2^2\otimes\overline{R}_2^2) + gR_1R_2\otimes\overline{R}_2\overline{R}_1\Big)\Big(-T\Big)^{\mathrm{p}}\\
&\qquad\qquad\times\Big(\mathbb{I}\otimes\overline{V}(x) + R_1(x)\otimes\overline{W}_1 + R_2(x)\otimes\overline{W}_2\Big)\,|r\rangle\\
&\quad + \langle\mathbb{I}|\,[Q, R_1]\otimes\Big([\overline{Q}, \overline{W}_1] + [\overline{V}, \overline{R}_1]\Big) + [Q, R_2]\otimes\Big([\overline{Q}, \overline{W}_2] + [\overline{V}, \overline{R}_2]\Big)\,|r\rangle\\
&\quad - \langle\mathbb{I}|\,\Big(\mu_1 R_1\otimes\overline{W}_1 + \mu_2 R_2\otimes\overline{W}_2\Big)\,|r\rangle\\
&\quad + \langle\mathbb{I}|\,\Big(cR_1^2\otimes(\overline{W}_1\overline{R}_1 + \overline{R}_1\overline{W}_1) + cR_2^2\otimes(\overline{W}_2\overline{R}_2 + \overline{R}_2\overline{W}_2)\Big)\,|r\rangle\\
&\quad + \langle\mathbb{I}|\,\Big(\frac{g}{2}R_1R_2\otimes(\overline{W}_1\overline{R}_2 + \overline{R}_2\overline{W}_1 + \overline{W}_2\overline{R}_1 + \overline{R}_1\overline{W}_2)\Big)\,|r\rangle\,\Big]\,.
\end{aligned} \tag{B.8}$$

where we made use of eq. (B.6) to arrive at (B.7) and (B.8) and T^{p} is the pseudo inverse of T, i.e. the inverse acting solely on the orthogonal complement of the kernel of T. Note that the tangent states in (B.5) can be seen as states with momentum zero (see eq. (1.2)) and can therefore not be orthogonalized to a finite constant in an infinite system but rather satisfy a δ-function normalization. The cost of calculating $\Big(-T\Big)^{\mathrm{p}}$ is naively $\mathcal{O}(D^5)$, but we can circumvent this by introducing the so called left energy matrix $\langle E_{\mathrm{L}}|$ which is the solution of

$$\begin{aligned}
\langle E_{\mathrm{L}}|\,T = -\,\langle\mathbb{I}|\,\Big([Q, R_1]\otimes[\overline{Q}, \overline{R_1}] + [Q, R_2]\otimes[\overline{Q}, \overline{R_2}] - \mu_1 R_1\otimes\overline{R}_1 - \mu_2 R_2\otimes\overline{R}_2\\
+ cR_1^2\otimes\overline{R}_1^2 + cR_2^2\otimes\overline{R}_2^2 + gR_1R_2\otimes\overline{R}_2\overline{R}_1\Big)\,.
\end{aligned} \tag{B.9}$$

The subtlety in taking the inverse of the rank deficient matrix T in (B.9) is best resolved by replacing $T \to T + |r\rangle\langle\mathbb{I}|$ while at the same time subtracting the ground state energy

expectation value from $\hat{H}$, i.e. $\hat{H} \to \hat{H} - E(Q, \overline{Q}, R_1, \overline{R}_1, R_2, \overline{R}_2)$. Note that the additional terms in the energy gradient arising from this substitution of $\hat{H}$ vanish since the left gauge condition (B.6) ensures orthogonality between the tangent states and the ground state ($\langle \Phi[\overline{V}, \overline{W}_1, \overline{W}_2] | \Psi(Q, R_1, R_2) \rangle = 0$). The solution of the linear equation eq. (B.9) can be iteratively calculated with a computational cost of $\mathcal{O}(D^3)$. With (B.9) we can write (B.8) as

$$\begin{aligned}
&\langle \Phi[\overline{V}, \overline{W}_1, \overline{W}_2] | \, \hat{H} \, | \Psi(Q, R_1, R_2) \rangle = \\
&2\pi\delta(0) \Big[\langle E_{\mathrm{L}} | \left(\mathbb{I} \otimes \overline{V}(x) + R_1(x) \otimes \overline{W}_1 + R_2(x) \otimes \overline{W}_2 \right) | r \rangle \\
&\quad + \langle \mathbb{I} | \, [Q, R_1] \otimes \left([\overline{Q}, \overline{W}_1] + [\overline{V}, \overline{R}_1] \right) + [Q, R_2] \otimes \left([\overline{Q}, \overline{W}_2] + [\overline{V}, \overline{R}_2] \right) | r \rangle \\
&\quad - \langle \mathbb{I} | \left(\mu_1 R_1 \otimes \overline{W}_1 + \mu_2 R_2 \otimes \overline{W}_2 \right) | r \rangle \\
&\quad + \langle \mathbb{I} | \left(c R_1^2 \otimes (\overline{W}_1 \overline{R}_1 + \overline{R}_1 \overline{W}_1) + c R_2^2 \otimes (\overline{W}_2 \overline{R}_2 + \overline{R}_2 \overline{W}_2) \right) | r \rangle \\
&\quad + \langle \mathbb{I} | \left(\frac{g}{2} R_1 R_2 \otimes (\overline{W}_1 \overline{R}_2 + \overline{R}_2 \overline{W}_1 + \overline{W}_2 \overline{R}_1 + \overline{R}_1 \overline{W}_2) \right) | r \rangle \Big] \, . \qquad \text{(B.10)}
\end{aligned}$$

Furthermore, the matrices (V, W_1, W_2) also have to be related to $(\dot{G}, \dot{D}_1, \dot{D}_2)$, which results in a non trivial Gram matrix originating solely from the parametrization in (B.4). We find that

$$\begin{aligned}
V = \dot{Q} &= -1/2 \left(\dot{R}_1^\dagger R_1 + R_1^\dagger \dot{R}_1 + \dot{R}_2^\dagger R_2 + R_2^\dagger \dot{R}_2 \right) - \mathrm{i}\dot{K} \\
W_1 = \dot{R}_1 &= -G^{-1} \dot{G} R_1 + G^{-1} \dot{D}_1 G + R_1 G^{-1} \dot{G} \\
W_2 = \dot{R}_2 &= -G^{-1} \dot{G} R_2 + G^{-1} \dot{D}_2 G + R_2 G^{-1} \dot{G} \, . \qquad \text{(B.11)}
\end{aligned}$$

The first line can be re-expressed as

$$\dot{K} = \frac{\mathrm{i}}{2} (\dot{R}_1^\dagger R_1 - R_1^\dagger \dot{R}_1 + \dot{R}_2^\dagger R_2 - R_2^\dagger \dot{R}_2) \qquad \text{(B.12)}$$

using (B.6). The specific structure of $\dot{K}$ guarantees that K stays hermitian during the time evolution to first order in dt and hence also the left-canonical form is preserved under time evolution. Equation (B.11) also ensures that the relation $\frac{\mathrm{d}}{\mathrm{d}t}[R_1, R_2] = [W_1, R_2] + [R_1, W_2] = 0$ holds exactly.

The last two lines of eq. (B.11) define a Gram matrix M of dimension $(D^2 + 2D)$ and together with the energy gradient found by reshaping (B.10) we find that the TDVP equations are given by

$$\mathrm{i}M \begin{bmatrix} \dot{D}_1 \\ \dot{D}_2 \\ \dot{G} \end{bmatrix} = \begin{bmatrix} u_1 \\ u_2 \\ u_3 \end{bmatrix} \qquad \text{(B.13)}$$

where the right hand side denotes the gradient with components u_i and the square brackets are assumed to be vectors of dimension $(D^2 + 2D)$. Note that the equation for $\dot{K}$ also contributes to (B.13) as $\dot{K}$ itself is a function of $\dot{D}_1$, $\dot{D}_2$ and $\dot{G}$.

There is another subtlety concerning the inversion of the matrix M. It turns out that M has a D-dimensional kernel which is a consequence of additional gauge degrees of freedom. Indeed, the matrices R_i are invariant under the transformation $G \to \Delta G$ where Δ is a diagonal matrix. These gauge transformations are special, in the sense that they are not of the general form $R_i \to \Theta R_i \Theta^{-1}$, $G \to \Theta G \Theta^{-1}$ for some invertible matrix Θ but are rather a consequence only of the parametrization in (B.4). The corresponding gauge transformation for $\dot{G}$ is then given by $\dot{G} \to \dot{G} + \Delta G$ which is the infinitesimal version of the gauge transformation for G. With this transformation at hand one can construct an isometry that projects M

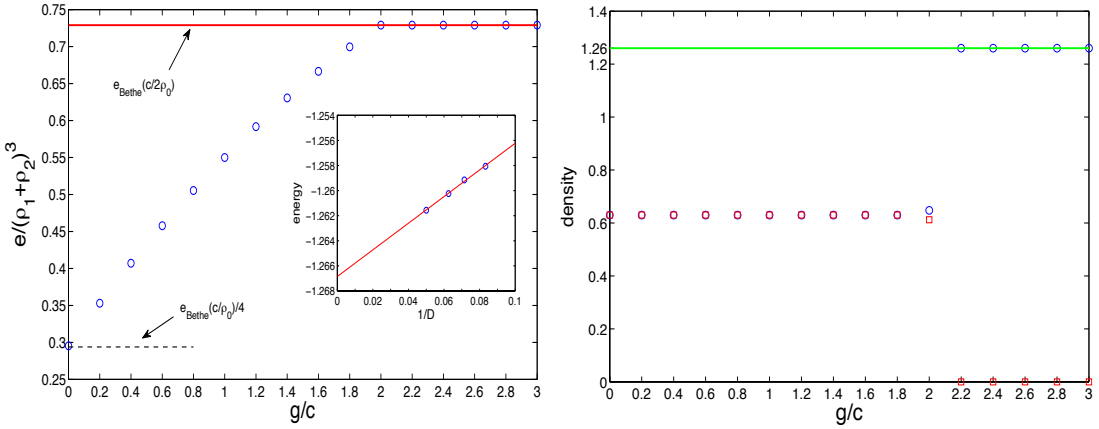

Figure B.1: Left: Ground state energy density as a function of the interspecies interaction g for $c = 1.5$ and $\rho_0 = 0.63$. Inset: Finite entanglement scaling of the ground state energy density at $c = 1.5$, $g = 1.2$ and $\rho = 0.63$. The dashed and solid line are the exact Bethe ansatz energies for the case of $g = 0$ and $g > 2c$ respectively. Right: Ground state density expectation values as a function of the interspecies interaction g for $c = 1.5$ and $\rho_0 = 0.63$. Blue circles: Density of species 1. Squares: Density of species 2. All simulations were done at $D = 20$.

onto the orthogonal complement of the space spanned by the D linearly independent vectors $\{[0_{(D,1)}; 0_{(D,1)}; n_i]\}|_{i=1}^{D}$ where $n_i = [e_i e_i^\dagger G]$ are each D^2-dimensional vectors and e_i is the standard basis. This isometry will thus reduce the dimensionality of eq. (B.13) by D and we end up with a full rank effective gram matrix and in total with $(D^2 + D)$ variational parameters.

In the left panel of Fig. B.1 the ground state energy density at $c = 1.5$ and $\rho_0 = 0.63$ is shown for several values of g below and above the demixing transition point at $g = 3$. If the inter-interaction exceeds this point, then one of the densities collapses to zero while the other density becomes twice as large as is shown in the right panel of Fig B.1. The system then turns into the single species Lieb-Liniger Hamiltonian at $\gamma = c/2\rho_0$. Calculating the precise critical point of a quantum phase transition with tensor networks is in general a subtle task since any finite D approximation always slightly shifts the effective numerical value and one has to perform a finite entanglement scaling to extract an accurate result [108]. This behaviour can also be observed in the right panel of Fig. B.1 as the density close to the transition point is not a perfect step function at this value of D but rather continuously changes from ρ_0 to $2\rho_0$ or 0 respectively.

In the case of $g = 0$ the ground state energy is simply twice the Lieb-Liniger ground state energy at $\gamma = c/\rho_0$. The expectation value of the inter-interaction then factories as $< \psi_1^\dagger \psi_2^\dagger \psi_2 \psi_1 > = < \psi_1^\dagger \psi_1 > < \psi_2^\dagger \psi_2 >$ as the two fields are then uncorrelated. In the left panel of Fig. B.2 we show the ground state expectation values of $< \psi_1^\dagger \psi_2^\dagger \psi_2 \psi_1 >$, $< \psi_1^\dagger \psi_1^\dagger \psi_1 \psi_1 >$ and $< \psi_2^\dagger \psi_2^\dagger \psi_2 \psi_2 >$ for different values of g. At $g = 0$ the cMPS approximation of $< \psi_1^\dagger \psi_2^\dagger \psi_2 \psi_1 >$ indeed factorises to ρ_0^2 and decreases for increasing g as the two fields start to repell each other leading to an antibunching effect of the two species visible in the density-density correlation function shown in the right panel of Fig. B.2.

All simulations were done at $D = 20$. At this bond dimension the relative error of the energy w.r.t. the asymptotic value calculated from the $1/D$ scaling is found to be $\epsilon_{\text{rel}} \approx 4 \times 10^{-3}$.

Finally, we will briefly discussion how the parametrization proposed in this chapter compares to the tensor product based parametrization recently introduced in [99, 100]. There the authors made the choice of $R_1 = \tilde{R}_1 \otimes \mathbb{I}$ and $R_2 = \mathbb{I} \otimes \tilde{R}_2$ where $\tilde{R}_1$ and $\tilde{R}_2$ are full matrices of dimension $\tilde{D}$. The species are then coupled by choosing $K = \tilde{K}_1 \otimes \mathbb{I} + \mathbb{I} \otimes \tilde{K}_2 + \sum_{p=0}^{P} Z_1^{(p)} \otimes$

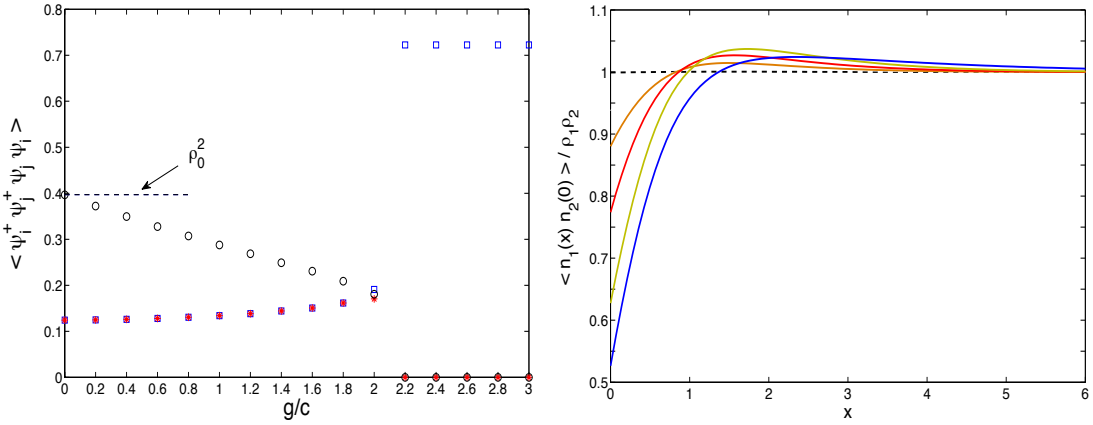

Figure B.2: Left: Ground state ecpectation values of $< \psi_1^\dagger \psi_1^\dagger \psi_1 \psi_1 >$ (blue squares), $< \psi_2^\dagger \psi_2^\dagger \psi_2 \psi_2 >$ (red stars) and $< \psi_1^\dagger \psi_2^\dagger \psi_2 \psi_1 >$ (red circles) for $c = 1.5$ and $\rho_0 = 0.63$. Right: Interspecies density-density correlation function at $c = 1.5$ and $\rho_0 = 0.63$. From top to bottom: $g = 0$ (dashed line), $g = 0.6$ (orange), $g = 1.2$ (red), $g = 2.1$ (green), $g = 2.7$ (blue).

$Z_2^{(p)}$ with P pairs of $\tilde{D}$-dimensional matrices $(Z_1^{(i)}, Z_2^{(i)})$. The authors observed that already moderate values of P up to $P = 3$ are enough to get reasonable results. This ansatz has a very elegant physical motivation as the coupling between the two species is adiabatically turned on by starting from the uncoupled solution given by $(\tilde{R}_1, \tilde{R}_2, \tilde{K}_1, \tilde{K}_2)$. As far as the ground state energies are concerned this ansatz and the one proposed in this chapter give the same results. On the one hand, the tensor product based parametrization has the advantage that solutions where the R matrices have Jordan Blocks are very well defined. The ansatz in this chapter is based on diagonalizing these matrices and thus does not allow for Jordan Blocks. However, it remains to be investigated whether or not this makes any difference in practice. On the other hand, when it comes to systems with more than two species the ansatz proposed in this chapter might be advantageous as it can be straightforwardly generalised to the multi species case. Moreover, the multi component tangent states as defined in (B.5) can be used as an ansatz for low lying excitations similar to what has been done in chapter 1. This would pave the way to systematically study the intriguing properties of the excitations in this system such as the phenomena of bosonic spin-charge separation. Moreover, the ansatz proposed in this chapter also allows the study of quasi two-dimensional systems by simply adding a Josephson coupling to the Hamiltonian of the form

$$\hat{H}_J = -g_\perp \int \mathrm{d}x \; \hat{\psi}_\alpha^\dagger(x) \hat{\psi}_\beta(x) + \mathrm{h.c.} \tag{B.14}$$

with a perpendicular coupling $g_\perp$ between the layers. Such a setting is especially relevant for experiments where systems are typically not constructed in isolation but rather in a coupled arrays [16, 105].

Lebenslauf

Persönliche Daten

Name:	Mag. Damian Draxler
Geburtsdatum:	10. Juli 1984
Geburtsort:	Graz, Österreich
Nationalität:	Österreich

Ausbildung und Tätigkeiten

06 / 2004	Reifeprüfung am Bundes-Oberstufenrealgymnasium Hegelgasse
10 / 2004 – 09 / 2005	verpflichtender Zivildienst beim Roten Kreuz
10 / 2005 – 06 / 2010	Studium der Physik an der Universität Wien
10 / 2010 – 10 / 2016	Doktorand an der Fakultät für Physik der Universität Wien

Publikationsliste

- D. Draxler, J. Haegeman, T. J. Osborne, V. Stojevic, L. Vanderstraeten, and F. Verstraete, "Particles, holes and solitons - a matrix product state approach", *Phys. Rev. Lett.* **111**, 020402 (2013)
- V. Zauner, D. Draxler, L. Vanderstraeten, M. Degroote, J. Haegeman, M.M. Rams, V. Stojevic, N. Schuch, F. Verstraete,
"Transfer Matrices and Excitations with Matrix Product States", *New J. Phys.* **17**, 053002 (2015)
- V. Zauner, D. Draxler, L. Vanderstraeten, J. Haegeman, F. Verstraete,
"Symmetry breaking and the Geometry of Reduced Density Matrices", *e-print* arXiv:1412.7642, 2016, submitted
- J. Haegeman, D. Draxler, V. Stojevic, J. I. Cirac, T. J. Osborne, F. Verstraete,
"Quantum Gross-Pitaevskii Equation", *e-print* arXiv:1501.06575, 2016, submitted to PRA: Rapid Communications
- D. Draxler, J. Haegeman, F. Verstraete, M. Rizzi,
"Atomtronics - a continuous matrix product state approach", *e-print* arXiv:1609.09704, 2016, submitted to PRB